

AD-A086 523

NAVAL POSTGRADUATE SCHOOL MONTEREY CA

F/G 17/2

FIBER OPTIC LINK DESIGN FOR AN OPEN-OCEAN SHALLOW-WATER TRACKIN--ETC(U)

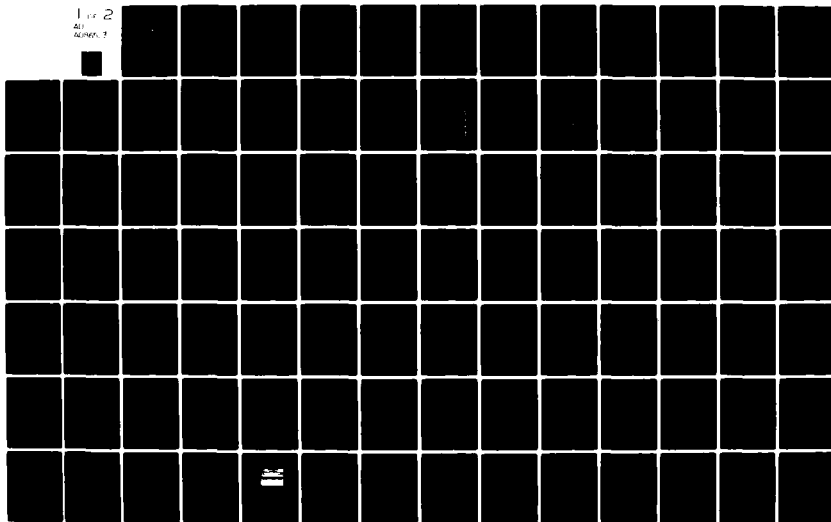
MAR 80 D N NICHOLSON, J P POWERS

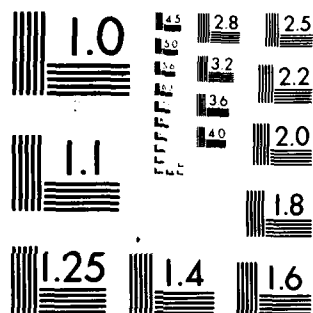
UNCLASSIFIED

NPS-62-80-007

NL

1 of 2  
ALL  
REMOVED





MICROCOPY RESOLUTION TEST CHART  
NATIONAL BUREAU OF STANDARDS 1963 A

**LEVEL**

(2)  
B.S.

**NAVAL POSTGRADUATE SCHOOL**  
**Monterey, California**

ADA 086523



**DTIC**  
**ELECTED**  
**S** JUL 15 1980

**THESIS**

FIBER OPTIC LINK DESIGN  
FOR AN  
OPEN-OCEAN SHALLOW-WATER TRACKING RANGE

by

David Norman Nicholson

March 1980

Thesis Advisor:

J.P. Powers

Approved for public release; distribution unlimited

Prepared for:

Naval Undersea Warfare Engineering Station (Code 0115)  
Keyport, Washington 98345

DDC FILE COPY.

80 7 14 105

NAVAL POSTGRADUATE SCHOOL  
Monterey, California

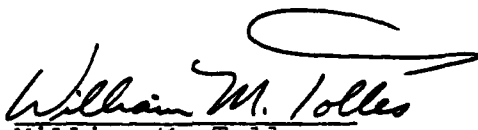
Rear Admiral John J. Ekelund  
Superintendent

Jack R. Borsting  
Provost

This thesis prepared in conjunction with research supported in part by Naval Undersea Warfare Engineering Station under work request number N0025380WR00032.

Reproduction of all or part of this report is authorized.

Released as a  
Technical Report by:

  
William M. Tolles  
Dean of Research

UNCLASSIFIED

SECURITY CLASSIFICATION OF THIS PAGE (When Data Entered)

REPORT DOCUMENTATION PAGE		READ INSTRUCTIONS BEFORE COMPLETING FORM	
1. REPORT NUMBER 14 NPS-62-80-007	2. GOVT ACCESSION NO. AD-A086523	3. RECIPIENT'S CATALOG NUMBER	
4. TITLE (and Subtitle) 6 Fiber Optic Link Design for an Open-Ocean Shallow-Water Tracking Range.		5. TYPE OF REPORT & PERIOD COVERED 9 Master's Thesis, March 1980	
7. AUTHOR(s) 10 David Norman Nicholson and John P. Powers		6. PERFORMING ORG. REPORT NUMBER	
8. PERFORMING ORGANIZATION NAME AND ADDRESS Naval Postgraduate School Monterey, California 93940		9. CONTRACT OR GRANT NUMBER(s)	
11. CONTROLLING OFFICE NAME AND ADDRESS Naval Postgraduate School Monterey, California 93940		10. PROGRAM ELEMENT, PROJECT, TASK AREA & WORK UNIT NUMBERS N0025380WR00032	
12. MONITORING AGENCY NAME & ADDRESS (if different from Controlling Office) Naval Undersea Warfare Engineering Station Code 0115 Keyport, Washington 98345		11. REPORT DATE March 1980	
		12. NUMBER OF PAGES 129	
13. DISTRIBUTION STATEMENT (of this Report) Approved for public release; distribution unlimited		13. SECURITY CLASS. (of this report) Unclassified	
14. DISTRIBUTION STATEMENT (of the abstract entered in Block 20, if different from Report)		14a. DECLASSIFICATION/DOWNGRADING SCHEDULE	
15. SUPPLEMENTARY NOTES			
16. KEY WORDS (Continue on reverse side if necessary and identify by block number) Fiber Optic Communications Open-Ocean Shallow-Water Tracking Range Fiber Optic Link Design Digital Signal Formats			
20. ABSTRACT (Continue on reverse side if necessary and identify by block number) This thesis is an investigation into the feasibility of using fiber optics in a shallow-water tracking range at the Naval Undersea Warfare Engineering Station. After a review of the requirements and constraints imposed on the system, a study of optical fiber cables is presented. The engineering parameters for a fiber optic system were reviewed and sample calculations made based on commercially available optical components. The signal formats available for transmission over a fiber optic system were also reviewed. A description of the electronics used to construct one of the possible signal formats and			

DD FORM 1473  
1 JAN 73  
(Page 1)EDITION OF 1 NOV 68 IS OBSOLETE  
S/N 0102-014-4401

UNCLASSIFIED

SECURITY CLASSIFICATION OF THIS PAGE (When Data Entered)

UNCLASSIFIED

SECURITY CLASSIFICATION OF THIS PAGE/When Data Entered

#20 - ABSTRACT - CONTINUED

a spread spectrum version of that signal are provided.

Accession For	
NTIS 3.2241	<input checked="checked" type="checkbox"/>
DOC TAB	<input type="checkbox"/>
Unannounced	
Justification	
By	
Distribution/	
Availability Codes	
Dist	Available/or special
A	

DD Form 1473  
Jan 73  
S/N 0102-014-6601

2

UNCLASSIFIED

SECURITY CLASSIFICATION OF THIS PAGE/When Data Entered

Fiber Optic Link Design  
for an  
Open-Ocean Shallow-Water Tracking Range

by

David Norman Nicholson  
Captain, United States Army  
B.S., United States Military Academy, 1972

Submitted in partial fulfillment of the  
requirements for the degree of

MASTER OF SCIENCE IN ELECTRICAL ENGINEERING

from the

NAVAL POSTGRADUATE SCHOOL  
March 1980

Author

*David N Nicholson*

Approved By:

*J. J. Powers*

Thesis Advisor

*R. Paulhofer*

Second Reader

*D. E. Kite*

Chairman, Department of Electrical Engineering

*William M. Toller*

Dean of Science and Engineering

# ABSTRACT

This thesis is an investigation into the feasibility of using fiber optics in a shallow-water tracking range at the Naval Undersea Warfare Engineering Station. After a review of the requirements and constraints imposed on the system, a study of optical fiber cables is presented. The engineering parameters for a fiber optic system were reviewed and sample calculations made based on commercially available optical components. The signal formats available for transmission over a fiber optic system were also reviewed. A description of the electronics used to construct one of the possible signal formats and a spread spectrum version of that signal are provided.



## TABLE OF CONTENTS

I.	INTRODUCTION-----	11
II.	SYSTEM REQUIREMENTS AND CONSTRAINTS-----	14
	A. MODULATION FORMAT-----	14
	B. RANGE PARAMETERS-----	19
III.	OPTICAL FIBER CABLES-----	21
	A. ADVANTAGES-----	21
	B. DISADVANTAGES-----	26
	C. OPTICAL FIBER STRENGTH IN THE PRESENCE OF WATER-----	27
	D. OPTICAL CABLES: A SOLUTION-----	31
IV.	OPTICAL SYSTEM ENGINEERING-----	47
	A. OPTICAL FIBER SELECTION-----	47
	B. OPTICAL SOURCE SELECTION-----	52
	C. OPTICAL DETECTOR SELECTION-----	54
	D. OPTICAL LINK DESIGN-----	59
	E. OPTICAL MODULATOR DESIGN-----	61
	F. RECEIVER CIRCUIT DESIGN-----	65
V.	SIGNAL FORMAT AND DATA RECOVERY-----	74
	A. ANALOG OR DIGITAL ?-----	74
	B. SFSK SIGNAL SIMULATOR-----	78
	C. DATA RECOVERY CIRCUIT-----	86
	D. DATA SPREADING-----	102
VI.	CONCLUSIONS-----	123
	LIST OF REFERENCES-----	125
	INITIAL DISTRIBUTION LIST-----	126

## LIST OF TABLES

I.	CABLE COMPARISONS-----	22
II.	CABLE A CHARACTERISTICS-----	35
III.	ARMORED CABLE A CHARACTERISTICS-----	38
IV.	ATTENUATION CALCULATIONS-----	51
V.	OPTICAL SOURCE CHARACTERISTICS-----	55
VI.	OPTICAL DETECTOR CHARACTERISTICS-----	58
VII.	OPTICAL DETECTOR NOISE CALCULATIONS-----	60
VIII.	POWER CALCULATIONS FOR TRANSIMPEDANCE AMPLIFIER-----	70
IX.	BAND 2 FREQUENCIES IN kHz-----	87

## LIST OF FIGURES

1. Shallow-Water-Tracking-Range Subsystems-----	12
2. Spaced Frequency Shift Keying-----	15
3. Bandpass Characteristics of Non-recurrent Tones and Spaced Frequency Shift Keying-----	17
4. Signal Construction Timing Diagram-----	18
5. Shallow-Water-Tracking-Range-----	20
6. End View of Cables-----	24
7. Attenuation vs Frequency-----	25
8. Stress vs Strain for Optical Fibers and Copper-clad Steel Wire---	32
9. Cable A Composition-----	35
10. Cable A Performance Under Load-----	36
11. Armored Cable A Composition-----	38
12. Tapered Epoxy Plug Bulkhead Penetrator-----	41
13. Epoxy Filled Hypo Needle Bulkhead Penetrator-----	42
14. Elastomeric Bulkhead Penetrator-----	43
15. Glass Window With $\frac{1}{4}$ Pitch Selfoc Rod Bulkhead Penetrator-----	44
16. $\frac{1}{2}$ Pitch Selfoc Rod Bulkhead Penetrator-----	45
17. Attenuation Calculations for Hydrophone to Multiplexer Link-----	62
18. Attenuation Calculations for Multiplexer to Shore Link-----	63
19. Analog Optical Modulators-----	64
20. Digital Optical Modulators-----	66
21. Transimpedance Amplifier-----	69
22. Integrating Front-end Amplifier-----	69
23. Tone Generator With Variable Doppler-----	79
24. Programmable Data Generator-----	81

# LIST OF FIGURES (CONT)

25. Programmable Data Generator-----	82
26. SFSK Generator (Modulator)-----	84
27. SFSK Signal Generated by Signal Simulator-----	85
28. 567 Tone Detector-----	88
29. Narrowband Tone Detector With Adjustable Overlapping Locking Ranges-----	89
30. Locking Range Adjustment For Detection of Narrowband Signal With 567 Tone Detector-----	91
31. Monostable Multivibrator-----	91
32. Clock Recovery Circuit-----	92
33. Original Message Recovery-----	94
34. Timing Diagram of Data Recovery-----	95
35. Block Diagram of Circuit Which Recovers Original Message-----	96
36. SFSK Signal and Data Reccovered With 10010110 Programmed-----	97
37. SFSK Signal and Data Recovered With 11010010 Programmed-----	97
38. 3 Band Multiplexer-----	99
39. Transimpedance Amplifier Calculations-----	100
40. BER vs SNR For ASK Signals-----	103
41. 31-Bit Spreading Circuit-----	106
42. Spreading Sequence [5,3] -----	107
43. Spreading Sequence [5,3] -----	107
44. Spreading Sequence [5,2] -----	108
45. Spreading Sequence [5,2] -----	108
46. Despreading Circuit to Detect [5,3] or [5,3] -----	110
47. Theoretical and Measured Results [5,3] Transmitted-----	111
48. Theoretical and Measured Results [5,3] Transmitted-----	112
49. Theoretical and Measured Results [5,2] Transmitted-----	113

# LIST OF FIGURES (CONT)

50.	Theoretical and Measured Results	$\overline{[5,2]}$	Transmitted-----	114
51.	Theoretical and Measured Results	$\overline{[5,2]}$	$\overline{[5,3]}$ Transmitted-----	115
52.	Theoretical and Measured Results	$\overline{[5,2]}$	$\overline{[5,3]}$ Transmitted-----	116
53.	Theoretical and Measured Results	$\overline{[5,2]}$	$\overline{[5,3]}$ Transmitted-----	117
54.	Theoretical and Measured Results	$\overline{[5,2]}$	$\overline{[5,3]}$ Transmitted-----	118
55.	Theoretical and Measured Results	$\overline{[5,2]}$	$\overline{[5,3]}$ $\overline{[5,2]}$ $\overline{[5,3]}$ Transmitted-----	119
56.	Theoretical and Measured Results	$\overline{[5,2]}$	$\overline{[5,3]}$ $\overline{[5,2]}$ $\overline{[5,3]}$ Transmitted-----	120
57.	Theoretical and Measured Results	$\overline{[5,2]}$	$\overline{[5,3]}$ $\overline{[5,2]}$ $\overline{[5,3]}$ Transmitted-----	121

#### ACKNOWLEDGEMENT

The author is extremely grateful to his thesis advisor, Dr. John Powers for his guidance and encouragement; to Dr. Steve Cowan (NOSC, San Diego), George Wilkens and Frank Armogida (NOSC, Hawaii), Ted Thompson and Rich Tiedemann (Keyport) for their expert advise and technical assistance; and finally to his wife Carol for her moral support and expert typing.

## I. INTRODUCTION

Optical fibers are fast becoming one of the primary transmission mediums for modern communications systems. They are now seriously being considered as an alternative to copper cable because of their bandwidth capability, small size, and lower system cost. The Naval Undersea Warfare Engineering Station in Keyport, Washington, is presently developing an open-ocean shallow-water tracking range and has requested a study on the feasibility of utilizing optical fibers to replace the proposed underwater copper cables. To this end three objectives will be undertaken in this presentation. The first is to ascertain whether fiber optics are a viable and even possibly better solution to the transmission of the signal from the underwater tracking device to the landbased signal processor. The second is to review the procedure for engineering a fiber optic system and to make sample calculations based on the requirements of the shallow-water range. The third is to evaluate various signal formats that could be used between the underwater tracking device and the signal processor. It is not the intention here to engineer a complete system for the Keyport facility but merely evaluate new technology that could be considered for future application.

The shallow-water range will be composed of four subsystems, one of which can be considered for the application of fiber optics. A basic diagram of the subsystems is presented in Fig. 1. The first subsystem is a pinger housed in the torpedo or other device to be tracked. The acoustic signal emitted by the pinger is received by the second subsystem, a hydrophone mounted on the ocean floor. The third subsystem is an underwater cable transmission link which is composed of the electronics to convert

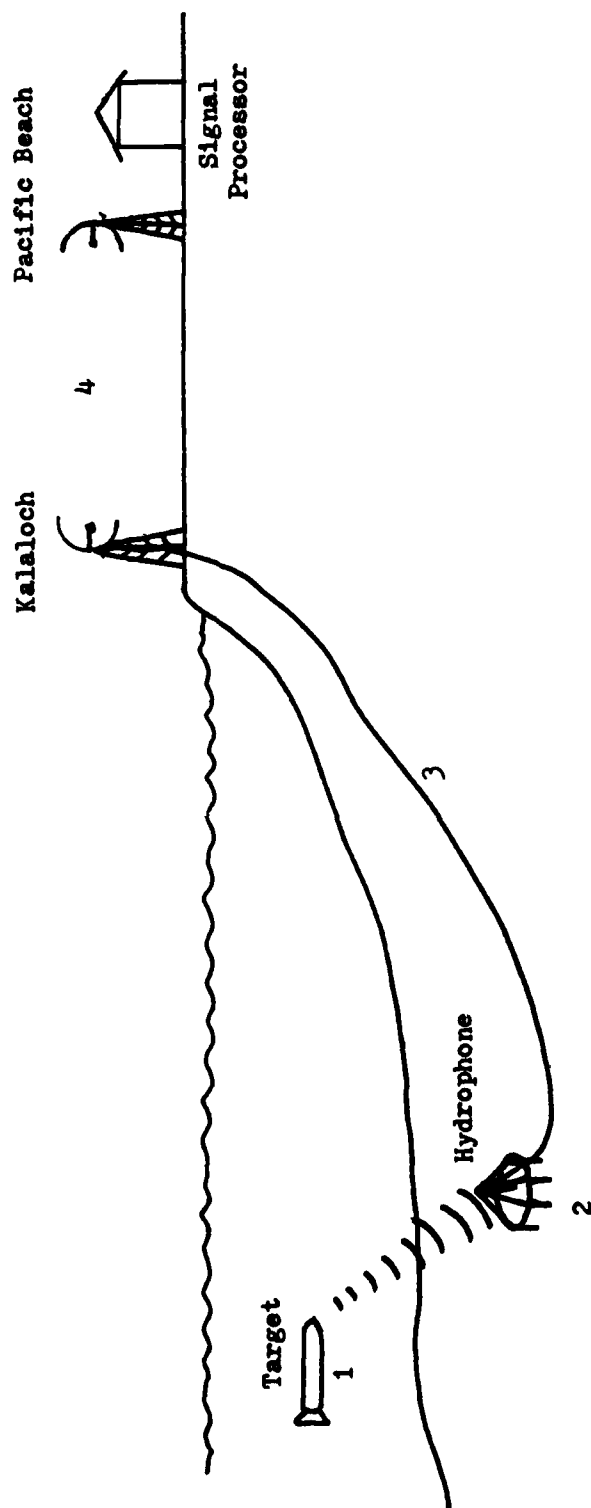


Figure 1. Shallow-Water-Tracking-Range Subsystems



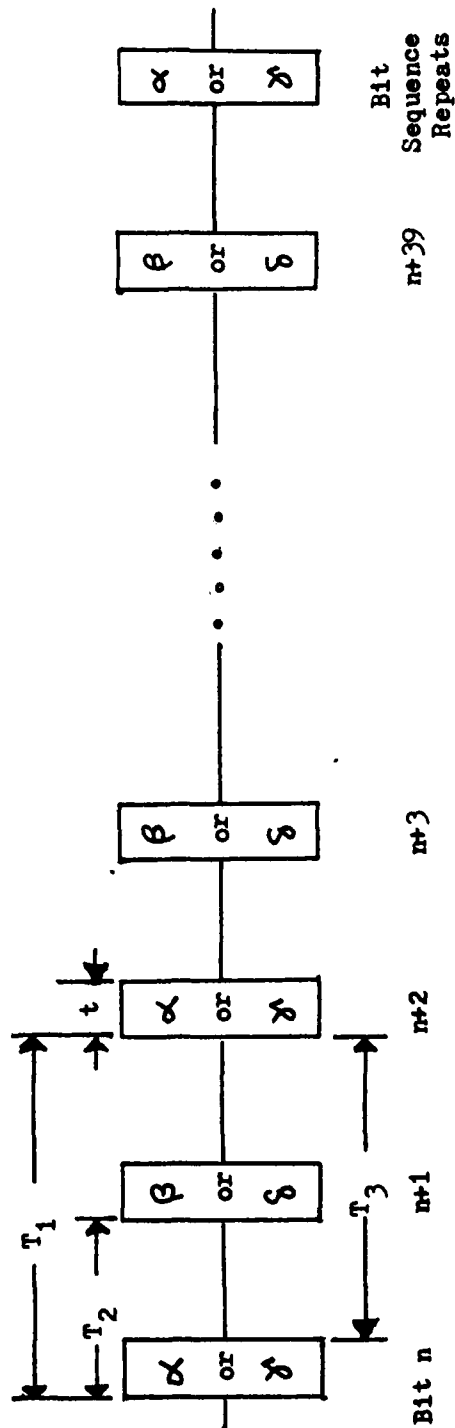
the voltage output of the hydrophone into a signal compatible with the cable and the cable itself which connects the hydrophone with the shore-line at Kalaloch, Washington. The fourth subsystem is a microwave system including the signal conversion electronics and radio path that connects Kalaloch with the Pacific Beach Tracking and Control Center. At the Pacific Beach facility the information is processed for evaluation. Subsystem three, the underwater link, is the concern of this investigation.

## II. SYSTEM REQUIREMENTS AND CONSTRAINTS

In order to determine the feasibility of replacing the proposed copper cables with an optical fiber it is necessary to examine the system requirements and constraints that have been set by the Keyport Station as well as those that exist due to the undersea environment. The reader is advised that the final engineering guidelines for the shallow-water range have not, at the time of writing, been solidified. Therefore many of the values and even concepts presented in this section may not be valid. Nevertheless, what is presented is representative of what the actual requirements and constraints will be and therefore with slight modification the results of this presentation are valid.

### A. MODULATION FORMAT

The modulation format chosen for the shallow-water range is Spaced Frequency Shift Keying (SFSK). This system uses four non-recurrent tones to transmit the data. Two separate data streams, timing and telemetry, are interleaved to produce the transmitted message. As shown in Fig. 2, the odd numbered bits are composed of a twenty bit code that can identify the target and establish timing by correlating the transmitted code with a stored replica at the tracking station. The even numbered telemetry bits consist of a ten-bit error-correcting code for depth and five uncoded bits each for x and y position. The forty bit sequence continuously repeats as the target maneuvers the range with the telemetry data being updated every second. Each data bit will be about three milliseconds ( $t$ ) in duration with a period of 50 milliseconds ( $T_1$ ). The interleaved data will therefore have a period of 25 milliseconds ( $T_2$ ). Thus each of the codes is transmitted



Odd Numbered Bits: Identify, Timing, Framing  
 Even Numbered Bits: Programmable; i.e. 10-bit error-correcting  
 coded depth & 5-bits each for X & Y

Figure 2. Spaced Frequency Shift Keying

at 20 bits per second and the interleaved data stream, which is the actual transmitted message, is at 40 bits per second.

Four distinct frequencies will be used to modulate the data: one tone, represented by  $\alpha$ , for a timing bit "1"; a second,  $\beta$ , for a telemetry bit "1"; and two more,  $\gamma$  and  $\delta$ , for a "0" bit of timing and telemetry respectively. As shown in Fig. 3 each successive tone,  $\alpha$  through  $\delta$ , is spaced in frequency five per cent higher than the previous tone. This results in a 10.25 per cent separation between corresponding "1" and "0" bits with the "1" tone being the lower frequency. The tracking range will utilize three bands of four frequencies in the range from 27 to 50 KHz. Two bands will be used to track single high speed targets and the third will be used to track up to two slower speed targets simultaneously. This enables up to four targets to be tracked at one time.

The SFSK format was selected to allow compensation for Doppler and for multipath effects. The four per cent bandwidth about each tone (Fig. 3) allows for  $\pm 2$  per cent Doppler or targets traveling at speeds up to 60 knots. The 47 millisecond spacing ( $T_3$ ) between each bit and the next related bit allows for decay of reverberation due to multipath effects. SFSK is dependent on frequency but insensitive to amplitude variations and therefore ignores any varying attenuation of the signal. In addition, the use of codes with good autocorrelation and low cross-correlation will allow three errors in the twenty bit identification and timing sequence. The result of modulating the interleaved timing and telemetry sequences with SFSK is depicted in a - d of Fig. 4. The transmitted signal (d) is a clean signal but due to multipath effects and Doppler shift the signal received at the hydrophone would appear as in (e) of Fig. 4 where  $\epsilon$  represents a frequency shift of the transmitted tone due to Doppler shift.

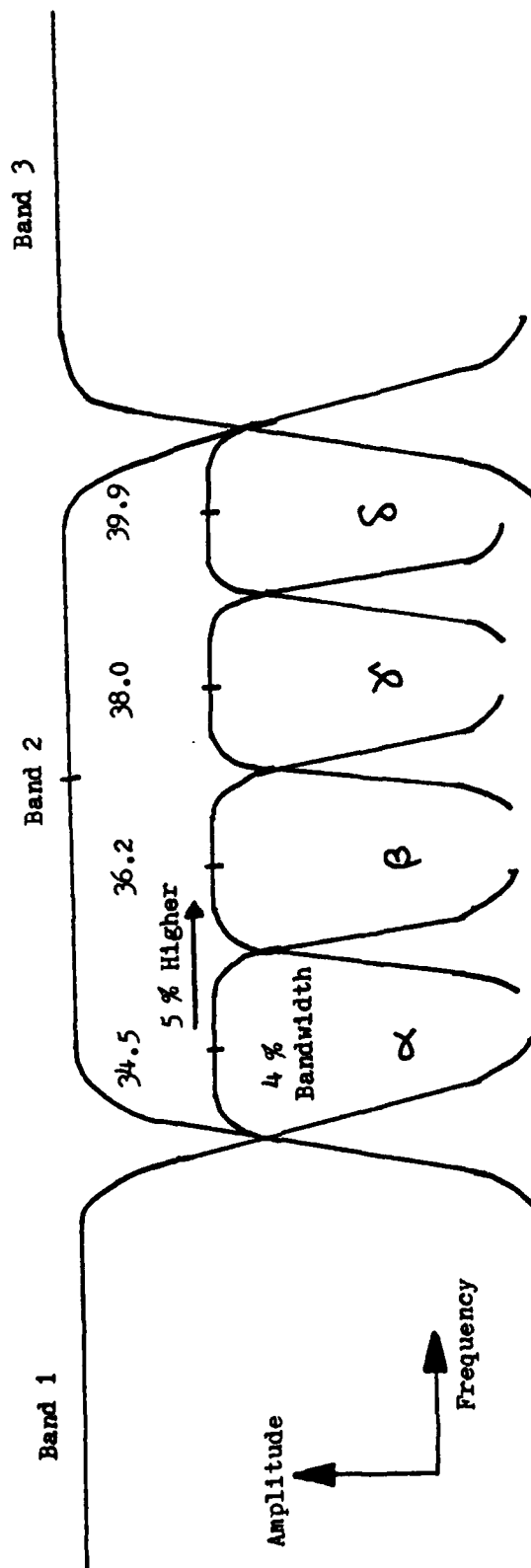


Figure 3. Bandpass Characteristics of Non-Recurrent Tones and Spaced Frequency Shift Keying

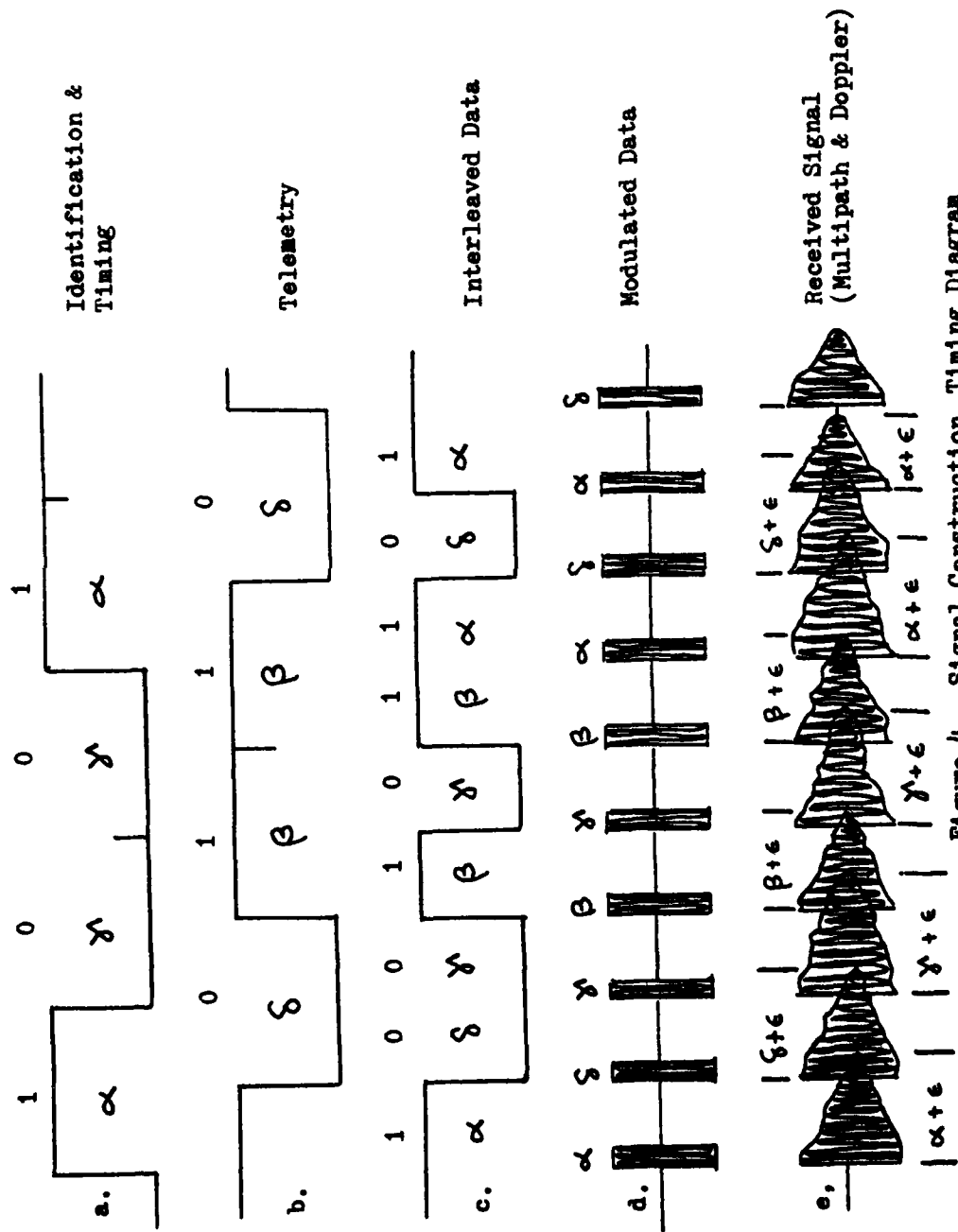


Figure 4. Signal Construction Timing Diagram

## B. RANGE PARAMETERS

The shallow-water tracking range, as depicted in Fig. 5, will be approximately two by four nautical miles in size and located seven nautical miles from the microwave link at Kalaloch in Olympic National Park. The range will consist of thirteen hydrophones placed 2000 yards apart. The hydrophones will each be tied to a central location 3400 yards east of the central hydrophone where the individual signals will be multiplexed together and then transmitted via a single cable to Kalaloch. The cables from the hydrophones to the multiplexer will range from 1950 yards to 5950 yards in length. The multiplexer should be capable of handling up to 16 signals. The hydrophones will be mounted three feet above the ocean floor in water ranging in depth from about 80 to 140 feet.

The range equipment and cables will be exposed to the ocean environment. This indicates the requirement to withstand turbulences due to high sea states. The ocean bottom in the area chosen is a flat, sandy, and featureless with minimum slope. The last nautical mile of the multiplexed-signal cable will transverse through the surf zone and must therefore be amply protected from the additional turbulence. Other ocean environmental constraints that must be considered include sea-water effects, sea-life attacks and fouling due to anchors and trollers.

Finally, several desired features have been proposed for engineering the range. These include hermetically sealed electronics, CMOS components to minimize power requirements, and the mobility capable of a system that can be installed, repaired and recovered by divers.

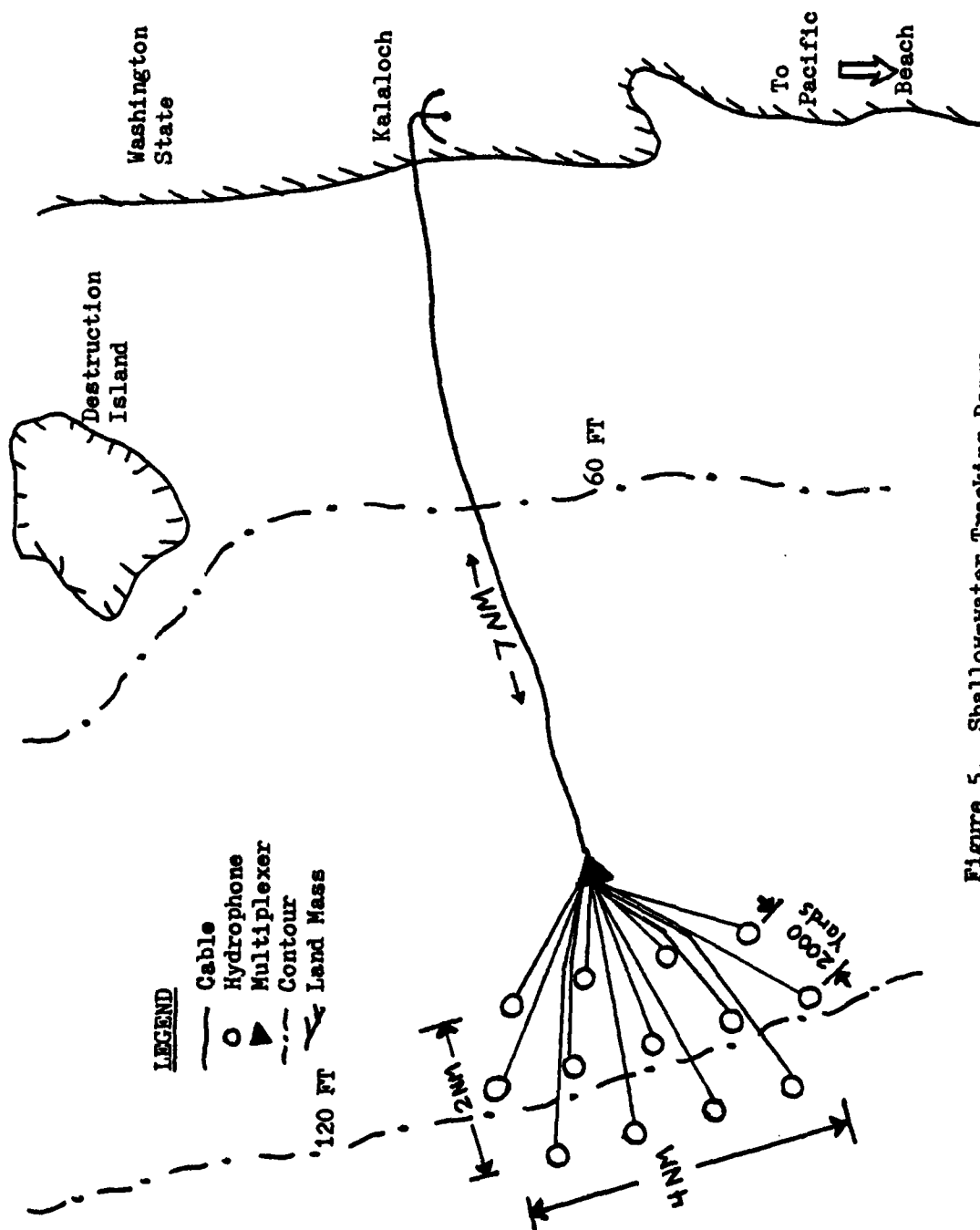


Figure 5. Shallow-water Tracking Range



### III. OPTICAL FIBER CABLES

Having established the requirements and constraints of the underwater cable subsystem, the feasibility of utilizing optical fibers as the communications path can now be examined. The first step is to determine the advantages of optical fibers over copper cables. Then the pertinent disadvantages must be examined to determine those that could preclude the use of fibers, and if and how they can be overcome.

#### A. ADVANTAGES

The advantages of optical fibers over copper cables are numerous. Those which are of interest in this application are smaller size, less weight, greater bandwidth capability, lower attenuation at high bandwidths, immunity to radio-frequency interference and electromagnetic radiation, and lower system cost.

The present plan for the shallow-water range is to use three different copper cables. Between the hydrophones and the multiplexer a quad-type armored ocean cable is to be used. The cable consists of four insulated conductors twisted together around a center filler and then covered with armor wires and a polyethelene outer covering. The cables that will be used to link the multiplexer to the shore subsystem are a single-armor and a double-armor submarine coaxial cable. The first six nautical miles will be composed of the single-armor coaxial cable while the last nautical mile, which includes the surf zone region, will be composed of the double-armor coaxial cable. In Table I the size and weights of those cables have been listed along with the size and weight of International Telephone and Telegraph Corporation (ITT) T-1211 graded-index buffered optical cable.

CABLE TYPE	OVER ALL DIAMETER (in.)	WEIGHT IN AIR (lb/NM)	WEIGHT IN SEA WATER (lb/NM)	MINIMUM BREAKING STRENGTH (lbf)	CABLE MODULUS (NM)	SPECIFIC GRAVITY RELATIVE TO SEA WATER
QUAD CABLE	0.50	375	250	$4 \times 10^3$	15.0	3.00
SINGLE-ARMOR COAXIAL CABLE	1.25	6600	3950	$3 \times 10^4$	7.6	2.50
DOUBLE-ARMOR COAXIAL CABLE	1.75	54600	31400	Info not available	2.35	
ITT T-1211 OPTICAL FIBER CABLE	.02	2.1	0.38	1.9	5.0	1.22

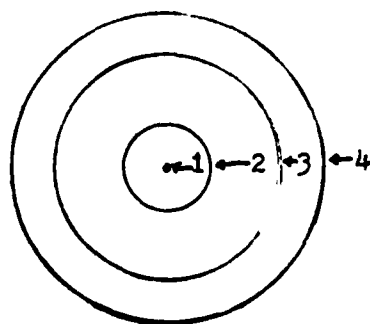
TABLE I. CABLE COMPARISONS

Figure 6 presents an end-view look at the relative size of these various cables. The outer diameter of the glass fiber (cladding) itself is only .005 inches or one quarter of the optical cable's total diameter. Cable modulus is the minimum breaking strength of the cable (ultimate tensile strength) divided by its weight in sea water and is an absolute measure of the strength of the cable during installation which is when the stress on a cable is greatest.

The obvious advantage to be gained from the fiber is ease of installation. The large size and weight of the copper cables makes it necessary to use cable laying ships to install and recover them. The optical fiber can easily be installed by divers or from a small boat. This ease of installation is the primary advantage of interest for the shallow-water tracking range.

Optical fibers, which are modulated at optical frequencies, are capable of very large modulation bandwidths. For example, the ITT T-1211 optical cable in Fig. 6, is commercially available with an electrical bandwidth-length of greater than 400 MHz-NM. This means, for example, a capability of carrying a 40 MHz signal a distance of ten nautical miles. In copper cable the bandwidth is proportional to the size of the conductors. Therefore to obtain a large bandwidth a large cable is required. An optical fiber's bandwidth capability is not dependent on size but on the purity of the material from which it is constructed.

Signal attenuation in copper cables is also a function of size. Again this is not the case in optical cables. Fig. 7 shows a comparison of the two types of copper cable (the single and double armor coaxial cables have the same attenuation) and ITT T-1211 optical cable. At low bandwidths the coaxial cable has lower attenuation than this particular optical cable. However optical fibers with attenuation as low as .37 dB/NM have been re-



1. Optical Fiber Cable (T-203 & T-1211)
2. Quad Cable
3. Single-Armor Coaxial Cable
4. Double-Armor Coaxial Cable

Figure 6. End View of Cables

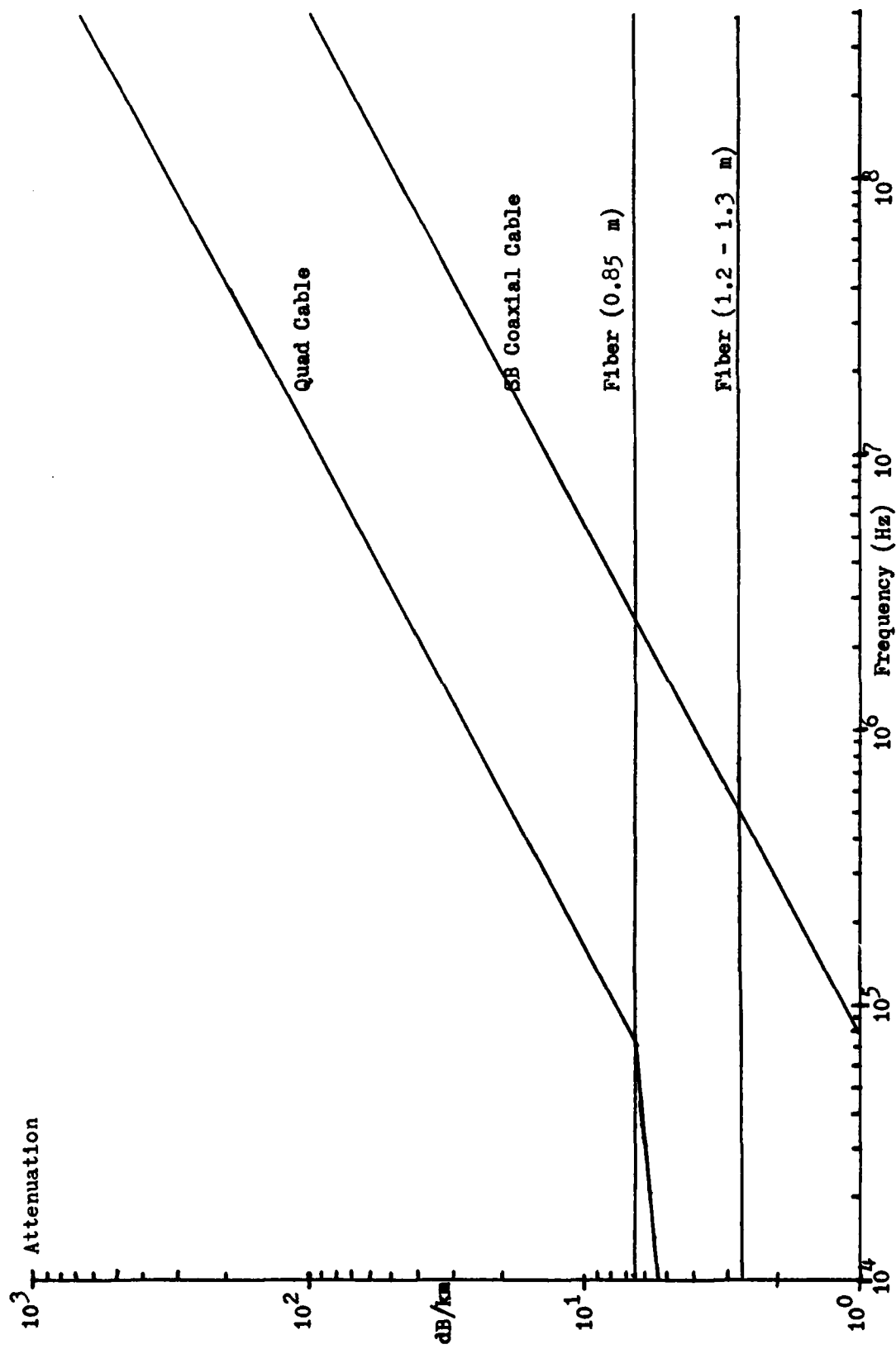


Figure 7. Attenuation vs Frequency

ported at an optical wavelength of  $1.55 \mu\text{m}$ . These very low loss fibers will be commercially available in the near future. As can be seen in Fig. 7, a fiber modulated at a wavelength of  $1.25 \mu\text{m}$  can carry a signal with nearly 1000 times the bandwidth of the coaxial cable for a distance of one nautical mile with equal attenuation. Because processing gain (the improvement in signal-to-noise ratio) due to bandwidth spreading is proportional to the amount of spread, the fiber offers a capability of nearly 30 dB improvement. Likewise, the larger bandwidth without increased attenuation enables the engineer to consider a larger variety of signal formats including digitized versions of the analog signal received at the hydrophone.

Coaxial cable is subject to picking up extraneous signals on the outer conductor while quad-cable is subject to crosstalk between pairs of conductors. Because optical cables carry information at light frequencies rather than radio frequencies and require no return path they are immune to these effects of radio-frequency interference. Since optical cables are composed of non-conducting materials they are also immune to electromagnetic radiation.

In engineering any system one of the primary concerns is cost. At present the cost of T-1211 optical cable is approximately one half the cost of the single armor coax. In addition, the cost of optical fiber is decreasing as its market increases while coax cost is increasing as copper becomes more expensive. Extensive savings can also be realized in installation costs since a cable laying ship would not be required to install optical cables.

#### B. DISADVANTAGES

In spite of the many advantages of optical fibers they do have several

problems which must be overcome before utilization as the transmission medium in the underwater subsystem is practical. The light weight of the fiber which is advantageous for handling could be a disadvantage if the fiber were bouyant in seawater or even if it did not have sufficient specific gravity to remain fast on the ocean floor in the presence of turbulence. Fibers are in fact immune to RFI and EMI, but on the other hand cannot carry electrical power which would be needed to operate the electronics at the hydrophones and multiplexer. The fact that optical fibers are composed of glass leads to the question of strength and survivability in an ocean environment. One of the primary causes of attenuation in optical fibers is the presence of Hydroxyl Ions,  $\text{OH}^-$ , which are numerous in the presence of moisture and therefore the effects of seawater on fiber attenuation are of concern. If in fact optical fibers are vulnerable in water, the problem of connectors and optical-to-source or detector interfaces must also be addressed. Finally there is the problem of a lack of standardization in industry which to a large extent forces the user to purchase systems rather than components and keeps the cost of fiber optics high.

The problems of keeping the fiber on the ocean floor and providing power to the underwater electronics are unimportant if the undersea environment proves to be fatal to the survivability of optical fibers. As will be seen, in the process of insuring the fiber survives in the ocean environment the problem of weight (specific gravity) and power handling are overcome.

#### C. OPTICAL FIBER STRENGTH IN THE PRESENCE OF WATER

Theoretically the ultimate tensile strength, pulling force at fracture, of glass fiber is greater than  $2.9 \times 10^6$  pound-force per square inch ( $\text{lbf/in}^2$ )

while a value of only  $0.25 \times 10^6$  lbf/in<sup>2</sup> is typical for high-carbon steel wire. However, in reality the strength of glass fibers is much lower than the theoretical value. In addition, the theoretical maximum strain, per cent of elastic stretching, prior to fracture for glass fibers is near ten per cent but typical safe values for strained fibers are closer to one per cent or less. It is commonly believed that the cause of glass fibers falling short of theoretical values is the existence of flaws, especially those on the surface which are referred to as microcracks. Glass, unlike steel, is not ductile nor does it have the ability to flow and evenly distribute stress. Therefore, an applied stress becomes concentrated at the tip of a surface crack causing local failure of the material's atomic bonds. This results in fracture of the fiber even though the average applied stress is well below the ultimate tensile strength for the material. This fracturing effect is utilized in preparing fibers for splicing or connector application via the scribe and break technique. A diamond cutting edge is used to barely scratch the surface of the fiber after which a gentle tug causes a clean fracture. Although effective for fiber end preparation, the microcrack fracture must be avoided along the entire length of a communications channel.

Theory predicts and practice verifies that the strength of a fiber is a function of the most severe flaw. The ultimate tensile strength for a length of fiber can therefore be predicted if the geometry and size of this most severe flaw is known. In 1920, Griffith [4] described fracture strength ( $\sigma$ ) by the equation

$$\sigma = (2E\gamma/\pi L)^{\frac{1}{2}} \quad (1)$$

where  $E$  is Young's modulus,  $\gamma$  is the surface energy and  $L$  is the halfcrack length. Griffith predicted that fracture results when the strain-energy



release rate caused by extension of the surface flaw exceeds the surface-energy increase rate. For any length of fiber the distribution and characteristics of surface flaws are random. Therefore, fiber strength can only be described statistically. Assuming that the flaws are independent and randomly distributed, the probability of failure of a specified length of fiber can be described by a Weibull distribution [6].

$$G(s, f^*, t) = 1 - \exp \left[ - \left( \frac{f^* - f_m}{f_o - f_m} \right)^p \left( \frac{t}{t_o} \right)^b \left( \frac{s}{s_o} \right) \right]. \quad (2)$$

This equation describes the probability that a fiber with surface area  $s$  will fail under stress  $f^*$  in time  $t$  where

- $f_m$  is stress below which failure never occurs
- $f_o$  is stress above which failure always occurs
- $t_o$  is a crack growth time constant
- $s_o$  is a scale factor for equivalent surface area
- $p, b$  are experimentally determined powers.

The various parameters are determined experimentally by testing sufficient samples to fracture.

The problem of microcrack stress fracture is further complicated when the fiber is placed in an active environment. The result is a growth of the surface flaw which lowers the ultimate tensile strength. Static fatigue is the term used to describe this crack growth behavior when it occurs due to a constant stress being applied which is below the materials inert strength. Unfortunately water is such an active environment for glass fibers. This time dependent behavior of static fatigue on a glass fiber in the presence of water is referred to as stress corrosion. If the constant applied stress is less than 20 per cent of the ultimate tensile strength for the fiber, stress

corrosion occurs very slowly and would take decades to result in fracture. However at 40 per cent of the ultimate strength the corrosion rate is rapid and fracture occurs in hours.

The average tensile strength in short lengths of high quality optical fiber is greater than  $5 \times 10^5$  lbf/in<sup>2</sup> at an ultimate strain of five per cent. This value is typically much lower in long fiber lengths since the longer the fiber the greater the probability of a more severe surface flaw occurring.

Unfortunately the only way to determine the exact tensile strength of a length of glass fiber is to stress it to fracture. In addition, it is not sufficient to test a small portion of the entire length. The continuous testing of each section left after fracture results in numerous short lengths, hardly a practical means of obtaining the needed information for a long length of usable optical fiber. To overcome this problem fiber manufacturers have developed the technique of proof testing [4]. The long length of fiber is subjected to a standard tensile load, typically  $10^5$  lbf/in<sup>2</sup> at one per cent elongation, which is hopefully greater than any expected stress the fiber would be subjected to in future handling or use. If the fiber fractures it is discarded. This guarantees that the maximum surface flaw is smaller than a predictable value. From the Griffith equation for a stress of  $10^5$  lbf/in<sup>2</sup> the maximum crack depth is .19  $\mu$ m. The proof test assures the user that the fiber can withstand any instantaneous stress up to the proof strength. It also enables the prediction of minimum lifetime for a stress corroding environment at constant applied stresses below the proof test level.

It has been shown that fiber tensile strength is dependent on surface flaw initiation and growth. Therefore to improve the ultimate tensile strength of a glass fiber the number and size of surface flaws must be

minimized both during and after manufacturing. To accomplish this a protective coating is applied to the glass to protect against rough handling, abrasion and exposure to water [7]. In addition, glass fibers are characterized as brittle, meaning their capacity to absorb energy and deform plastically is low. To prevent fracture from an anisotropic stress, such as an impact, the protective buffer must also be capable of converting the applied stress into a more isotropic one or absorb and evenly distribute the stress in all directions. Several materials have proven suitable. The ITT T-1211 fiber is buffered with RTV 184, a silicone rubber, and then with Hytrel 7246, a polyester elastomer. These buffers provide hundreds of hours of isolation from water contamination at high hydrostatic pressures. In addition, they are applied in the fiber drawing process and therefore provide immediate protection against flaw initiation.

#### D. OPTICAL CABLES: A SOLUTION

Optical fibers are theoretically stronger in tension than steel wire and even in practice are nearly as strong. Figure 8 shows the stress-strain relationship for these two materials. To compute the proof strength, the actual load that the fiber can support, the tensile strength must be multiplied by the cross sectional area for a given strain. For the ITT T-1211 fiber with cladding diameter of 125  $\mu\text{m}$  the proof strength is 1.9 pound-force which is not an ideal upper limit to have on a communications cable. The low proof strength is due to the small size of optical cable, only 2.5 times the size of a human hair. The solution to the problem is cabling the fiber with another material that serves as the load bearing element. As noted earlier, glass fiber is subject to stress corrosion only when stressed in the presence of an active environment such as water. Thus the additional load bearing element will not only add needed proof strength but also prevent stress corrosion.

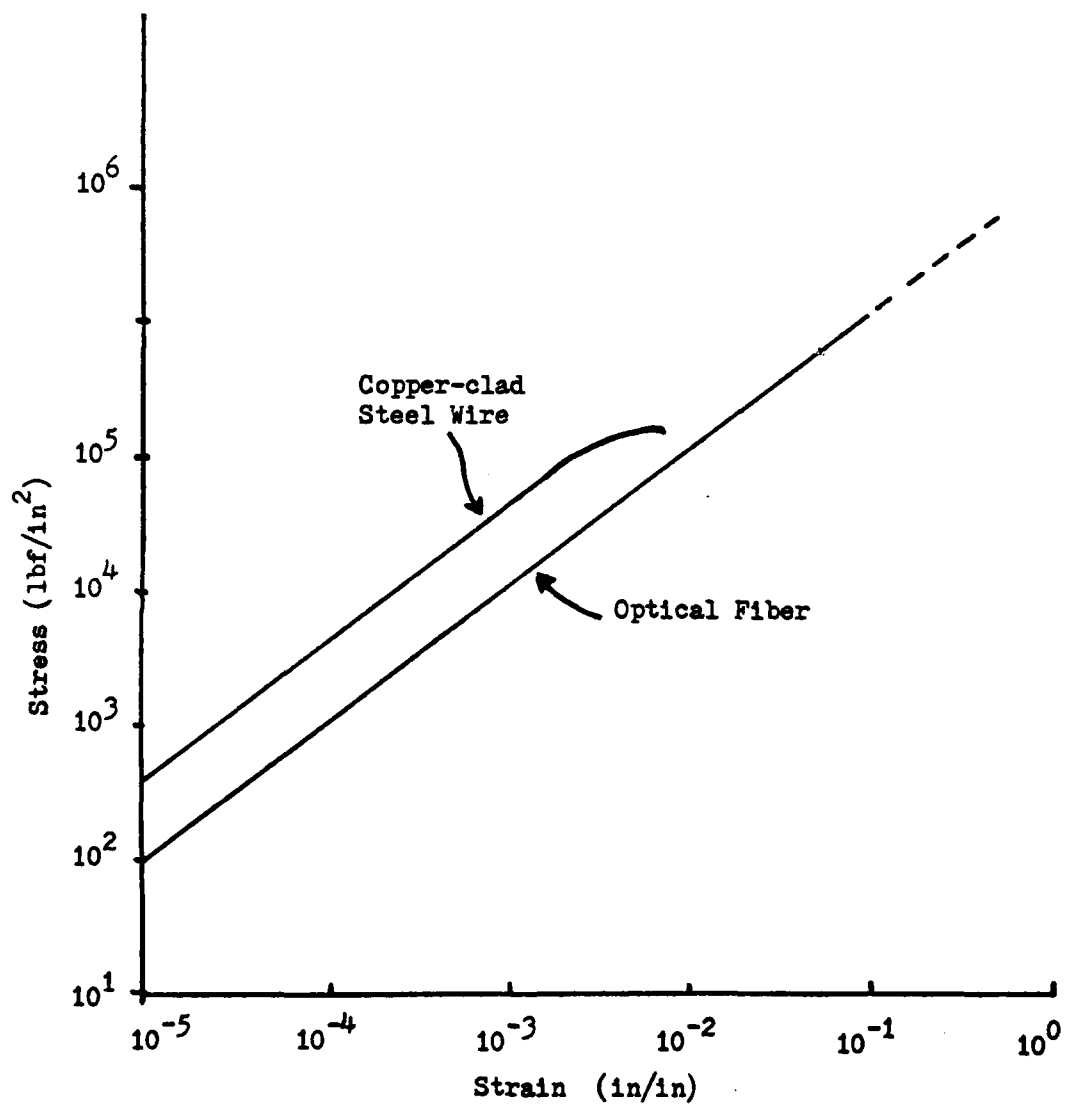


Figure 8. Stress vs Strain for Optical Fibers and Copper-clad Steel Wire

Several materials including copper-clad-steel, Kelvar 49, and S-glass have been successfully used in cabling optical fibers and achieving the desired proof strength. Extensive work in this area has been done by George Wilkens [11, 12] at Naval Ocean Systems Center, Hawaii.

In designing optical cables it is convenient to limit cable and thus fiber strain rather than pull strength. Glass fibers have ultimate strains of near ten per cent but often fail at less than one per cent. Ideally then, a strength member is needed that increases proof strength while limiting proof strain to less than one per cent.

To insure the fiber is not strained beyond the established limit, the strength members must take up the strain first. The relationship used to insure this is  $\sum E_i A_i \gg N E_f A_f$  (3) where  $E$  is Young's modulus,  $A$  is the cross sectional area,  $N$  is the number of fibers,  $i$  represents the strength members and  $f$  is the fiber [5,7]. For a single material load element and a single fiber this equation reduces to  $E_i A_i \gg E_f A_f$  (4). Since most materials have a Young's modulus less than the silica glass used in glass fibers the cross sectional area of the load element must be significantly greater than that of the fiber. In addition the proof strength ( $T$ ) that results from the cable is related to the proof strain ( $S$ ) by  $T = S \sum_j E_j A_j$  (5) where  $j$  represents each element in the cable. For proper design the strength member should dominate resulting in  $T \approx S E_i A_i$ .

An alternate solution to limiting the strain on the fiber is to place it in the cable in such a manner as the length of the fiber exceeds the length of the cable. This must be done such that under load the other elements in the cable stretch to their limit before the fiber is strained. An evaluation done by Wilkens [11] shows that assembling the fiber in a helix does not solve the strain relief problem. He concludes that strain relief must be achieved through (a) inclusion of load bearing members

(b) cabling the fiber around a larger nonoptical core and/or (c) obtaining fibers with a higher minimum fracture strain.

NOSC, Hawaii, has designed and/or tested several optical cables for undersea applications [12]. These cables were evaluated for use in sea-floor communications, diver support and tethering information gathering devices. These cables utilized steel wire, Kelvar 49 and/or S-glass as the strength members to support a single ITT T-203 (the predecessor to T-1211) graded index optical fiber. One of the cables evaluated, hereafter designated Cable A, was designed and manufactured by ITT for use as a data link between fixed points in which electrical power must be supplied by the cable. The composition of Cable A is shown in Fig. 9 and pertinent data is listed in Table II. Of particular interest is the proof strength of 132 lbf, a 7000 per cent improvement over the uncabled glass fiber. Two tests of interest which were performed on Cable A were flexure under load and optical performance under load. In the flexure test the fiber was exposed to a  $\pm 28^\circ$  flexure at 20 per cent of the proof strength. Failure occurred on the average after 710,000 cycles. As a comparison a 1.85-mm-diameter cabling-steel wire failed consistently in 2000 - 2500 flexure cycles. In the optical performance test the cable was loaded up to 40 per cent of the proof strength while attenuation of an optical signal was measured. The results, shown in Fig. 10, indicate that up to 14 per cent of the proof strength attenuation actually decreased and even at the 40 per cent level was only equal to the original attenuation of the unloaded cable.

The copper-clad steel wires in Cable A serve a dual function. As has been shown, they serve as the cable's primary strength member increasing proof strength nearly 7000 per cent. In addition, they can provide the necessary power carrying capability not available with an optical fiber.

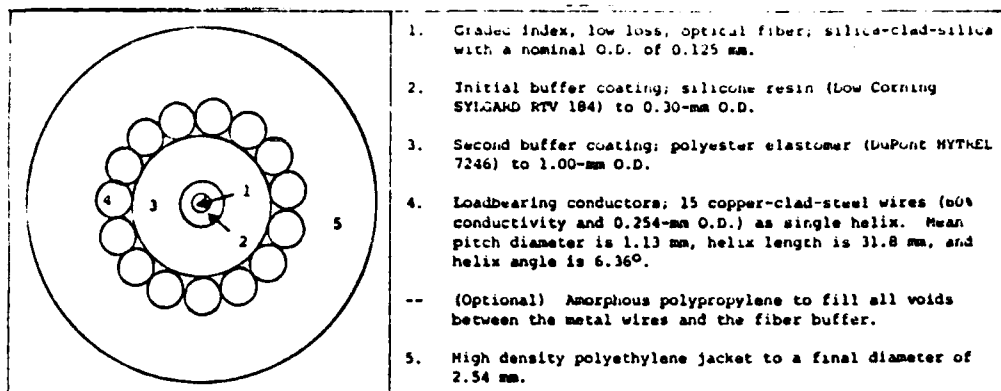


Figure 9. Cable A Composition

CABLE A

Component	Specific Gravity	Cross Section (cm <sup>2</sup> )	Weight (kg/km)	
			In Air	In Seawater
1	2.2	.000128	.027	.014
2	1.05	.000584	.062	.002
3	1.25	.007147	.895	.161
4	8.15	.007600	6.200	5.415
-	0.85	.000300	.026	-.005
5	1.0*	.04920	3.492	-.087
Total	2.12	.050669	10.702	5.500

Specific Gravity	2.12
Ultimate Tensile Strength (copper-clad steel wire)	110 klbf/in <sup>2</sup>
Ultimate Strain	.79%
Proof Strength	132 lbf
Weight In Air	22.8 lb/NM
Weight In Seawater	11.7 lb/NM
Cable Modulus	13 NM
Specific Gravity Relative To Seawater	2.06

\* Several coatings are available for use in submarine cables. These include Polyethylene (.95), Polyvinyl Chloride (1.30), and Polyurethane (1.11).

TABLE II. CABLE A CHARACTERISTICS

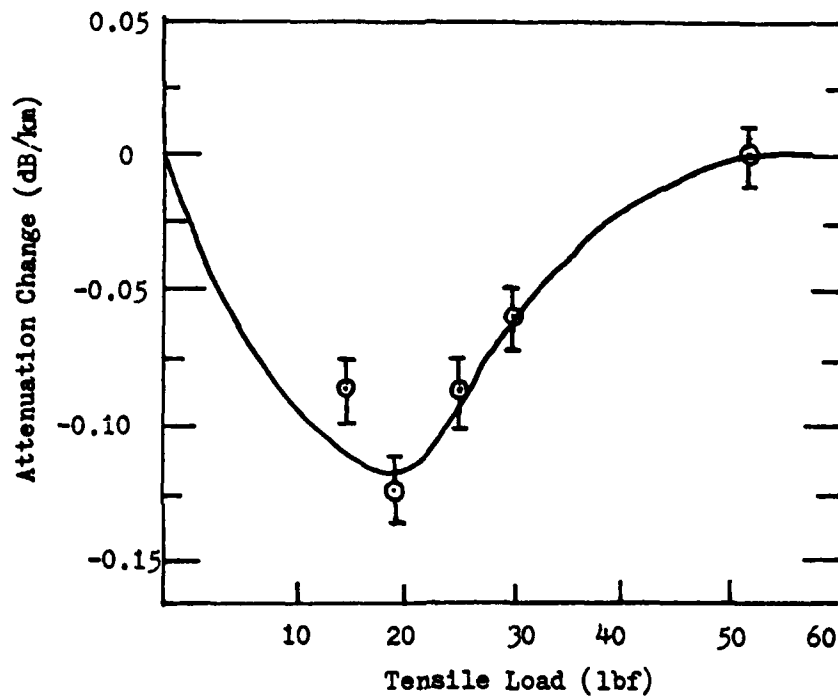


Figure 10. Cable A Performance Under Load



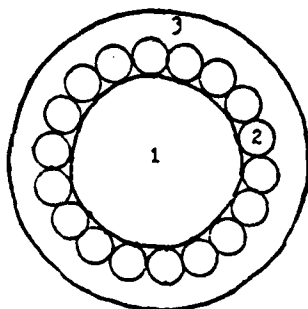
The cable resistance is 38 ohms/km and can support an applied voltage of up to 750 volts at a 1930 V/mm stress level. The jacket has a resistance of nearly 800 megohm/km.

Cable A has been shown to have a proof strength of 132 lbf resulting in a cable modulus of nearly 13 NM. This is accomplished at a cost of an increase in ten times the weight in air, 30 times the weight in water, and two and a half times the diameter of the buffered fiber. In spite of the improved strength of Cable A over the T-203 fiber the cable must be armored if it is to be capable of surviving abrasion and various other environmental hazards on the ocean floor. Any amount of armoring can be applied to Cable A that is desired, but only with the drawback of increased weight and diameter. An example of Cable A with armor is shown in Fig. 11. The armored cable has 18 strands of .02 in. copper-clad steel surrounded by a polyethylene jacket. The jacket can be treated with chemicals to make it distasteful to sea life. Table III provides the pertinent data on the armored cable. The proof strength for the cable was computed as

$$T \approx SE_1 A_1 = .0079 \times (14 \times 10^6 \frac{\text{lbf}}{\text{in}^2}) \times (6.83 \times 10^{-3} \text{ in}^2) = 755 \text{ lbf.} \quad (5)$$

The armor protection increases proof strength nearly sixfold but at a cost of increase in weight (9.3 times the weight in air and 10.8 times the weight in water) and diameter (two times) over Cable A. Also, with the armoring, the cable's modulus is reduced from 13 NM to less than six NM.

For the optical fiber cables to be useful in an ocean bottom application it is necessary that they have sufficient weight to sink to the bottom and bury in the sand. Any object that has a specific gravity relative to sea water of greater than two will accomplish this. Both Cable A and the armored version of Cable A have specific gravities greater than the minimum



1. Cable A
2. Armor: 18 copper-clad-steel wires (.02-in. O.D.) as single helix.
3. High density polyethylene jacket to a final diameter of .2 in.

Figure 11. Armored Cable A Composition

Armored Cable A

Component	Specific Gravity	Cross Section (cm <sup>2</sup> )	Weight (kg/km)	
			In Air	In Seawater
1	2.12	.05067	10.702	5.500
2	8.15	.03648	29.731	25.992
3	1.0	.11553	11.553	-.289
Total	2.57	.20268	51.986	31.203

Specific Gravity	2.57
Ultimate Strain	.79%
Proof Strength	755 lbf
Weight In Air	212.2 lb/NM
Weight In Seawater	127.4 lb/NM
Cable Modulus	6 NM
Specific Gravity Relative to Seawater	2.5

TABLE III. ARMORED CABLE A CHARACTERISTICS

(2.06 and 2.50 respectively). The greater the specific gravity the more rapid the sink and bury process. Therefore armoring can improve the ability of Cable A to accomplish this. Because of the light weight of the optical cables divers could install them, including burying, thus rapidly insuring proper cable positioning and survivability.

Attenuation in a glass fiber is dependent on the quantity of Hydroxyl ions,  $\text{OH}^-$ , present when the fiber is being manufactured. A sea water environment causes stress corrosion in an optical fiber which is under stress but does not increase attenuation. The light path in a fiber is confined primarily to the core. If the sea water should reach the core of a glass-on-glass fiber, the cladding would either have had to fracture and the cable failed, or possibly permeated through the cladding, which would take much longer than the lifetime of the system.

Other factors which cause attenuation in optical fibers include microbends and small radius of curvature bends. Both of these cause radiation of higher order modes and mode coupling of lower to higher order modes. Microbends are due to small surface discontinuities which can result when a fiber is cabled. Larger bends occur when an optical cable is reeled and possibly when installed. Good cabling design and installation eliminate these problems and no additional attenuation is added to the fiber. This is the case with Cable A as reported by Wilkens [12]. Cabling induced attenuation on Cable A as compared with T-203 was measured to be no more than 0.4 dB/km and was often negative. As was shown in Fig. 9 when Cable A was stressed, as it would be in a hydrostatic environment, attenuation actually decreased. This was due to the straightening of the fiber under stress which reduced existing microbends.

A great deal of research has been devoted to developing optical fiber connectors for land line communications but not for undersea applications.

Alignment of the optical fibers by a connector is critical and the most difficult problem to overcome. For maximum transfer of light the fibers must be axially displaced no more than a few microns. In a sea water environment, particles could become seated between fiber ends within a connector while the connection is being made. The compression stress from these particles in the presence of water would result in damage to the fiber ends, leading to increased attenuation or fiber fracture. Optical fiber connectors developed for land use relieve tensile stress but generally not compression stress. An undersea connector would ideally then isolate the fiber ends from the sea water and light transfer would have to be made through some type of lens. Until a time when such underwater connectors are developed and marketed the optical cable would have to be permanently connected to the electronics container. Several schemes that have been used to connect a fiber through a bulkhead providing a hermetic seal between sea water and electronics are depicted in Figs. 12 - 14. In each case an epoxy impervious to water is used to seal the glass fiber insuring a water tight seal. In shallow water these bulkhead connectors have proven successful. Research is presently being conducted by NOSC, San Diego, into bulkhead penetrators capable of surviving at high hydrostatic pressures. NOSC is testing the concept of using a lens mounted in the bulkhead to interface fibers in the low and high pressure environment. Figures 15 - 16 depict this concept. The lenses are composed of a Selfoc rod which behaves like a graded index fiber in that it bends the various light modes back toward the axis of the rod. Selfoc rods cut to the proper length will collimate and refocus the light from fiber to fiber with losses of less than one decibel. If this work is successful, the Selfoc rod lens could be developed for undersea optical connectors and detachable bulkhead connectors.

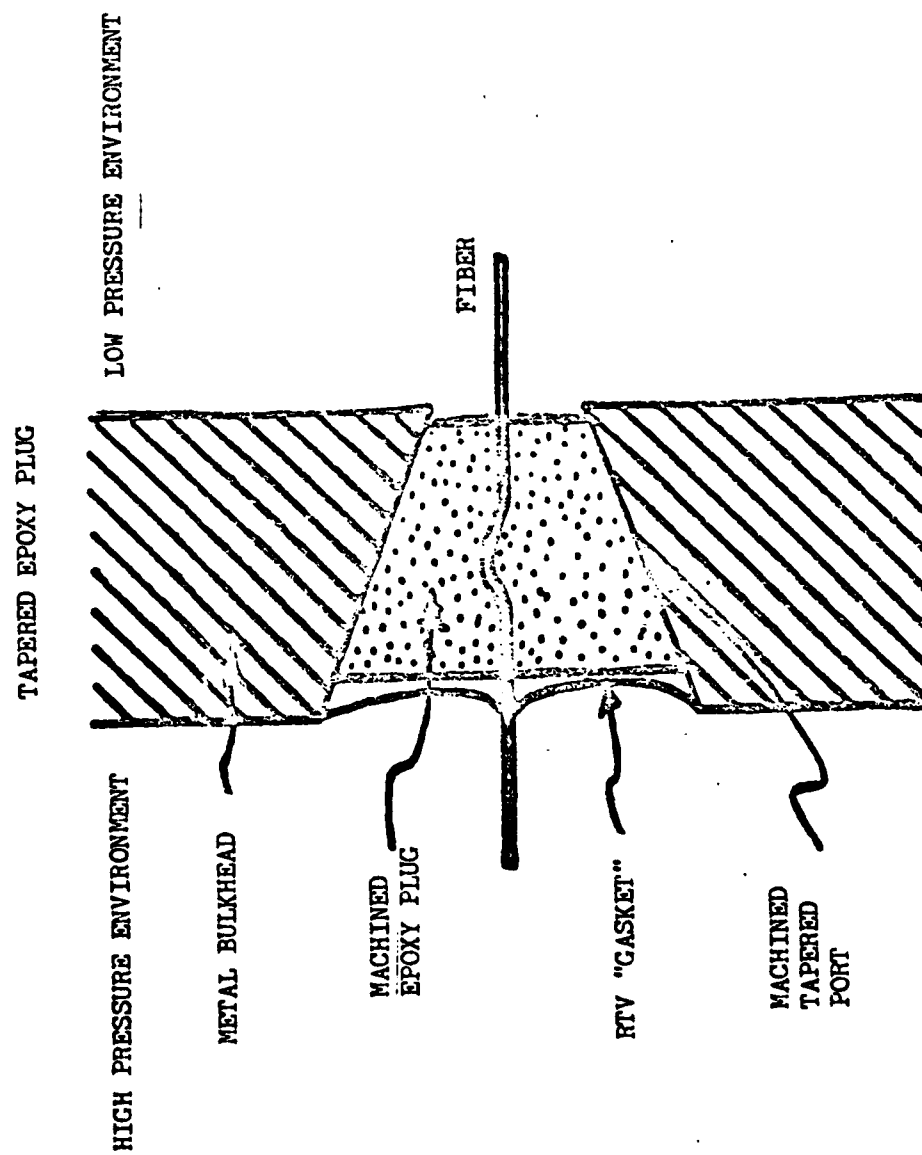


Figure 12. Tapered Epoxy Plug Bulkhead Penetrator

PRESSURE PENETRATOR EPOXY FILLED HYPO NEEDLE

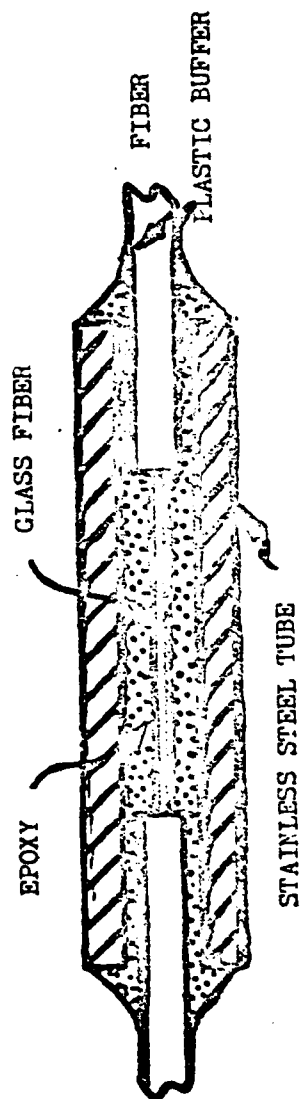


Figure 13. Epoxy Filled Hypo Needle Bulkhead Penetrator

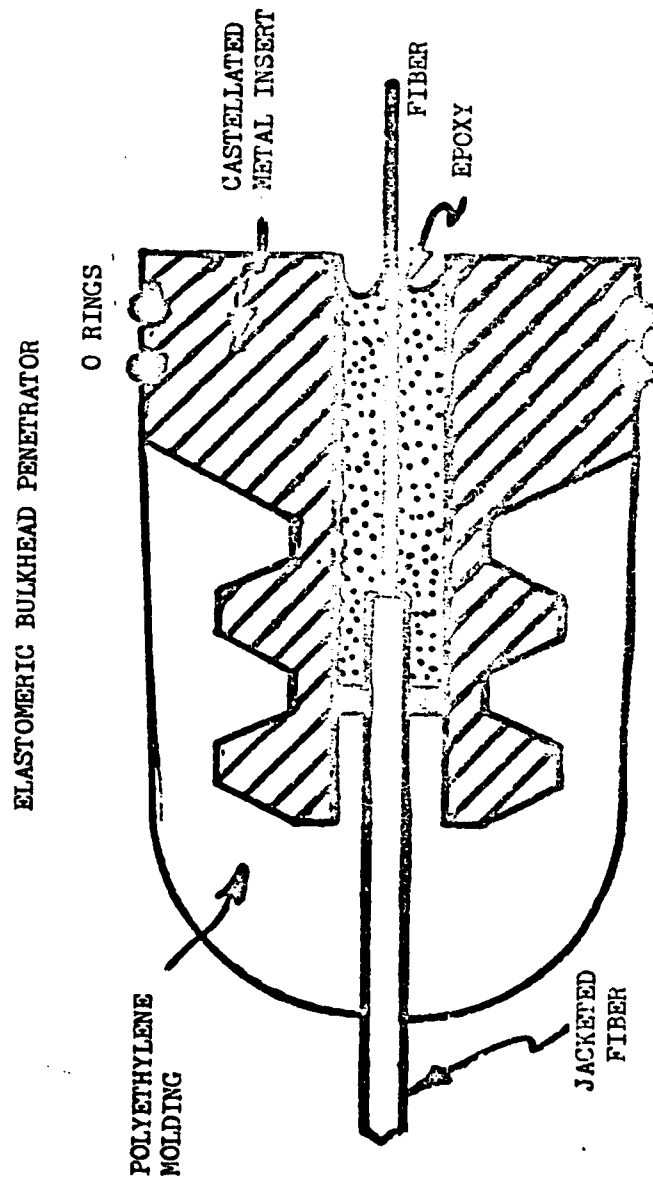


Figure 14. Elastomeric Bulkhead Penetrator

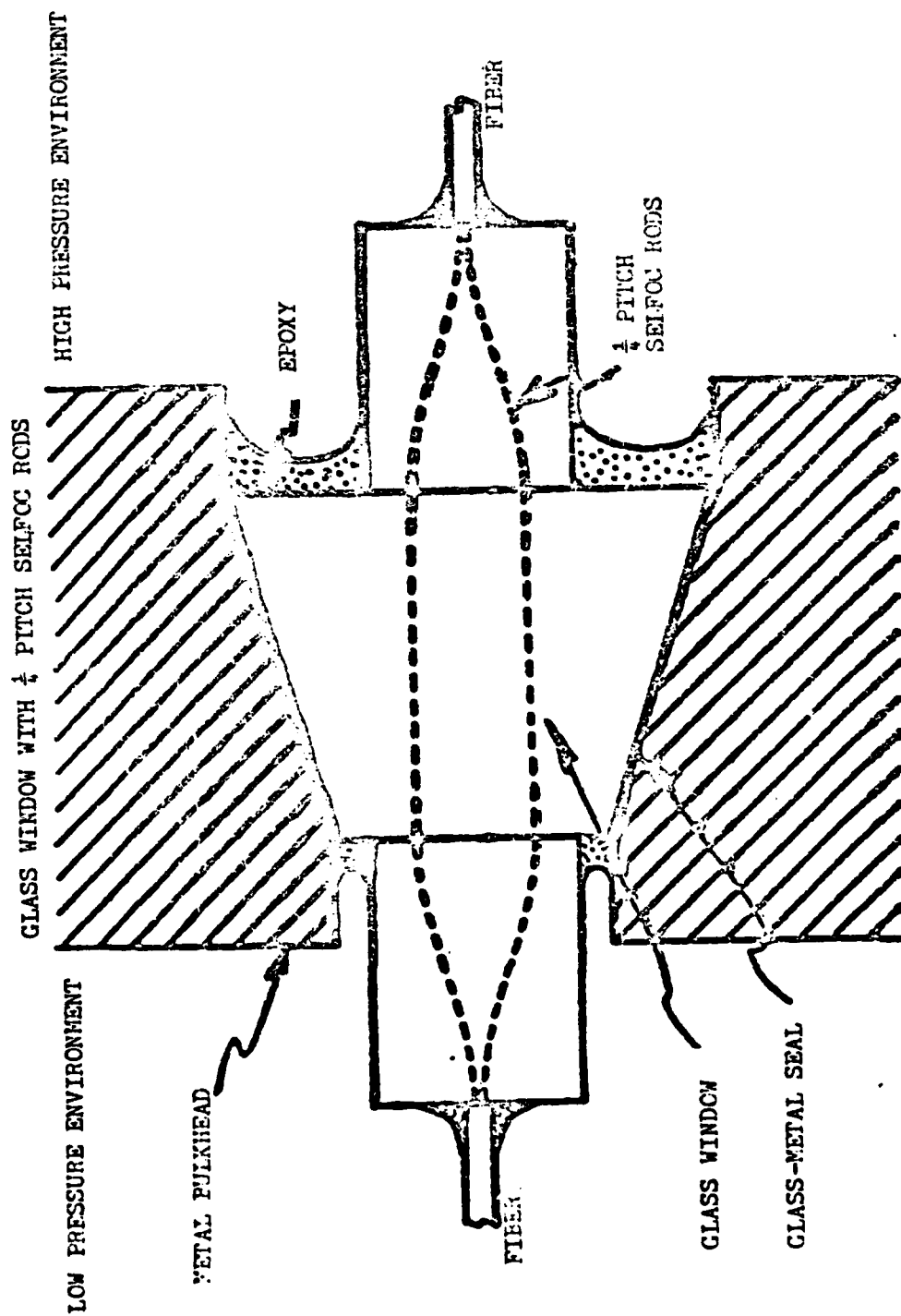


Figure 15. Glass Window With  $\frac{1}{4}$  Pitch Selfoc Rod Bulkhead Penetrator



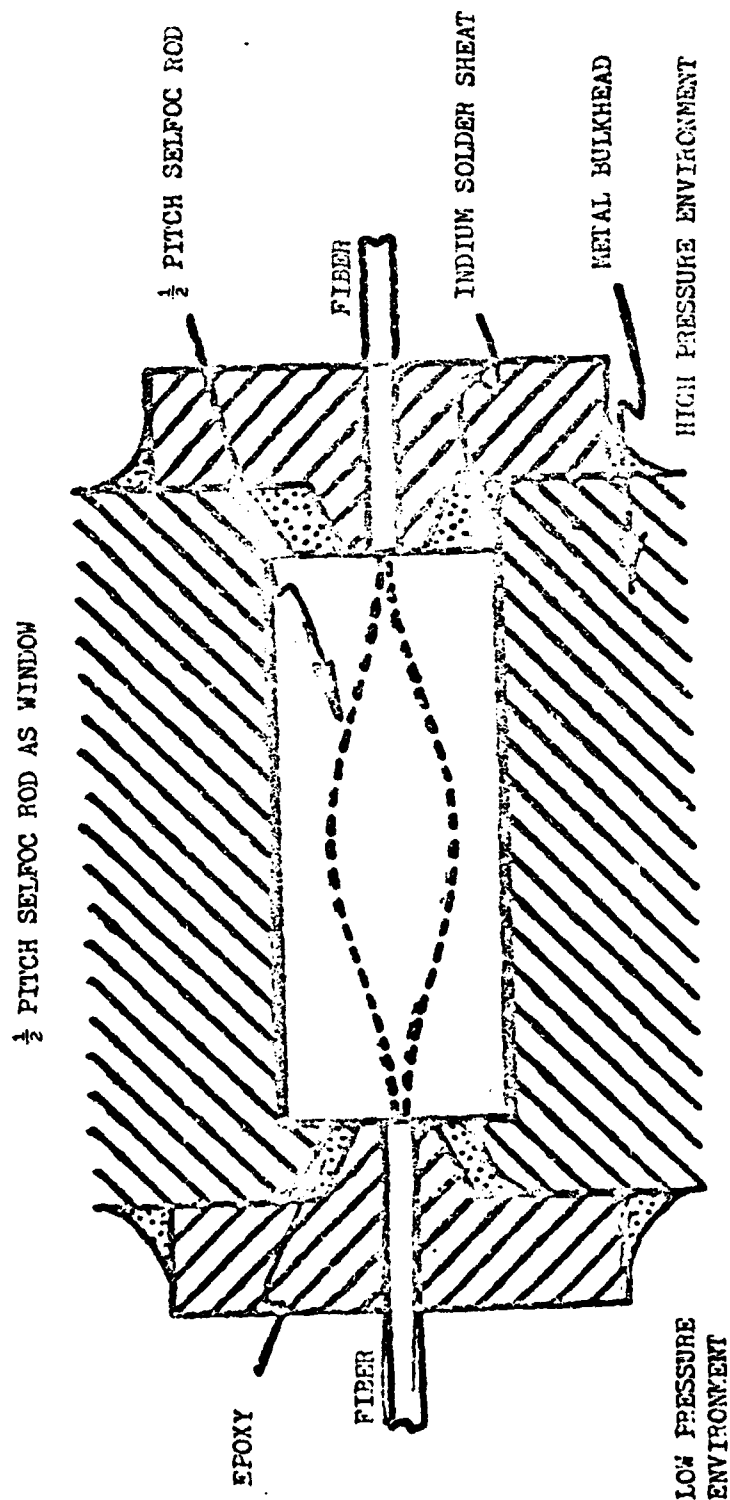


Figure 16.  $\frac{1}{2}$  Pitch Selfoc Rod Bulkhead Penetrator

Optical fiber cables can be manufactured for utilization in the shallow-water range. They will survive the turbulence and abrasion in an ocean environment. The primary area of concern would be in the surf zone where turbulence is at its greatest and the cable is most likely to be fouled by an anchor or troller line. In this region it would be advisable to bury the cable at a safe depth, immobilize the cable by the use of a split iron pipe or split PVC pipe, or a combination of burying and pipe. Since these procedures are normally applied for armored coaxial cable [7], the cost of installation would be no more for fiber than coax (probably less since a smaller diameter pipe could be used) and the survivability for either cable would be the same.

#### IV. OPTICAL SYSTEM ENGINEERING

A fiber optic system is composed of a transmitter, an optical fiber link and a receiver. Engineering a fiber optic system requires the design and/or component selection of a light source, an optical fiber, an optical detector, and signal recovery circuitry. The design and selection process is based on the signal and system parameters which are particular to any one system. What follows is a review of the guidelines for designing a fiber optic link with emphasis on the parameters that are pertinent to the shallow-water tracking range application. An actual finalized link design for the range is not attempted but rather a discussion of the various engineering alternatives and their implications is presented.

##### A. OPTICAL FIBER SELECTION

As with all communication links the driving parameters are signal power and bandwidth. The required strength of the transmitted signal is dependent on the minimum allowable received signal strength and the link losses. A good starting point then is to determine the attenuation and the bandwidth capabilities of the transmission link. In a fiber optic system the link loss is determined by the optical fiber. The bandwidth capability is a function of the light source and detector as well as the optical fiber. Therefore, the first step in engineering fiber optic link is to select an optical fiber. The selection of an optical fiber is dependent on optical parameters and cable strength. Since strength of an optical cable has been previously discussed the optical parameters must now be considered.

Those parameters which effect the fiber's ability to transmit the desired signal include; numerical aperture (NA), refractive index profile, core

diameter, attenuation and intermodal dispersion. Numerical aperture (NA) provides an engineer with a measure of the fiber's ability to accept light. The larger the NA the larger the angle of the cone in which light is accepted. A smaller NA requires more precise alignment between fiber and source as well as fiber-ends in a connector. Unfortunately, fibers with smaller NA also have less attenuation and in long fiber lengths (greater than one km) alignment preciseness is the price that must be paid for low loss. ITT T-1211 fiber has a NA of .23, which is a small value, or an acceptance angle from the axis of  $13.3^\circ$ . There are two types of refractive index profiles, step and graded. The profile determines the intermodal dispersion within the fiber and thus limits the bandwidth capability of the fiber. Single-mode step-index fibers, which allow only one mode, have no intermodal dispersion but have core diameters on the order of five microns, making them extremely fragile and difficult to couple light into. Graded-index fibers have range-bandwidth capabilities on the order of 500 MHz-km while step-index have a capability on the order of 50 MHz-km. Even though the range-bandwidth of the step-index fiber might be sufficient for the shallow-water range, graded-index fibers are commercially available with lower attenuation rates than equivalent step-index fibers. ITT T-1211 is a graded-index fiber with an attenuation of 3.5 dB/km, at  $0.85 \mu\text{m}$ , while ITT's step-index fiber, T-103, has an attenuation of 5 dB/km. Attenuation at  $1.25 \mu\text{m}$  is approximately 2 dB less for both types of fiber. Core diameter, like NA, effects the required precision of alignment to maximize light coupling. Larger core diameter generally means higher attenuation so once again there is a trade off.

Although graded-index optical fibers for long haul communications have not yet been standardized, the trend is towards 50 - 70  $\mu\text{m}$ . T-1211 fiber has a 55  $\mu\text{m}$  core. Fiber attenuation is the primary cause of system loss in present fibers. However, as fibers are developed and become available

that approach the expected lower limit of about .2 dB/km, the primary system loss will become fiber-to-fiber and fiber-to-source connectors which in quality connections are about .5 dB and 4 dB respectively. Intermodal dispersion, which is a function of the index of refraction profile, is specified in nanoseconds per kilometer (ns/km) and determines the range-bandwidth capability of the fiber. The approximate electrical bandwidth can be computed by

$$\text{Range-BW (MHz-km)} \approx 222 \div \text{Intermodal Dispersion} \quad (6)$$

T-1211 fiber has an intermodal dispersion of 0.3 which gives an electrical bandwidth-range capability of 740 MHz-km or 400 MHz-NM.

From the shallow-water range parameters and the specifications on T-1211 fiber, typical optical fiber link attenuations were computed. A simple formula for computing the link loss in dB is

$$\text{Loss} = A_F l + A_{SF} + A_{FD} + n A_{FF} + A_M \quad (7)$$

where

- $A_F$  = optical fiber attenuation (dB/km)
- $l$  = length of fiber (km)
- $A_{SF}$  = source-to-fiber coupling loss (dB)
- $A_{FD}$  = fiber-to-detector coupling loss (dB)
- $A_{FF}$  = fiber-to-fiber connector loss (dB)
- $n$  = number of connectors
- $A_M$  = attenuation margin for temperature effects, time-dependent component degradation and unexpected excess loss.

Optical fiber attenuation ( $A_F$ ) is dependent on the light wavelength used. Values for T-1211 fiber are 3.5 dB/km at 0.85  $\mu\text{m}$  and 1.5 dB/km at 1.25  $\mu\text{m}$ . Source-to-fiber loss is accounted for in source power output when

a pigtail is utilized (discussed in the following section on sources) and is assumed to be zero. Fiber-to-detector coupling loss is typically one dB. Fiber-to-fiber connector losses are typically about .5 dB but for a connection through a lens as in an underwater application a 1.5 dB loss is assumed. The number of connectors is two, one at each end of each optical link. Therefore, the link loss for a system operating at 850 nm reduces to

$$\text{Loss} = (3.5 d + 4 + A_M) \text{ dB} \quad (7)$$

and at 1.25  $\mu\text{m}$  reduces to

$$\text{Loss} = (1.5 d + 4 + A_M) \text{ dB} \quad (7)$$

where  $d$  is the distance of the optical link in km. Utilizing these formulas and the cable links of 1.78 to 5.44 km between hydrophone and multiplexer and 13 km between multiplexer and Kalaloch, the various link losses, excluding loss margin, were tabulated in Table IV.

The bandwidth requirement placed on the optical fiber will depend on the signal format selected. The two alternatives for signal format are analog and digital. For either case the maximum bandwidth requirement will be on the cable carrying the multiplexed signal. For the analog signal, using frequency division multiplexing (FDM), this equates to 50 kHz per channel, plus a 5 kHz guard-band for each of 16 channels or 880 kHz. Because of intermodulation products the actual bandwidth requirement is closer to one MHz. For the digital case, assuming worst case of eight bit pulse code modulation (PCM) of the baseband signal, this equates to 25 kHz times the Nyquist sampling rate of two times eight bits per sample or 400 kbps. Using time division multiplexing (TDM) and sampling each of the 16 channels plus one synchronizing channel at the Nyquist rate the total bandwidth is 13.6 MHz.

T-1121 Optical Fiber

<u>Link Distance (km)</u>	<u>Loss at 0.85 <math>\mu</math>m (dB)</u>	<u>Loss at 1.25 <math>\mu</math>m (dB)</u>
1.78	10.2	6.7
5.44	23.0	12.2
13.0	49.5	23.5

TABLE IV. ATTENUATION CALCULATIONS

If the signal at the hydrophone is digitized without converting down to baseband these values are increased by a factor of two. Since T-1211 fiber has a bandwidth capability of 740 MHz-km, it is capable of supporting the PCM signal for a distance of greater than 50 km. Therefore, for optical fibers in the shallow-water range application, bandwidth capability is not a problem and signal attenuation is the driving engineering parameter.

#### B. OPTICAL SOURCE SELECTION

The two primary light sources for fiber-optics communication systems are the high radiance LED and the injection laser diode. The engineering parameters for both which determine bandwidth and power are modulation scheme, spectral width, beam width, lifetime, power output, center frequency and cost.

The LED and the laser diode are directly modulated by varying the current to the anode. Both devices behave fairly linearly at constant temperature and can therefore be modulated with analog as well as digital signals. The maximum rate of modulation is a function of minority carrier lifetime and recombination rate. LEDs are capable of modulation rates of several hundred MHz while laser diodes are capable of GHz.

Material dispersion is the limiting factor for bandwidth in any optical fiber. Various light frequencies, or wavelengths, traverse from one end of the fiber to the other at different speeds causing pulse dispersion. The degree of pulse spreading is a function of length of the fiber and the spectral width of the source. LEDs have spectral widths in the range of 400 nm. This large bandwidth of light limits an LED to a typical modulation rate of 50 Mb/s for a five km fiber link. Laser diodes, because of the coherent quality of their output, have spectral widths on the order of 40 nm and are capable of modulation rates of hundreds of MHz over long fiber lengths.



The beamwidth of an optical source is a measure of how fast the light output spreads and together with the NA of the fiber determines how much light is coupled into the fiber. Optical source-to-fiber coupling loss accounts for a major portion of any system's loss. LEDs have large beamwidths while laser diodes have much smaller ones. Because of the precision alignment necessary, typical losses of 15 dB were encountered in the past when source-to-fiber couplings were made. To overcome this problem, optical source manufacturers offer sources with pigtails, a short length of fiber, already attached, thus minimizing the coupling loss. Still the minimum coupling loss is close to four dB.

The lifetime of an LED is typically greater than  $10^5$  hours. Laser diodes have recently been reported with lifetimes of  $10^5$  hours, however to limit turn-on time and thus obtain maximum response time the laser diode must be biased to threshold which tends to reduce the lifetime. Still a value of greater than  $2 \times 10^4$  hours is readily available and more than sufficient for the shallow-water range.

For the shallow-water range it has been determined that link attenuation is the driving design parameter. Therefore, optical power output is the primary parameter of interest for source selection. LEDs have typical output power levels of hundreds of microwatts while laser diodes have typical values in the tens of milliwatts.

Fiber attenuation was shown to be approximately two dB/km less at a wavelength of  $1.25 \mu\text{m}$  than at  $0.85 \mu\text{m}$ . Unfortunately, most of the optical sources that have been developed are composed of GaAlAs and have a spectral peak near  $0.85 \mu\text{m}$ . A great deal of research is being done with other materials, such as InGaAsP/InP, which operate near  $1.27 \mu\text{m}$  and even materials at  $1.55 \mu\text{m}$  where silica fibers have their lowest attenuation.

The least expensive optical source available is the LED ( $0.85 \mu\text{m}$ ). LEDs are also inexpensive to operate since they require a minimum amount of temperature compensation circuitry. Laser diodes ( $0.85 \mu\text{m}$ ) cost twice as much (or more) as LEDs and require accurate temperature compensation circuitry for linear operation. Sources operating at the higher wavelengths have recently become commercially available but are extremely expensive ( $\sim \$1000$ ) because of research and development costs.

For the purpose of computing sample values for the shallow-water range, two sources are assumed to be available. These are the Laser Diode IRE-160FB high radiance LED and the RCA 86000E laser diode. Typical data for each of these sources is presented in Table V.

### C. OPTICAL DETECTOR SELECTION

The PIN photodiode and the avalanche photodiode (APD) are the optical detectors commonly used in fiber-optics applications. Both devices are reverse-biased photon detectors. The engineering parameters for these devices are device capacitance, reverse-bias speed, responsivity, noise equivalent power (NEP), dark current, detector surface area, center frequency and cost.

The model for a photodiode is a current source in parallel with a capacitance. These devices emit a quantity of electrons that is statistically proportional to the quantity of photons incident upon them. The efficiency of this operation is typically on the order of 50 per cent. The device resistance ( $50 \Omega$ ) is small in relation to the load resistance and can be ignored. The junction capacitance and package capacitance of the device must be considered in determining the speed of operation and therefore bandwidth capability. For both the PIN diode and APD these capacitances are on the order of two picofarads resulting in a device capacitance on the order of four picofarads.

Both the PIN diode and the APD have reverse-bias rise and fall times

	<u>IRE-160FB (LED)</u>	<u>RCA 86000E (Laser Diode)</u>
Spectral width	40 nm	4 nm
Optical Power Out (available from pigtail)	100 $\mu$ W (-10 dBm)	4 mW (+6 dBm)
Rise time	14 ns	1 ns
Peak wavelength	.82 $\mu$ m	.82 $\mu$ m
Forward Voltage (at 100 mA)	2.2 v	2 v
Cost (with pigtail)	\$325.00	\$615.00

TABLE V. OPTICAL SOURCE CHARACTERISTICS

on the order of one nanosecond. They therefore are capable of detecting bandwidths of several hundred MHz.

Responsivity provides the engineer with a measure of current output for a given optical power input and is given in amps per watt (A/W). For the PIN diode responsivity ( $r$ ) is related to device efficiency by

$$r = \text{efficiency} \times \text{wavelength} \div 1.24 \quad (8)$$

and is therefore typically about 0.4 A/W. APDs provide current gain through avalanche multiplication. The gain is dependent on temperature and reverse-bias level and responsivity typically ranges from 5 A/W to 250 A/W.

Noise equivalent power (NEP) is a measure of the level of optical power incident on a detector required to produce a unity rms signal-to-noise ratio. NEP is a bandwidth normalized value with units watts per  $\text{Hz}^{\frac{1}{2}}$ . It is computed for a given wavelength, frequency, temperature and bandwidth which must be considered when comparing detectors from various manufacturers. NEP provides the engineer with a method of comparing the quantum limited noise (shot noise) of various detectors.

Dark current is that current which flows in the device when no light is incident upon the detection area and therefore manifests itself as noise. Typical values for PIN diodes are about two nanoamperes. For APDs the dark current is dependent upon gain and thus bias level. Typical values range from 10 nA at low bias to 200 nA at avalanche-threshold bias.

Detector surface area should be chosen such that it is much larger than the surface area of the fiber's core. This minimizes fiber-to-detector coupling loss and makes alignment easier since the cone of light emitted from the fiber (determined by the NA of the fiber) will be entirely incident on the detection area. Most detectors are available with detection area greater than  $1 \times 10^{-3} \text{ cm}^2$  which is sufficient for the 55  $\mu\text{m}$  core ( $3 \times 10^{-5} \text{ cm}^2$ )

surface area).

Cost and center frequency considerations for optical detectors are the same as for sources. Again the most common devices operate near  $0.85 \mu\text{m}$  but research is being done at higher wavelengths. PIN diodes ( $0.85 \mu\text{m}$ ) can be purchased as cheaply as one dollar but more typically cost near \$20. APDs are very difficult to manufacture which drives the cost up to several hundred dollars each. The avalanche diodes also require high bias voltages ( $\sim 300 \text{ v}$ ) and accurate temperature control while PIN diodes operate with low bias ( $\sim 15 \text{ v}$ ) and are much less temperature sensitive.

Again, for the purpose of computing sample values for the shallow-water range, two detectors will be assumed available. These are the HP-4205 PIN Diode and the RCA-C30908E avalanche photodiode. The engineering parameters for each is listed in Table VI.

The minimum power required at the detector is computed using the device's design parameters. Signal power required is specified by the desired signal-to-noise ratio (SNR) and the detector noise. For an optical detector, shot noise is the quantum limit. The shot noise ( $P_n$ ) is computed by

$$P_n = NEP \cdot B^{\frac{1}{2}} \quad (9)$$

where B is bandwidth and the noise current ( $i_n$ ) is computed by

$$i_n = P_n \cdot r. \quad (10)$$

The noise power and noise current for the selected detectors are listed in Table VII. The quantum noise current for both devices at the specified bandwidth is less than the manufacturer's specified dark current. Because dark current ( $I_d$ ) is considered a contributing factor to the shot noise, the

	<u>HP-4205 (PIN DIODE)</u>	<u>RCA C30908E (APD)</u>
Capacitance	.7 pf	1.6 pf
Reverse bias speed	1 ns .	.5 ns
Responsivity	.5 A/W	77 A/W (@220 v) 10 A/W (@150 v)
NEP	$1.4 \times 10^{-14} \text{ W/Hz}^{\frac{1}{2}}$	$3 \times 10^{-15} \text{ W/Hz}^{\frac{1}{2}}$
Dark Current	.15 nA	15 nA (@220 v) 12 nA (@150 v)
Surface Area	$3 \times 10^{-3} \text{ cm}^2$	$.625 \times 10^{-3} \text{ cm}^2$
Peak Wavelength	0.80 $\mu\text{m}$	0.82 $\mu\text{m}$
Bias Voltage (Breakdown)	50 v	225 v
Cost	\$30.00	\$300.00
Efficiency ( $\eta$ )	75%	77%

TABLE VI. OPTICAL DETECTOR CHARACTERISTICS

noise current is assumed to be at least as high as the dark current. Since the dark current figure supplied by the manufacturer is a maximum, the assumption is a conservative one. The signal current ( $i_s$ ) required is computed by

$$i_s = I_d \cdot \text{SNR} . \quad (11)$$

A required SNR of 10 is assumed. From the required signal current the minimum signal power is determined by

$$P_s = i_s \div r . \quad (12)$$

Because the calculated shot noise current for both devices (Table VII) was below the specified dark current for all bandwidths of concern, the signal power does not depend on bandwidth. Using the above equations the minimum signal power for the PIN diode is 3nW (-55 dBm) and for the APD is 2nW (-57 dBm). It appears that no significant advantage is obtained by using the ADP. However, it will be seen that in designing the receiver circuit the ADP offers a major advantage over the PIN diode.

#### D. OPTICAL LINK DESIGN

From the design parameters of the optical source, waveguide and detector, the optical link can be designed. Assuming a fiber is chosen, the optical loss can be computed. From the optical loss, a source and a detector are then selected such that a specified attenuation margin ( $A_m$ ) is satisfied. Using the components specified in the previous sections, and assuming a minimum required attenuation margin of 6 dB, link designs are given in Fig. 17 and Fig. 18.

The computations for the optical link between the hydrophone and multiplexer are given in Fig. 17. The maximum distance of fiber, which results

	<u>HP 4205</u>	<u>RCA C30908E</u>
<u>B = 400 kbps</u>		
$P_n$ (pW)	8.85	1.9
(dBm)	-80.0	-87.0
$i_n$ (pA)	4.425	146.0
<u>B = 15 Mbps</u>		
$P_n$ (pW)	58	12
(dBm)	-72	-79
$i_n$ (pA)	29	900

TABLE VII. OPTICAL DETECTOR NOISE CALCULATIONS



in maximum loss, is 5.44 km. In this figure the power levels computed for the various optical devices (Table IV, Table V, and the end of section IV-C) have been compiled to determine the available power margin for any possible combination of source and detector. From Fig. 17 it can be seen that the LED with an output of -10 dBm and the PIN diode which requires a minimum received power of -55 dBm allow a link loss of 45 dB. Because the fiber loss including connector was only 23 dB, an attenuation margin of 22 dB results. Thus, the inexpensive LED plus PIN diode combination is more than sufficient for the hydrophone to multiplexer link.

The calculations for the 13 km optical link between the multiplexer and the shore are provided in similar fashion in Fig. 18. In this case the LED does not provide sufficient power out and a laser diode is required. It appears that the laser diode can be used with either the PIN diode or APD and sufficient attenuation margin is obtained.

#### E. OPTICAL MODULATOR DESIGN

The optical sources used for fiber optics are typically modulated by varying the anode current. For most devices the current is typically modulated between a minimum of five milliamps and a maximum of 150 milliamps. Any electronic circuit that can source or sink current can be used to modulate the optical source.

For analog modulation the current-controlling circuit must provide an output that is linear with respect to the input signal. In addition, the optical source must be biased to a quiescent level (e.g. 70 mA) and modulated about this point (e.g. from 10 mA to 130 mA). Examples of simple analog modulators requiring only an op amp and one transistor are shown in Fig. 19.

For digital (binary) modulation, there is no requirement for linear response since only two distinct current levels are required. In addition,

Maximum Link Length - 5.44 km  
Wavelength - .85  $\mu$ m  
Maximum Bandwidth - 400 kHz  
Fiber Loss - 23.0 dB

LED + PIN                -10 - (-55) = 45 dB  
Margin                    45 - 23 = 22 dB

LED + APD               -10 - (-57) = 47 dB  
Margin                    47 - 23 = 24 dB

Laser Diode + PIN      6 - (-55) = 61 dB  
Margin                    61 - 23 = 38 dB

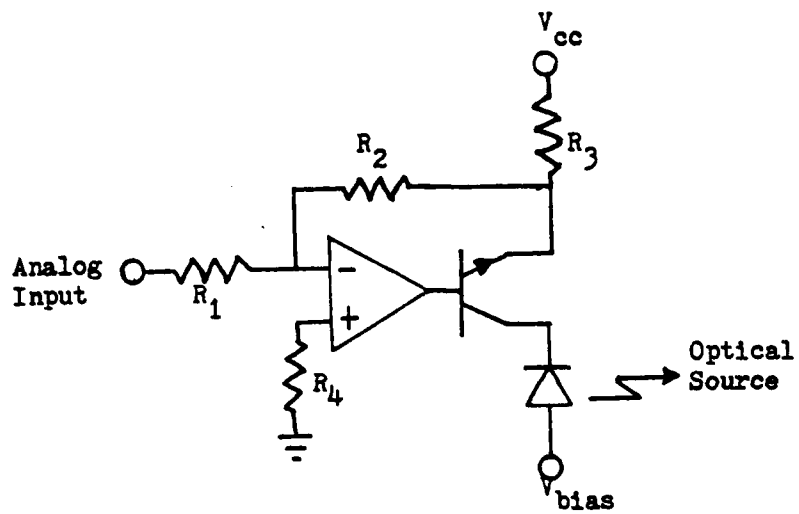
Laser Diode + APD      6 - (-57) = 63 dB  
Margin                    63 - 23 = 40 dB

Figure 17. Attenuation Calculations for  
Hydrophone to Multiplexer Link

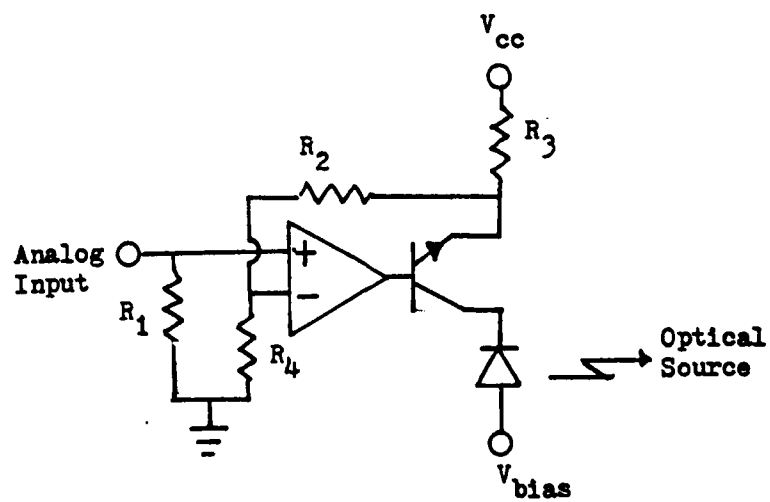
Maximum Link Length - 13 km  
Wavelength - .85  $\mu$ m  
Maximum Bandwidth - 15 MHz  
Fiber Loss - 49.5 dB

LED + PIN	$-10 - (-55) = 45$ dB
Margin	$45 - 49.5 = -4.5$ dB
LED + APD	$-10 - (-57) = 47$ dB
Margin	$47 - 49.5 = -2.5$ dB
Laser Diode + PIN	$6 - (-55) = 61$ dB
Margin	$61 - 49.5 = 11.5$ dB
Laser Diode + APD	$6 - (-57) = 63$ dB
Margin	$63 - 49.5 = 13.5$ dB

Figure 18. Attenuation Calculations for  
Multiplexer to Shore Link



Inverting Modulator



Noninverting Modulator

Figure 19. Analog Optical Modulators

the source need not be biased to a quiescent level (except for a small positive current to preclude complete device turn-off). Two simple TTL compatible digital modulators, one utilizing a discrete transistor and the other a hex inverter IC, are depicted in Fig. 20. The inverter preceding the transistor is necessary for TTL compatibility. With the hex inverter circuit the five paralleled inverters are capable of sinking 20 ma each, thus drawing about 100 ma through the source, while the sixth inverter provides TTL compatibility.

#### F. RECEIVER CIRCUIT DESIGN

The output of the optical detectors discussed earlier was a very small current on the order of nanoamperes. This small value of current is composed of the varying signal current as well as dark current, average signal or shot noise current and background current which are all DC currents that provide noise to the receiver. The receiver must be capable of converting these currents into voltage while adding as little additional noise as possible. Following the current to voltage conversion the receiver must amplify the voltage to a usable level. The noise that is added by the receiver is thermal noise from the load resistor. The expression for SNR from which the receiver circuit is designed is

$$\text{SNR} = \frac{2I_s^2 M^2}{2M^2 [I_b + I_d + I_s] F_q B + \frac{4kTB}{R_{\text{Eqv}}}} \quad (13)$$

where

$I_s$  = signal current (rms)

$I_b$  = background illumination current

$I_d$  = dark current

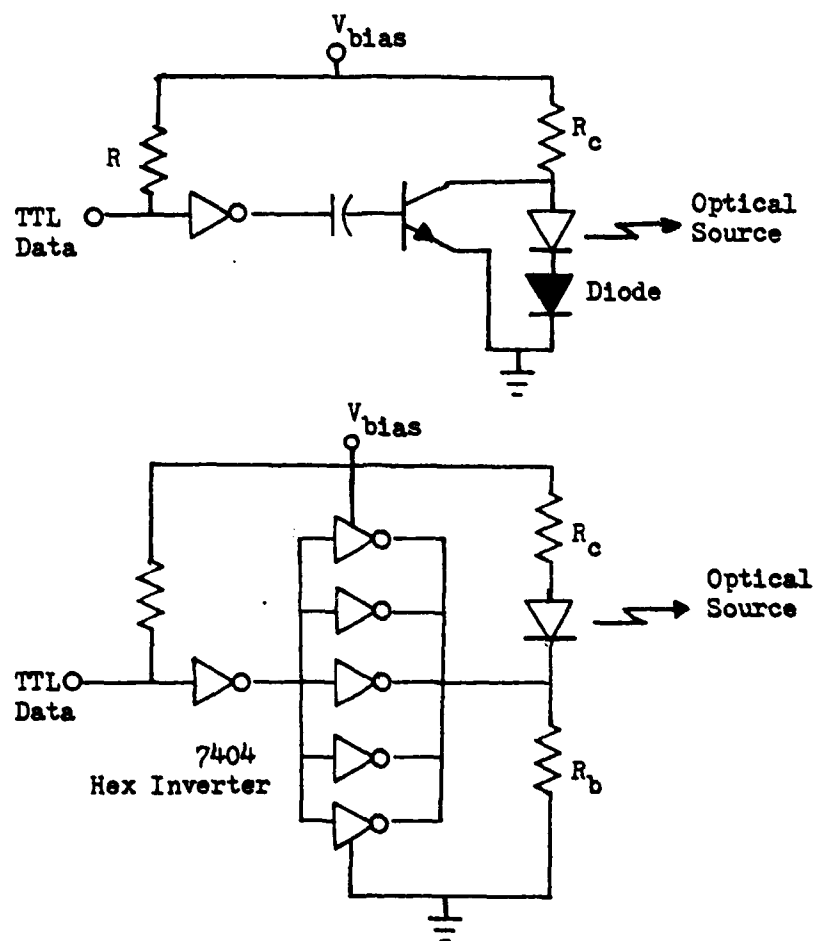


Figure 20. Digital Optical Modulators

- $I_s$  = average signal current
- $F$  = excess noise factor
- $B$  = bandwidth (signal)
- $M$  = photocurrent multiplication factor (gain)

The front-end amplifier which converts the current into voltage is the primary area of concern to the engineer. The stages which follow the front-end amplifier are merely voltage gain circuits and do not contribute significantly to the SNR of the receiver. The two most common front-end amplifiers used for fiber optics are the transimpedance amplifier and the integrating front-end.

The transimpedance amplifier, shown in Fig. 21, is the simplest front-end amplifier to design. It utilizes an operational amplifier with feedback resistance. When used with the PIN diode ( $M = 1$ ) the thermal noise dominates. The value of the feedback resistor is determined by

$$R_F(\Omega) = \frac{A_w}{2 \pi f_{3dB} C} \quad (14)$$

where  $f_{3dB}$  is the signal bandwidth,  $A_w$  is the operational amplifier gain and  $C$  is the sum of detector capacitance and amplifier capacitance. From the value of the resistor the noise current can be computed by

$$i_n = \left( \frac{4kTB}{R_F} \right)^{\frac{1}{2}} \quad (15)$$

where  $B$  is the signal bandwidth and  $T$  is the noise temperature. The minimum required optical signal level can then be computed by

$$P_{MIN} = i_n \times SNR_{MIN} / \text{Responsivity } (r) \quad (16)$$

where  $SNR_{MIN}$  is the ratio of signal current to noise current required to recover the message.

Sample calculations for the HP-4205 PIN diode operating at 400 kbps and 15 Mbps are given in Table VIII. The total capacitance was assumed to be 2.7 pf (.7 pf for the PIN diode and 2 pf from the amplifier). A noise temperature of 300 K is assumed. The required current SNR is 10. Operational amplifiers have constant gain-bandwidth products. For simplicity, it was assumed that an operational amplifier was selected such that the gain-bandwidth product is equal to the bandwidth of the input signal. Therefore  $A_w$  is equal to one. For the HP-4205 at bandwidths below 400 MHz the shot noise approaches the thermal noise. The ideal condition is when the two noise terms are equal. At higher bandwidths (e.g. 15 MHz) the thermal noise dominates and greatly increases the required power level necessary to achieve minimum SNR. When the transimpedance amplifier is used with an APD the thermal noise problem at large bandwidths is reduced because of the device's gain. From the SNR equation it can be seen that proper selection of M, the ADP gain, will increase the shot noise term to the level of the thermal noise term and simultaneously increase the level of the signal current power term. The noise term is then twice the value of the thermal noise. Since the minimum required power equals the minimum required signal current divided by the responsivity, it can be expressed as

$$P_{MIN} = \frac{i_s}{r} = \frac{SNR \cdot 2i_n}{rM^2} = 10 \left( \frac{8kTB}{R_F} \right)^{\frac{1}{2}} / rM^2 \quad (17)$$

where  $i_n$  is the thermal noise current. Responsivity for an APD is defined by

$$r = \eta \frac{\lambda}{1.24} M \quad (18)$$



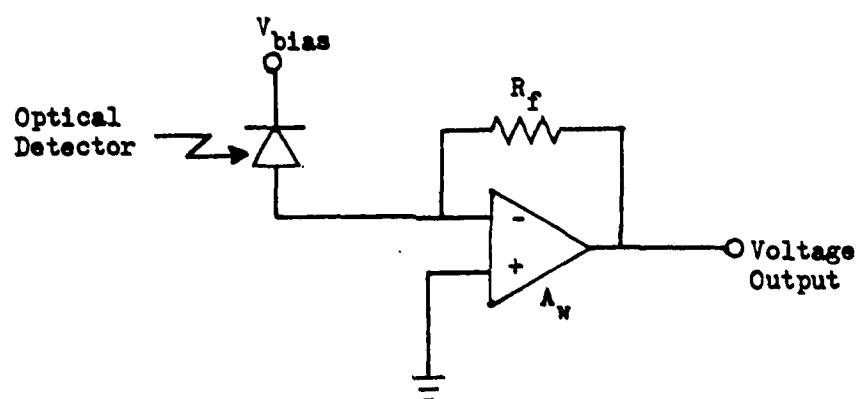


Figure 21. Transimpedance Amplifier

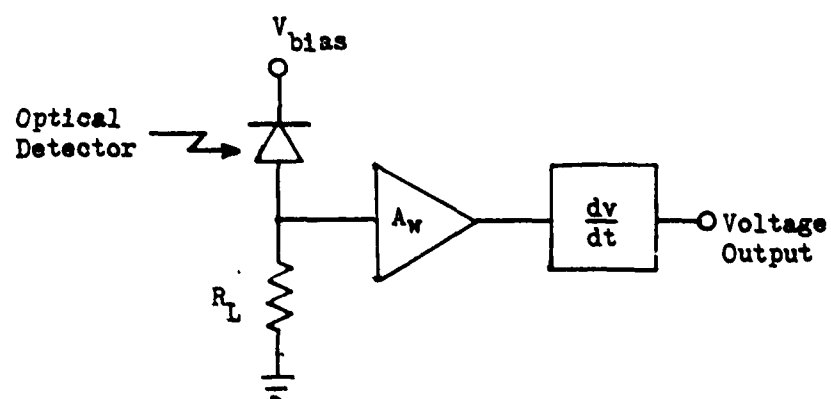


Figure 22. Integrating Front-end Amplifier

<u>Data Rate</u>	<u>400 kbps</u>	<u>15 Mbps</u>
$R = \frac{1}{2\pi f_{3dB} C}$	147 k $\Omega$	4 k $\Omega$
$i_n = \frac{4 KTB}{R}^{\frac{1}{2}}$	212 pA	8 nA
$P_{MIN} = \frac{i_n}{r} SNR$	4.25 nW (-54 dBm)	160 nW (-38 dBm)

TABLE VIII. POWER CALCULATIONS FOR TRANSIMPEDANCE AMPLIFIER

where  $i_n$  is in  $\mu\text{A}$ . Combining these equations minimum power can be computed by

$$P_{\text{MIN}} = \frac{17.54 i_n}{\eta \lambda M^2} \quad (19)$$

where  $i_n$  is the thermal noise current and  $M$  is set by that value of gain which results in shot noise equalling thermal noise. For the RCA C30908E this reduces to a value of  $215 \text{ nW/M}^2$ . Thus, if a value of gain equal to ten is required to equate shot and thermal noise, the optical power required is reduced to  $2.15 \text{ nW}$  or  $-56 \text{ dBm}$ .

The gain of the transimpedance amplifier is directly proportional to the feedback resistor. For the  $400 \text{ kbps}$  signal into the PIN diode the signal current was approximately  $2.12 \text{ nA}$ . Since the value of the feedback resistors was  $147 \text{ K}\Omega$  the voltage provided by the transimpedance amplifier is approximately  $0.3 \text{ mV}$ . This small voltage level is not sufficient for signal recovery and must be amplified by other amplifiers up to a usable level.

The transimpedance amplifier appears to be suitable and even sufficient for the receiver circuits in the shallow-water range. For the short low-bandwidth lengths between the hydrophone and the multiplexer a LED and PIN diode with a transimpedance amplifier provides  $21 \text{ dB}$  attenuation margin. For the longer high-bandwidth link between the multiplexer and the shore, the system requires a laser diode and APD with the transimpedance amplifier to obtain  $6.5 \text{ dB}$  of attenuation margin. Besides being simple and inexpensive the transimpedance amplifier has the features of a wide dynamic range and easy temperature stabilization.

The integrating front-end is primarily used for systems with extremely large bandwidths. It has the disadvantages of being difficult to temperature

stabilize, more complex to design and having a smaller dynamic range. A simplified diagram of the integrating front-end amplifier is shown in Fig. 22. For the receiver a value of load resistance ( $R_L$ ) is chosen that results in a bandwidth which is smaller than the signal bandwidth. This large value of load resistance keeps the thermal noise to a minimum and thus provides improved SNR over the transimpedance amplifier. The integrating effect due to the large  $R_L$  is overcome by following the amplifier with a differentiating equalizer. Below 50 MHz the amplifier is normally designed using an FET because it is inherently quieter than a bipolar transistor. Above 50 MHz a bipolar transistor is required.

From the fiber attenuation computations for the various links the minimum dynamic range required of the receiver can be computed. For fibers operating at  $0.85 \mu$  the hydrophone to multiplexer lengths (which vary from 1.78 to 5.44 km) result in an attenuation difference of nearly 13 dB. This requires a large dynamic range which favors the transimpedance amplifier. The link from the multiplexer to the shore station is a fixed distance and therefore has a minimal dynamic range. This link, because of the small attenuation margin with the transimpedance amplifier, the large bandwidth and distance, and the fact that the receiver electronics will be on shore where they can be easily controlled, warrants consideration for use of the integrating front-end.

Most manufacturers of optical-fiber products now offer system modules as well as individual components. Optical sources with driver modules and optical detectors with receiver modules are available off-the-shelf in a variety of packages with a variety of performance characteristics. As has been shown throughout this section, to optimize system design, which means minimizing noise, the system must be designed for the desired signal bandwidth. The off-the-shelf modules, for the most part, have been designed

for land-line computer-to-computer links and the design bandwidths do not coincide with those assumed for the shallow-water range. In addition, the off-the-shelf modules come with a variety of sources, detectors and fiber pigtails which result in optical link capabilities ranging from only hundreds of meters to several kilometers. Unfortunately, the long-distance link modules (5 km) are generally designed for high bandwidths ( $>100$  MHz) and cost thousands of dollars. The inexpensive low-bandwidth modules are generally only capable of distances of less than a kilometer. However, the fiber-optic market is rapidly expanding and it is possible that off-the-shelf modules will become available that satisfy the requirements of the shallow-water range application. Still, designing a customized system is not that difficult and offers the advantages of minimum noise and greater choice of optical components.

## V. SIGNAL FORMAT AND DATA RECOVERY

The purpose of a communications system is to transmit a message from one location to another. Basically, the communications system converts the message into a signal that can be transmitted through a medium, transmits the signal into that medium, then recovers the signal at some other location and converts the recovered signal back into the original message. The test of a good communications system is how consistently it can accurately recover the original message.

In an electrical communication system the message is a voltage. An analog message can take on any value of voltage in a range of continuous voltages while a digital message can take on only discrete values within that range. The signal can be any one of many forms including radio, optical, acoustical and electrical; however the signal format is either analog or digital.

In the shallow-water range application, the message is binary digital. The signal transmitted by the pinger and received by the hydrophone is acoustical with an analog format. Because the optical link is a communications system, the voltage from the hydrophone is considered to be the message. To complete the engineering of the fiber optic system it is therefore necessary to determine the best signal format for transmitting this message over an optical link.

### A. ANALOG OR DIGITAL ?

Fiber-optic systems are capable of carrying either analog or digital signals. In order to determine which signal format is most advantageous for the shallow-water range application it is necessary to investigate the

advantages and disadvantages of various optical modulation formats, analog and digital signal formats, and analog and digital multiplexing schemes.

A variety of optical modulation schemes are available for fiber optics. The modulation can be direct or heterodyne. The properties of the optical carrier that can be modulated include intensity, phase and polarization. These properties can be varied continuously or discretely. Discrete modulation of the optical-carrier's intensity can be accomplished by sampling an analog signal and utilizing pulse amplitude, pulse width, pulse position or pulse rate modulation, or by bi-level modulation of a binary digital signal. The most simple and most common form of modulation in fiber optics is a direct intensity modulation scheme. The sources and detectors discussed earlier are particularly suited to these forms of modulation.

The intensity of an optical source can be modulated by either an analog or digital signal. Because the message to be sent is analog, no message to signal conversion is required if analog modulation is utilized. Digital modulation requires that the message be converted into a digital signal format. Not only is analog-to-digital conversion circuitry required at the hydrophone but also digital-to-analog at the destination. Thus, analog modulation has the advantage of simplicity in this application.

The measure of performance in an analog system is the signal-to-noise ratio (SNR) at the destination. Noise once introduced into an analog system cannot be eliminated and degrades the signal. The limit of performance is therefore set by the total accumulated degradation. The total transmission distance of an analog system is a performance measure limited by the degradation. Assuming the required SNR at the signal processor is 10 dB and that the microwave link and multiplexed cable link each degrade the system by 6 dB, the required SNR after detection at the multiplexer is 22 dB. This

is a much more stringent signal-to-noise level than that assumed in the calculations made earlier.

The measure of performance in a digital system is bit-error-rate (BER). With a digital signal the circuitry at each detector must only make a decision of "1" or "0" sent. Once the decision is made the pulse shapes can be regenerated before retransmission. Therefore, perturbations are not passed on from section to section. This means virtually unlimited total transmission distance or signal quality which is independent of length. The BER performance is dependent on SNR at the decision point since the noise can cause a wrong decision. However the SNR that corresponds to the desired BER is the same at each decision point. Therefore, if 10 dB SNR is required at the signal processor only 10 dB is required at the multiplexer, which is the value used in the previous calculations. Thus, digital signals have better noise immunity than analog signals.

The performance of an analog system is dependent on the linearity of the system components while a digital system is dependent on their speed. Linearity in optical sources, especially lasers, is difficult to obtain. Linearity requires a low modulation index and extremely stable temperature. In optical detectors, especially APDs, linearity requires stable temperature and bias. Thus to obtain linearity in an optical system, expensive and complex temperature and gain control circuitry is required. Digital signals, on the other hand, are dependent only on switching between two distinct levels of intensity. Linearity and the associated control circuits are therefore not required. Whenever an analog signal is digitized the price paid is increased bandwidth and therefore faster switching speeds. If pulse amplitude, pulse width or pulse position modulation is utilized the bandwidth is doubled and if eight-bit pulse code modulation (PCM) is used the bandwidth is increased by 16. The bandwidth used in the previous optical calculations was based on



PCM bandwidths and, as was shown, the switching speeds were not a problem. Thus, for the shallow-water range digital signals have the advantage of not requiring linearity, but only at the expense of increased bandwidth (which is not a problem).

The multiplexing scheme used with analog signals is frequency-division multiplexing (FDM) and with digital signals is time-division multiplexing (TDM). The proposed coaxial system utilized FDM. Because of intermodulation products the required bandwidth is approximately one MHz for 16 signals. With a time division multiplexed eight-bit PCM signal the required multiplexed bandwidth was shown, in section IV-A, to be 13.6 MHz utilizing the baseband signal from the hydrophone and 27.2 MHz without down conversion to baseband. Again it can be seen that digital formats impose a significant increase in bandwidth. FDM requires expensive bandpass filters at the receiver to recover each of the upconverted signals. On the otherhand TDM requires only inexpensive low pass filters and circuits that can be easily built with readily available and inexpensive integrated circuits.

For the shallow-water range, digitizing the signal provides the advantage of improved noise immunity and eliminates the complex control circuitry necessary to obtain linearity in optical sources and detectors. These are accomplished at the expense of increased bandwidth, which increases the thermal noise in the receiver in the multiplexed link to the point where part of the noise immunity advantage is lost. In addition, there is the requirement for analog-to-digital and digital-to-analog circuitry.

Once the analog SFSK signal is recovered at the destination, the original 40 bps digital message must still be recovered. Since fiber optics favor a digital signal, the question of the feasibility of transmitting the original 40 bps message instead of the SFSK version over the fiber is raised. The low bandwidth of the original message is so far below that of the SFSK signal

that all the advantages of digital transmission would be obtained without the disadvantages. After considering the various signal-format alternatives for transmission over the optical link it was decided that the analog and digitized PCM version of the analog signal were straight forward. On the otherhand, recovering the original digital message at the hydrophone and transmitting this or a modified version merited further investigation.

#### B. SFSK SIGNAL SIMULATOR

The first step in the investigation into the feasibility of recovering the original message at the hydrophone for transmission over the fiber optic link was to construct a circuit which simulated the actual signal. Such a circuit must generate the various carrier frequencies including their Doppler shift. It must also generate a 40 bps data stream which is actually composed of two 20 bps interleaved data streams. The circuit must then be capable of combining the proper carrier frequency with the proper data bit to create SFSK.

At each hydrophone the signal received is composed of three bands of four frequencies for a total of twelve different frequencies. Because each of the three bands is identical, except for the different tones, and each carries only the information from one torpedo, it was sufficient to simulate one band of carriers (one set of  $\alpha$ ,  $\beta$ ,  $\gamma$  and  $\delta$ ) for the investigation. The band chosen, Band 2, was composed of the frequencies 34.5 kHz, 36.2 kHz, 38.0 kHz, and 39.9 kHz. With  $\pm 2\%$  allowed for Doppler the band of frequencies spans from 33.75 kHz to 40.85 kHz.

A phase-locked-loop tone generator was used to build each of the carrier generators. A typical carrier generator circuit is shown in Fig. 23. The 566 IC was chosen because of its capability of generating a single tone and simulating Doppler shift about that tone by varying the voltage applied at

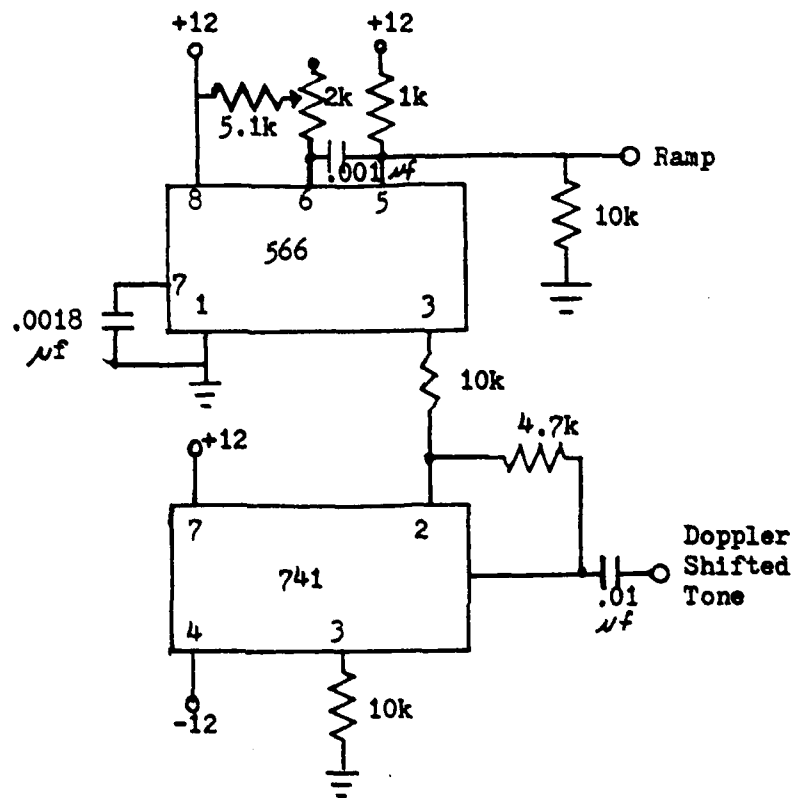


Figure 23. Tone Generator With Variable Doppler

pin 5. It was found that by applying a one volt peak-to-peak triangle wave at pin 5 the center frequency generated by the 566 IC would shift linearly the required  $\pm 2\%$ . Varying the frequency of the triangle wave allowed any rate of Doppler shift desired. The output of each tone generator was connected to a 741 operational amplifier configured as a non-inverting amplifier. This provided proper voltage level output and an interface between the analog 566 integrated circuit and the digital integrated circuits in the remaining portions of the simulator circuitry.

The circuitry which generates the digital message is shown in Fig. 24. The desired output of this circuit was four lines representing the four possible data bits, labeled  $\alpha$ ,  $\beta$ ,  $\gamma$  and  $\delta$ , which correspond to the four frequencies generated in the previous circuit. It was also desired that the outputs be programmable so as to allow simulation of various data streams. To simulate all possible basic combinations of the four outputs it was only necessary to allow eight variable inputs. In the interleaved data an  $\alpha$  or a  $\gamma$  can only be followed by a  $\beta$  or a  $\delta$ . Likewise a  $\beta$  or a  $\delta$  can only be followed by an  $\alpha$  or a  $\gamma$ . Therefore, the eight bit sequences ( $\alpha, \delta, \gamma, \beta, \gamma, \beta, \alpha, \delta$ ) and ( $\alpha, \beta, \alpha, \beta, \gamma, \delta, \gamma, \delta$ ) provide for each symbol to be immediately preceded and followed by all possible combinations. The eight switches were connected to the inputs of an eight-to-one multiplexer (74151) where  $D_1$  represents an  $\alpha$  or a  $\gamma$  and  $D_2$  represents a  $\beta$  or a  $\delta$ . The 74154 was driven by a four-bit binary counter (7493) which caused the eight inputs to be sequentially selected. The 7493 was clocked at the 40 bps data rate. A JK Flip Flop (7473) was used to divide a 40 bps clock by two and thus provide a synchronized 20 bps clock. The outputs of the 74151 and 7473 were connected to a 2-line to 4-line decoder (74155). The timing diagram depicted in Fig. 25 shows the inputs (A and B) and output (C) of the 74155

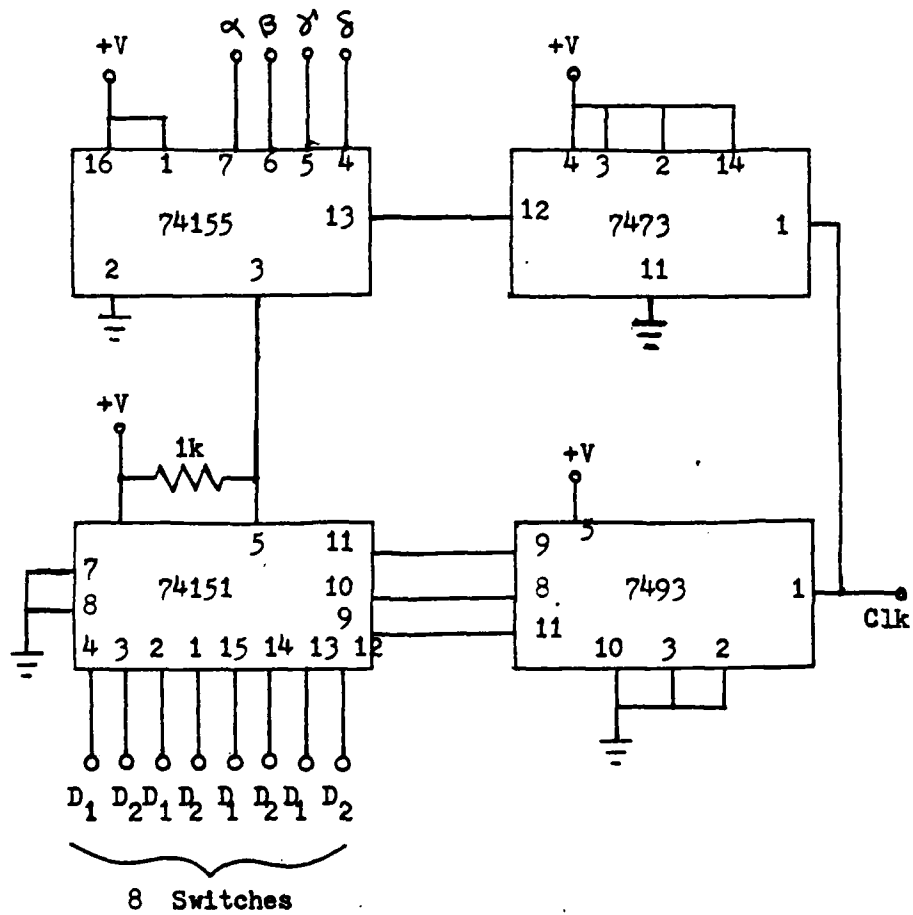


Figure 24. Programmable Data Generator

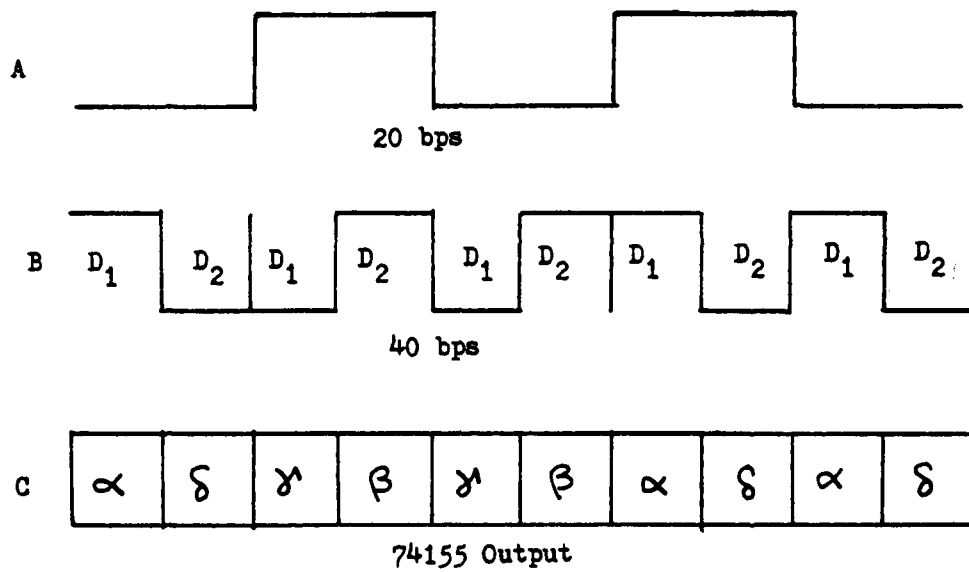


Figure 25. Data Circuit Timing Diagram

when the switches were programmed to produce the sequence ( $\alpha$ ,  $\delta$ ,  $\gamma$ ,  $\beta$ ,  $\gamma$ ,  $\beta$ ,  $\alpha$ ,  $\delta$ ). Each output symbol corresponds to an active low pulse on the corresponding output line of the 74125.

Having generated the data stream and the carriers with variable Doppler shift on eight separate lines, the results were then combined to produce the desired signal. The circuit used to modulate the data with the carrier tones is depicted in Fig. 26. The method of modulation chosen was switching the appropriate carrier on when the corresponding data bit was active. The switch chosen was the 4006 quad normal-open switch. Because the 4006 required active high pulses to trigger the proper switch, a 7404 hex inverter was utilized to convert the four data lines from active low to active high. Thus, when the data generator produced an  $\alpha$  the corresponding switch connected to the tone  $\alpha$  was closed and frequency  $\alpha$  was available at the output. At the same time the other three switches would be open. The four output lines from the 4006 were tied together utilizing a 741 as a summing amplifier.

The output of the SFSK signal simulator when the sequence ( $\alpha$ ,  $\delta$ ,  $\gamma$ ,  $\beta$ ,  $\gamma$ ,  $\beta$ ,  $\alpha$ ,  $\delta$ ) was programmed is shown in Fig. 27. As was shown in Fig. 4 the actual signal has variable frequency pulse duration and amplitude. The duration of any one tone varies from 3 to 40 ms depending on the multipath effect. The amplitude would also be a function of multipath with the direct path having the greatest amplitude. The signal simulator is based on the assumption that the output of the hydrophone is hard limited thus removing amplitude variations. The duration of any one arriving tone in the simulated signal is fixed at 25 ms. Although this is not the actual case, it is deemed sufficient to test the quality of the data recovery circuit discussed in the next section. As will be shown, the data recovery circuit was designed to allow for tone durations of up to 40 ms.

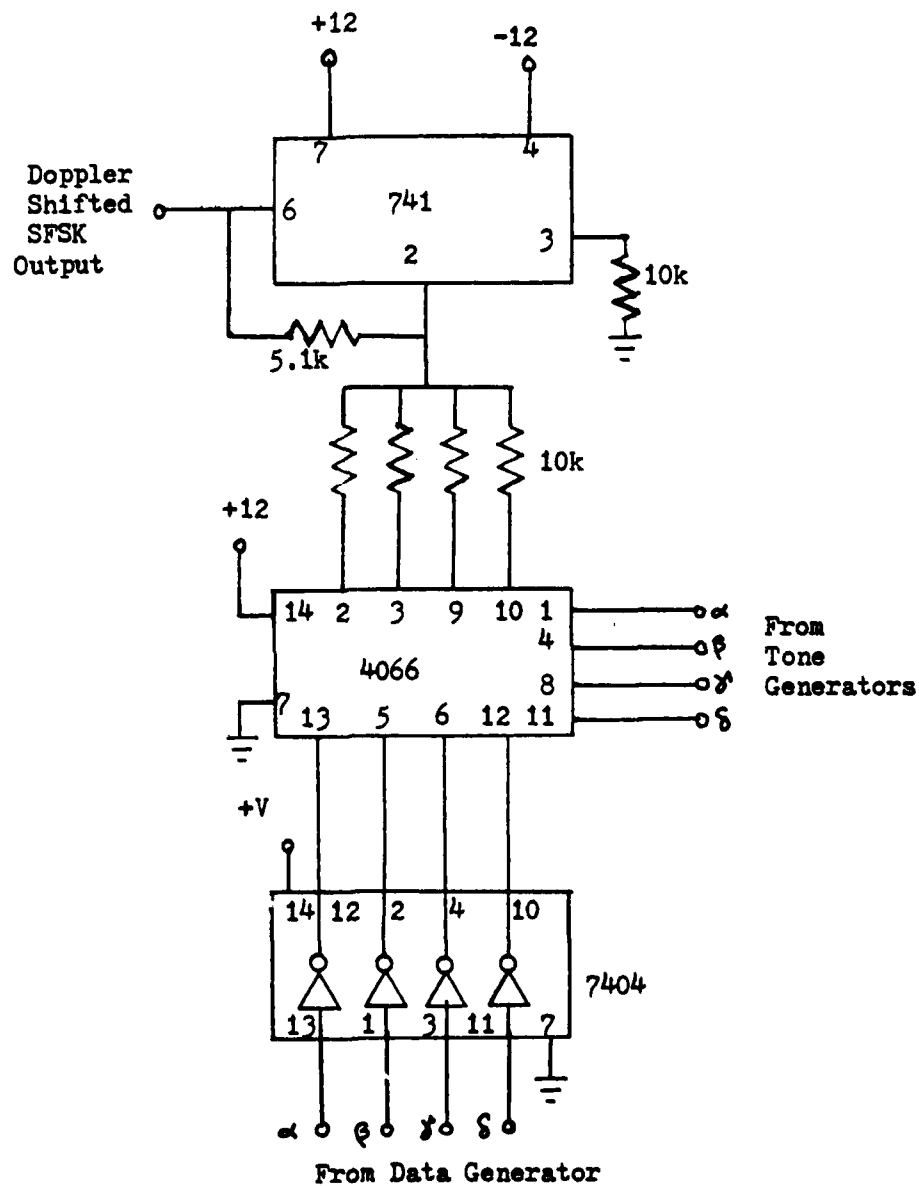


Figure 26. SFSK Generator (Modulator)



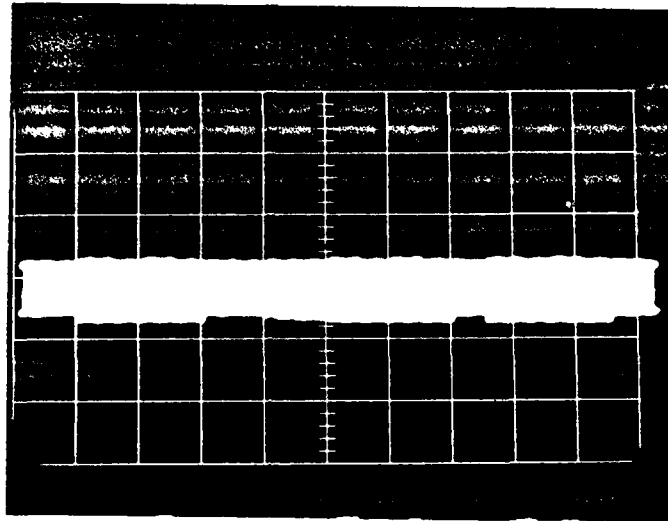


Figure 27. SFSK Signal Generated by  
Signal Simulator

### C. DATA RECOVERY CIRCUIT

Having simulated the output of the hydrophone, the next step was to design and construct a circuit capable of recovering the original digital message. This required a circuit capable of properly detecting which, if any, of four narrow bands of frequencies had a signal present. The four center frequencies and the  $\pm 2\%$  Doppler shift limits are listed in Table IX.

The first step was to select a circuit capable of detecting a narrow band of frequencies (four per cent of center frequency). Active bandpass filters are one alternative, but such narrow bandwidths with sharp cutoffs are difficult to design and expensive. The other alternative considered was the phase-locked-loop tone decoder, 567. It is inexpensive and capable of detection bandwidths from 0 to 14% with sharp cutoff.

A diagram of the 567 configured as a narrowband tone decoder is shown in Fig. 28. Whenever a frequency within the detection range appears at the input, the output of the 567 changes from high to low. The center frequency ( $f_0$ ) is selected by

$$f_0 \approx 1.1/R_1C_1 . \quad (20)$$

For a four per cent bandwidth the value of  $C_2$  is determined by

$$C_2 \approx 62 \times 10^3/f_0 \quad (21)$$

in  $\mu f$ . For the range of center frequencies of interest this corresponds to a value near 2.0  $\mu f$ . However, for minimum lock-up time the value of  $C_2$  should be as small as possible. When the data recovery circuit was constructed utilizing a single 567 for each carrier, the lock-up time was too long and the circuit would not consistently recover the data.

To alleviate this problem two 567s with overlapping locking ranges were used for each carrier. This configuration is shown in Fig. 29. The

<u>TONE SYMBOL</u>	<u>CENTER FREQUENCY</u>	<u>LOWER LIMIT</u>	<u>UPPER LIMIT</u>
$\alpha$	34.5	33.81	35.19
$\beta$	36.2	35.476	36.924
$\gamma$	38.0	37.24	38.76
$\delta$	39.9	39.102	40.698

TABLE IX. BAND 2 FREQUENCIES IN kHz

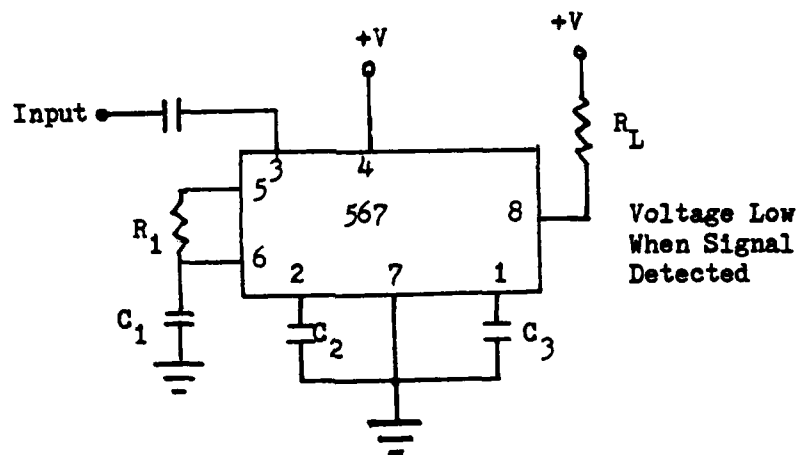


Figure 28. 567 Tone Detector

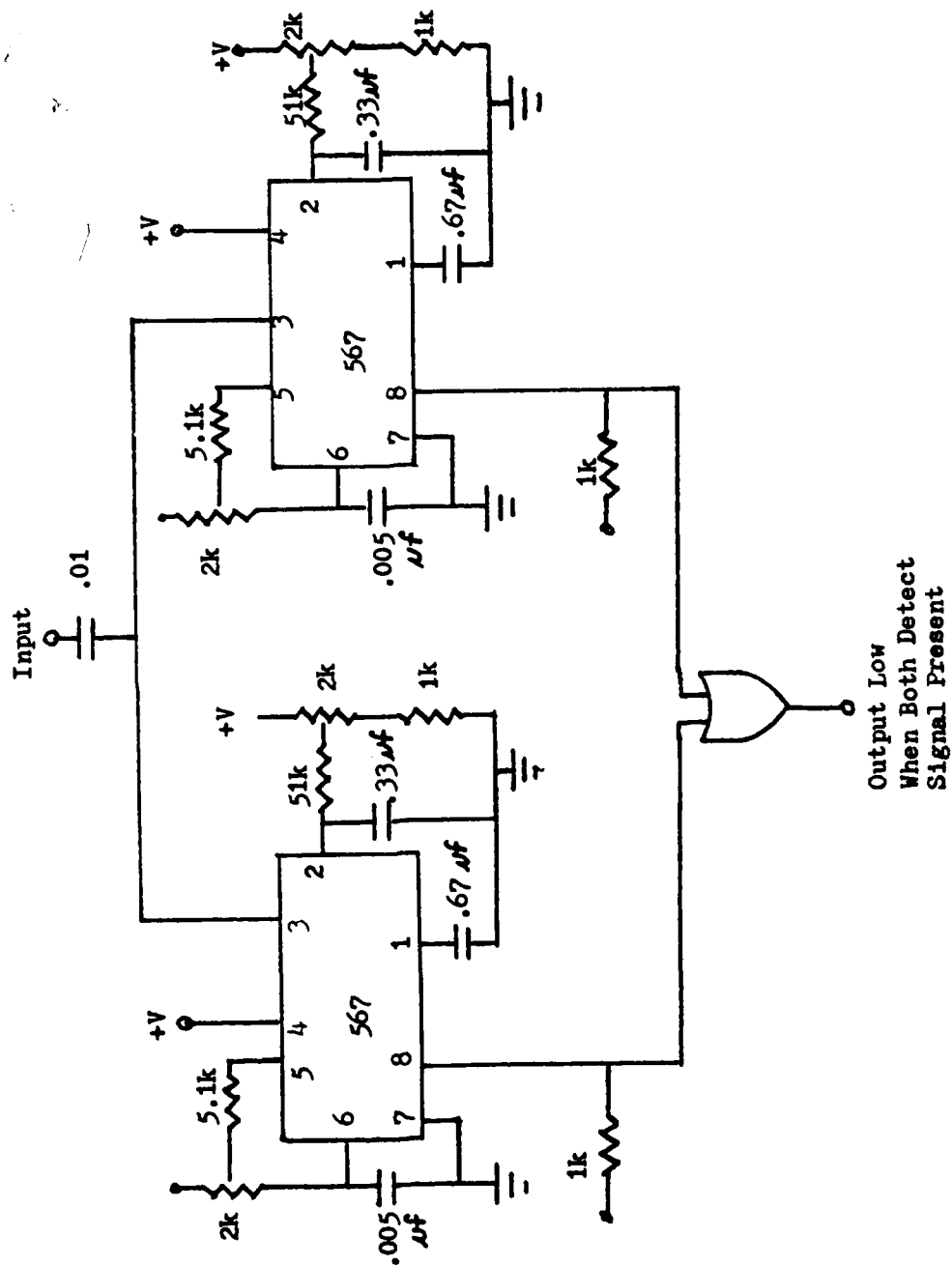
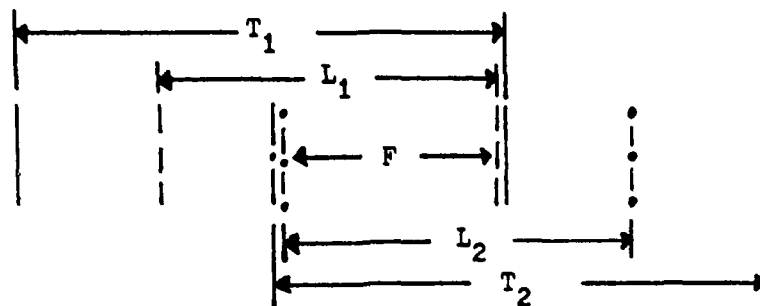


Figure 29. Narrowband Tone Detector With Adjustable Overlapping Locking Ranges

active low outputs of the two 567s were OR'ed to produce one active low output whenever the input frequency fell within the locking range of both 567s. Using two 567s allowed the detection bandwidth of both to be relaxed to 10%. Thus, the value of  $C_2$  was lowered allowing a faster lock-up time. It was discovered that for accurate detection the locking range of the lower frequency 567 had to be moved up to where it was near the upper limit of the tracking range. Likewise, the higher frequency tone detector had to have adjacent lower limits on both ranges. This configuration is depicted in Fig. 30. It was accomplished by the addition of the variable resistor circuit connected to pin 2 of the 567 as shown in Fig. 29. Thus, with eight 567s and one 7432 (quad dual input OR gate) four lines are available, each of which indicates the presence of  $\alpha$ ,  $\gamma$ ,  $\beta$  or  $\delta$  respectively.

Each of the output lines from the respective OR gate was then fed into a 555 timer as shown in Fig. 31. The 555 was configured as a nonretriggerable monostable multivibrator with an output period of 40 ms. Since the duration of the arriving tone varies because of multipath between 3 and 40 ms, the monostable multivibrator was necessary to eliminate the variable pulse lengths from the detector. To recover digital data it was also necessary to recover clock. As will be shown, the 40 ms monostable pulse limits the possibility of spurious tones causing an erroneous clock pulse.

The output of the 555 was then fed into a clock generating circuit and into circuitry which generated the original data stream of "1"s and "0"s. The clock generating circuit is depicted in Fig. 32. Each 40 ms output from the four 555's was fed into a 74121 monostable multivibrator designed to output a 10 ms active high pulse whenever the input goes high. Each 40 ms input pulse thus generates one 10 ms output pulse. Thus, spurious pulses from the detector are prevented from causing additional output pulses.



- $F$  = Desired detection range
- $T_1$  = Tracking range of 1st 567
- $T_2$  = Tracking range of 2nd 567
- $L_1$  = Locking range of 1st 567
- $L_2$  = Locking range of 2nd 567

Figure 30. Locking Range Adjustment For Detection of Narrowband Signal With 567 Tone Detector

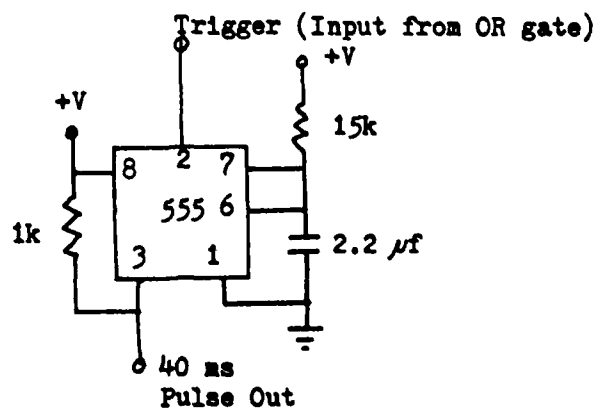


Figure 31. Monostable Multivibrator

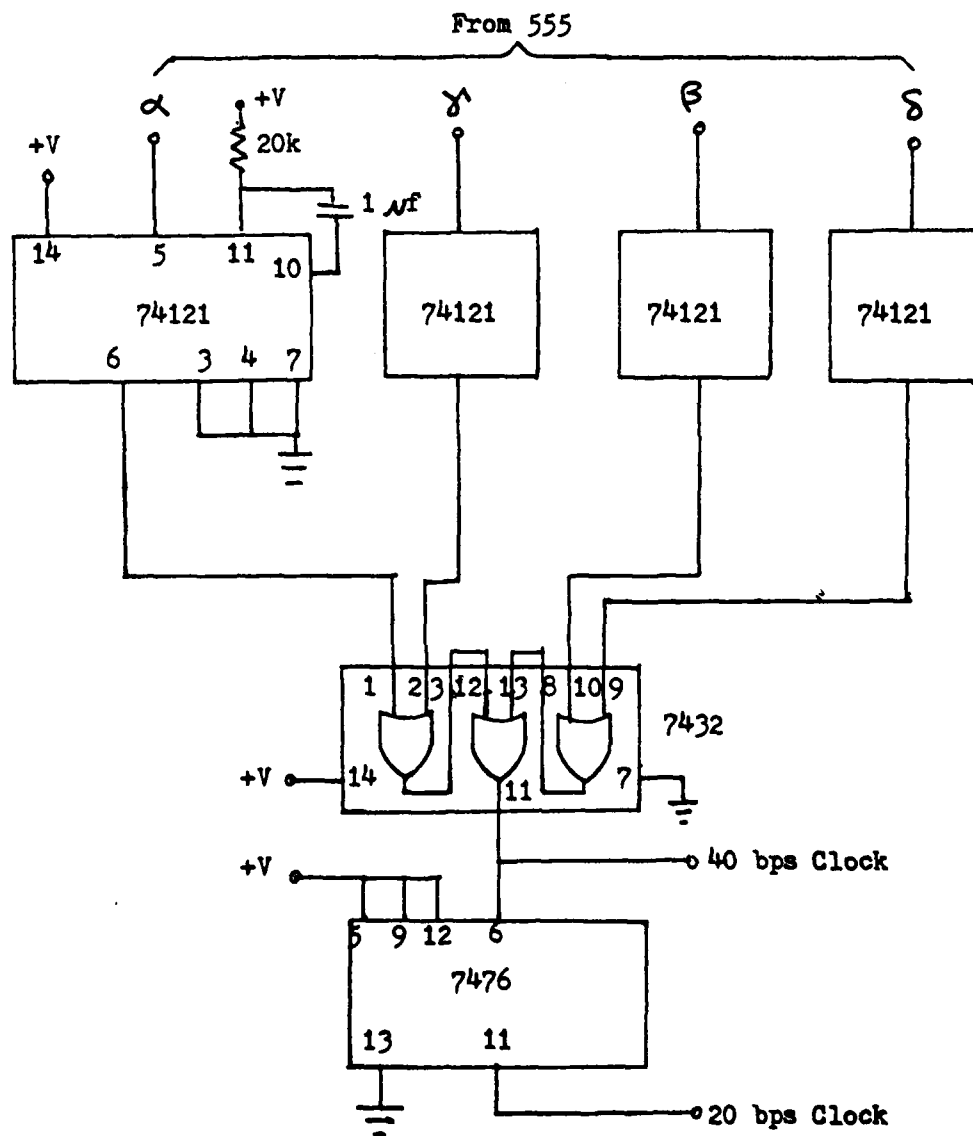


Figure 32. Clock Recovery Circuit



The outputs from the  $\alpha$  and  $\delta$  74121s were OR'ed utilizing one gate of a 7432, as were the  $\beta$  and  $\gamma$  outputs. This was done because when the hydrophone is receiving the SFSK signal, either  $\alpha$  or  $\delta$  (but not both) arrives and triggers the 40 ms pulse. The next  $\alpha$  or  $\delta$  does not arrive for 50 ms, the period of the timing code which was transmitted. Thus the output of the OR gate was a 10 ms pulse every 50 ms. Likewise  $\beta$  and  $\gamma$  will arrive every 50 ms, but only 25 ms after the preceding  $\alpha$  or  $\delta$ . Thus, when the two OR gate outputs were then put into a third OR gate the result was a 40 bps clock. The 40 bps clock was then divided by two utilizing a JK Flip Flop with J and K tied high.

The circuit which regenerates the original data required the 40 bps and the 20 bps clock. It is shown in Fig. 33. The 40 ms pulses from the 555 monostables were fed into JK Flip Flops. Because  $\alpha$  and  $\beta$  were "1"s in the original message they were connected to the J inputs. Similarly  $\delta$  and  $\gamma$ , which represent "0"s, were connected to the K inputs. The timing diagram in Fig. 34 shows the outputs  $Q_1$  and  $Q_2$  for the sequence ( $\alpha, \delta, \gamma, \beta, \gamma, \beta, \alpha, \delta$ ). These outputs were utilized as the inputs to a two-to-one multiplexer, 74157, which utilizes the 20 bps clock as its select line. The output of the 74157 was identical to the original message.

A simplified diagram of the entire data recovery circuit is shown in Fig. 35. To test the decoder the sequences (10010110) and (11010010) were programmed into the signal simulator and the Doppler generating triangle wave was set to produce a  $\pm 2\%$  sweep every 10 seconds. The results are shown in Fig. 36 and Fig. 37, respectively. These photographs show the generated SFSK signal (top) and the data recovered by the recovery circuit from the SFSK signal (bottom).

Having successfully recovered the 40 bps original message the next step

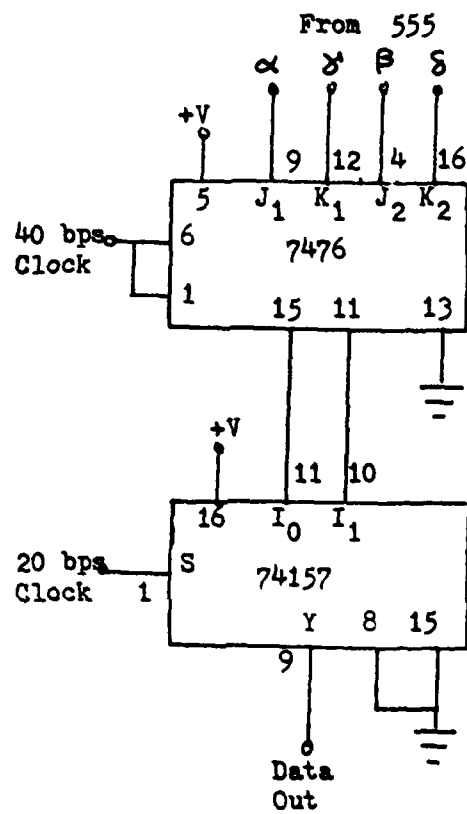


Figure 33. Original Message Recovery

AD-A086 523

NAVAL POSTGRADUATE SCHOOL MONTEREY CA

F/G 17/2

FIBER OPTIC LINK DESIGN FOR AN OPEN-OCEAN SHALLOW-WATER TRACKIN--ETC(U)

MAR 80 D N NICHOLSON, J P POWERS

UNCLASSIFIED

NPS-62-80-007

NL

2 11 2

AN  
ADONIS 1

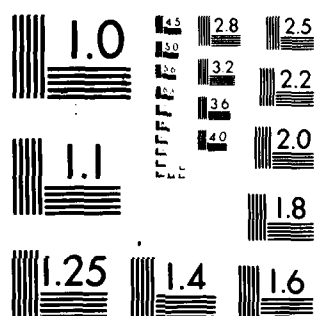
END

DATE

FILMED

8 80

DTIC



MICROCOPY RESOLUTION TEST CHART  
NATIONAL BUREAU OF STANDARDS 1963 A

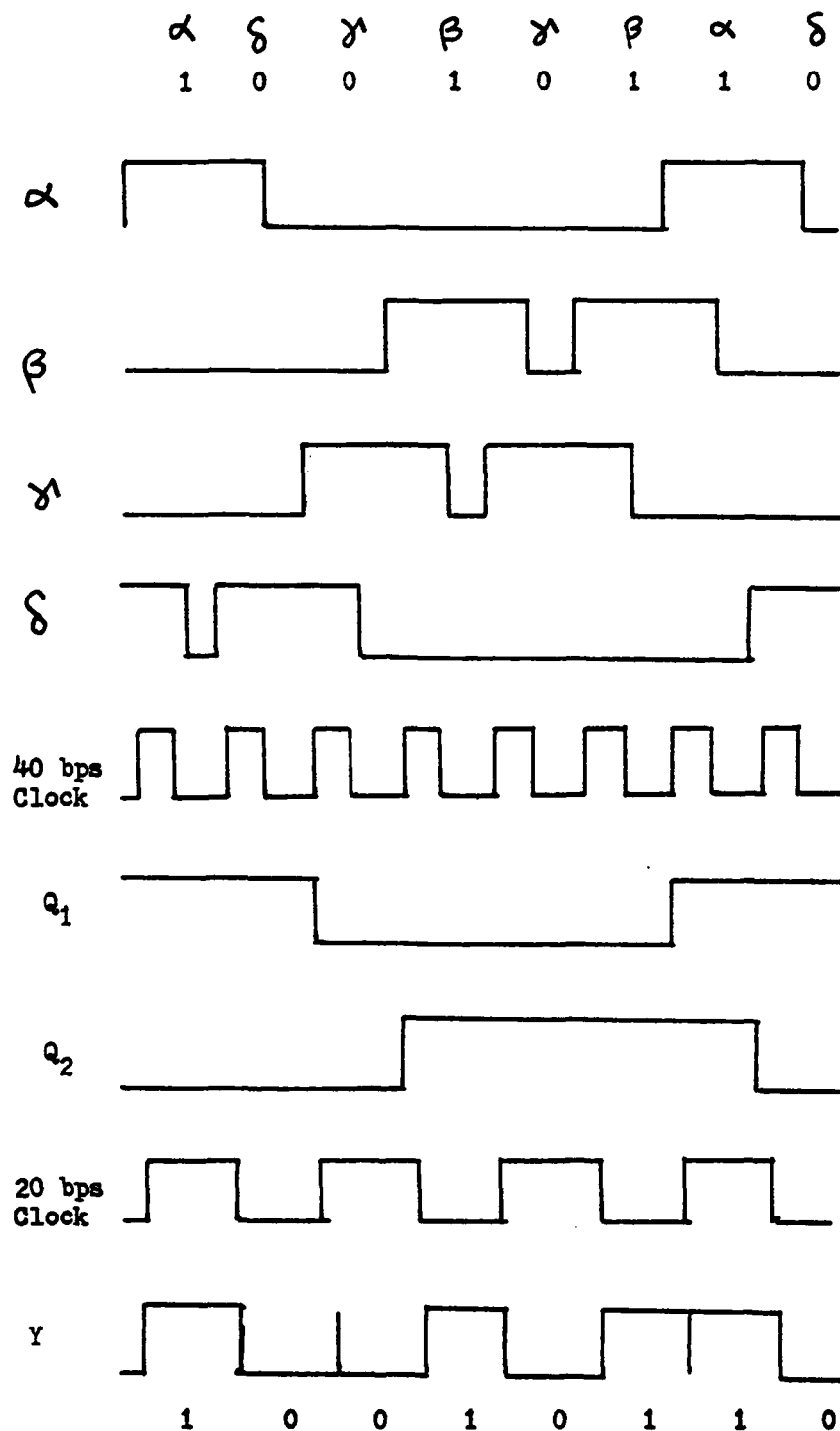


Figure 34. Timing Diagram of Data Recovery

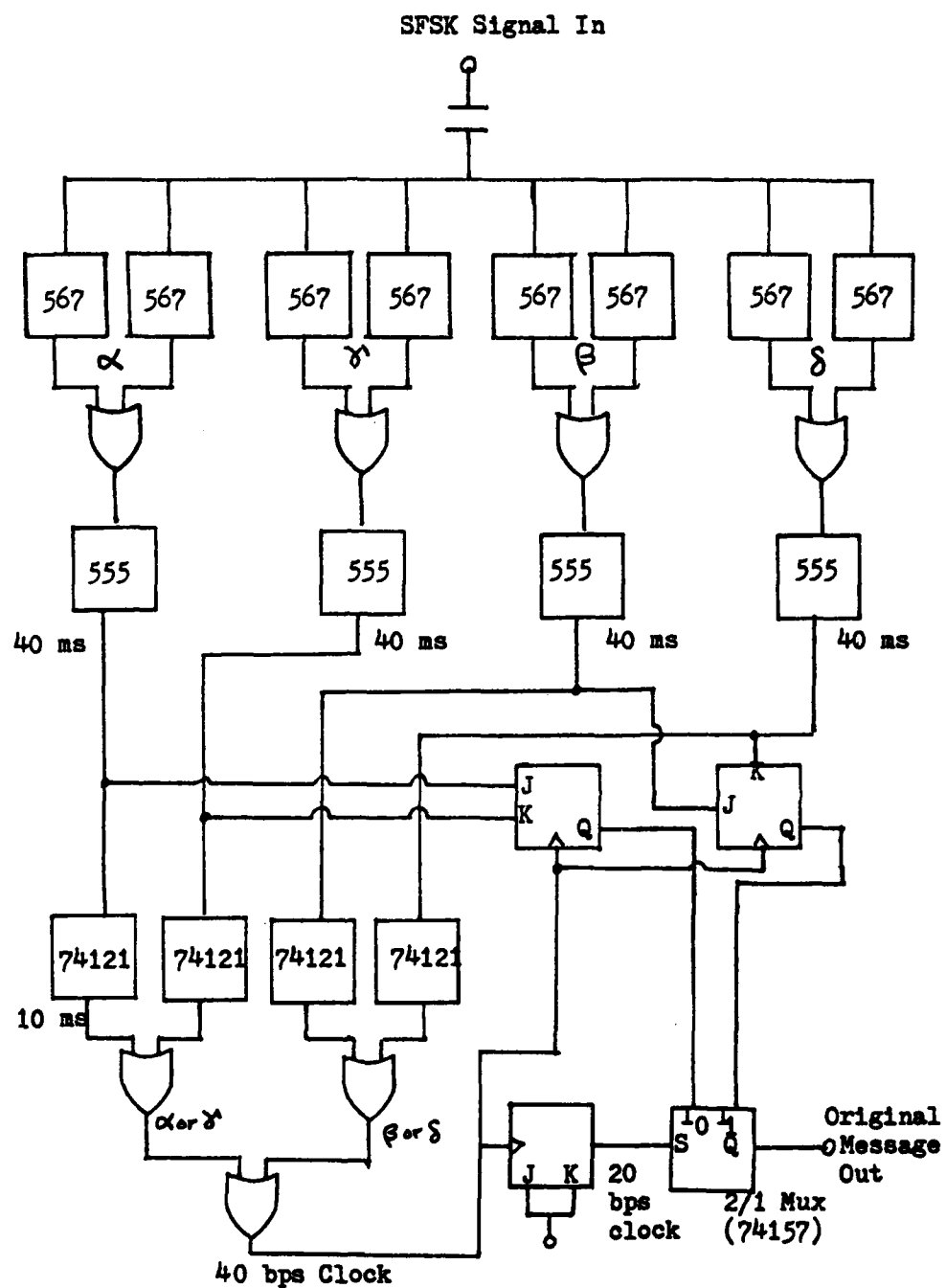


Figure 35. Block Diagram of Circuit Which Recovers Original Message

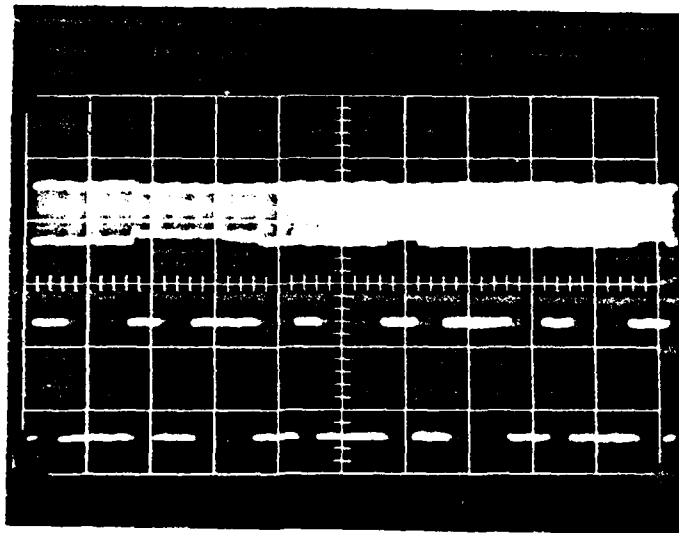


Figure 36. SFSK Signal and Data Recovered  
With 10010110 Programmed

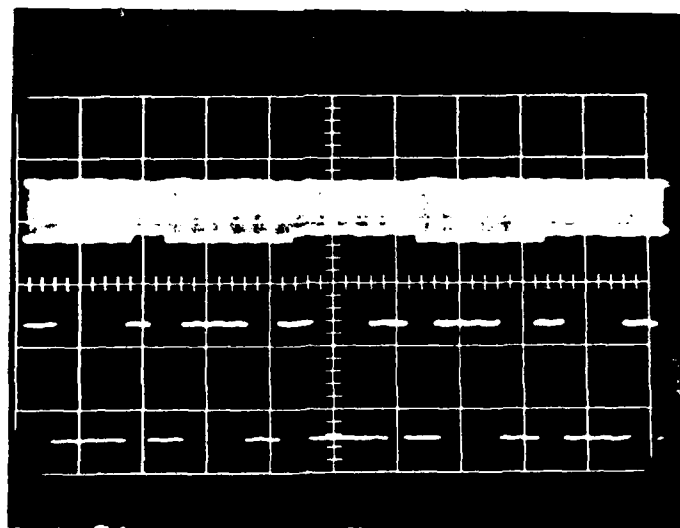


Figure 37. SFSK Signal and Data Recovered  
With 11010010 Programmed

was to evaluate the advantages and disadvantages of transmitting it. Because there are three bands each with one 40 bps recovered message at any one hydrophone, the three data streams would have to be multiplexed for transmission to the central multiplexer. A simple means of accomplishing this is depicted Fig. 38. Multiplexing the three frequency band outputs plus a synchronizing signal at twice the message rate requires a 320 bps clock which results in a data output rate of 320 bps. At the central multiplexer the output of 16 hydrophones must be multiplexed along with one synchronizing channel which results in an ultimate data rate of 10.88 kbps. For this signal format the total maximum bandwidth for 16 hydrophones is only 50 per cent of the bandwidth of one hydrophone using the analog signal and less than .08% of the bandwidth required for the multiplexed PCM signals. In Table VIII it was shown that for the high bandwidth TDM signal utilizing a transimpedance amplifier with a PIN diode, the minimum required received power for a SNR of 10 was -38 dBm. This high level of power forced the design to require an APD to obtain signal gain and which equated shot noise and thermal noise. The ADP decreased the minimum power required to -56 dBm. If the bandwidth of the TDM signal is only 10.88 kHz, the minimum required signal power as shown in Fig. 39 is only -55 dBm for the PIN diode with transimpedance amplifier. Thus the need for a APD is eliminated.

The major disadvantage of recovering the original signal at the hydrophone is the loss of the Doppler shift information present in the SFSK signal. For the most part the Doppler shift is merely a nuisance that the engineer must consider in designing a receiver. However, with signal processing the Doppler information can be recovered from the SFSK signal and provide information on the speed of the target. If the information from the Doppler is needed in the shallow-water range application additional signal processing circuitry would be required at the hydrophone. In this case the SFSK or PCM version would



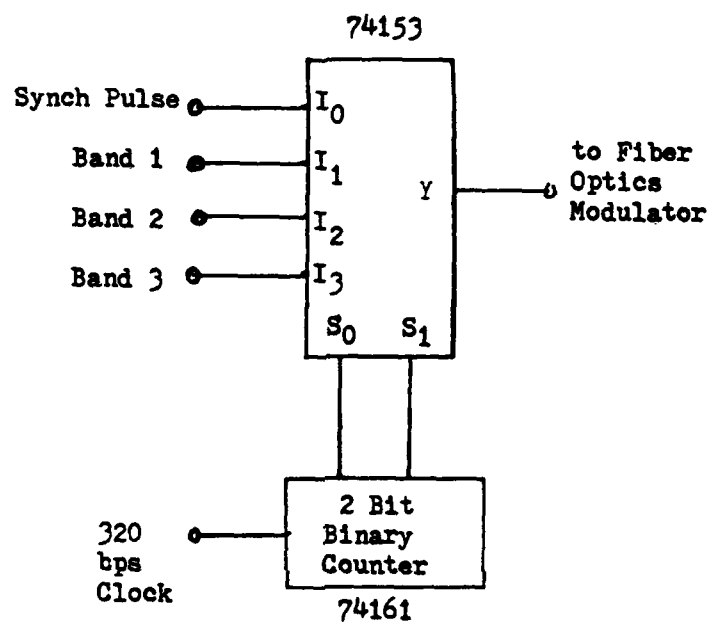


Figure 38. 3 Band Multiplexer

### TRANSIMPEDANCE AMPLIFIER

Op Amp Gain-Bandwidth Product (GB) =  $4 \times 10^5$

$$A_w = \frac{GB}{BW} = \frac{4 \times 10^5}{1.088 \times 10^4} = 36.8 \quad (22)$$

Feedback Resistor

$$R_F = \frac{A_w}{2\pi f_{3dB} C} = 200 \text{ M}\Omega \quad (14)$$

Thermal Noise Current

$$i_n = \left( \frac{4kTB}{R_F} \right)^{\frac{1}{2}} \approx 1 \text{ pA} \quad (15)$$

Dark Noise Current (Given)

$$I_D = 150 \text{ pA}$$

$\therefore$  Total Noise Current Equals Dark Noise Current

Minimum Required Power

$$P_{MIN} = \frac{I_D^2}{R} \times \text{SNR} = 3 \text{ nW or } -55 \text{ dBm} \quad (16)$$

Figure 39. Transimpedance Amplifier Calculations

Thus it appears that the bandwidth of the multiplexed signal must be increased while the SNR requirement for the desired BER is relaxed. The solution to this problem is spread spectrum.

There are many uses for signal spreading, one of which is detection of signals with negative SNR's. If a signal at 40 bps is spread 31 times to a bit rate of 1280 bps, the system attains a processing gain of 31 or 15 dB. Likewise if a 40 bps signal is spread 127 times to a bit rate of 5080 bps, the processing gain is 127 or 21 dB. This results in a reduction in SNR equal to the processing gain at the detector. Thus, signals with negative SNRs can be detected. In most communications systems spreading the bandwidth also increases the noise an equal amount since most systems are thermal noise limited. After the signal is de-spread, the SNR for a desired BER is unchanged. Thus, the only advantage is the ability to hide the signal in the noise for covert transmission. However, for optical transmission at 40 bps it was shown in Fig. 39 that the thermal noise current can be increased 150 fold before the total noise current is increased by a factor of two. It was also shown in Table VIII that at 400 kbps the thermal noise current approximately equals the shot noise current. This means the bandwidth increase which corresponds to a thermal-noise-current increase of 150 is nearly  $10^4$ . Thus, for the 40 bps message, it is possible to spread the signal by large amounts and obtain high BER's with negative SNR's. Examples for processing gains of 31 (center) and 127 (left) are also depicted in Fig. 40. Thus by spreading the 40 bps message 31 times a SNR of zero results in a BER of  $10^{-8}$  and by spreading 127 times the same BER is obtained with a SNR of -6 dB. Using these values of SNR as the required SNR for the system, the minimum power required is reduced from the original calculations by 10 dB for a bandwidth spread of 31 and 16 dB for a spread of 127. Thus, the required power level, utilizing the PIN diode with a

have to be transmitted back to the shore signal processor.

Another concern might be the result of message recovery at the hydrophone when the SFSK acoustic signal is distorted. In this case the data recovery scheme would be prone to make errors in its decisions. This would result in errors in the message received at the shore. However, if the incoming SFSK signal is so distorted that errors are made at the hydrophone where the SNR is a maximum, it is most likely that the signal would be too distorted to recover accurate information on shore where the SNR is a minimum. The message was designed to allow three errors in twenty bits which compensates partially for signal distortion. In the presently proposed system, signal processing is necessary to accurately recover the message. Similarly, if the original message is recovered at the hydrophone, signal processing performed on it at the Pacific Beach Station could be used to compensate for errors made at the hydrophone. Thus, it appears that the only real disadvantage of recovering the original message for transmission is the loss of Doppler information.

#### D. DATA SPREADING

In digital communications systems the measure of performance is bit error rate (BER). It is related to the received SNR as depicted in Fig. 40. The rightmost curve depicts BER versus SNR for PCM and amplitude shift keying (ASK) which are the digital signal formats available for the optical link. In the earlier calculations of minimum required signal power it was assumed that the required SNR was only 10 dB which can be seen to correspond to a BER of  $10^{-3}$ . A more realistic value of BER is  $10^{-6}$  which corresponds to a SNR of 13.5 dB. Thus, for the system design the required signal power would be actually 3.5 dB higher. This makes transmitting the original message over the long multiplexed link impractical because at such a low bandwidth, the shot noise due to dark current dominates and no advantage is obtained by using the gain of an ADP.

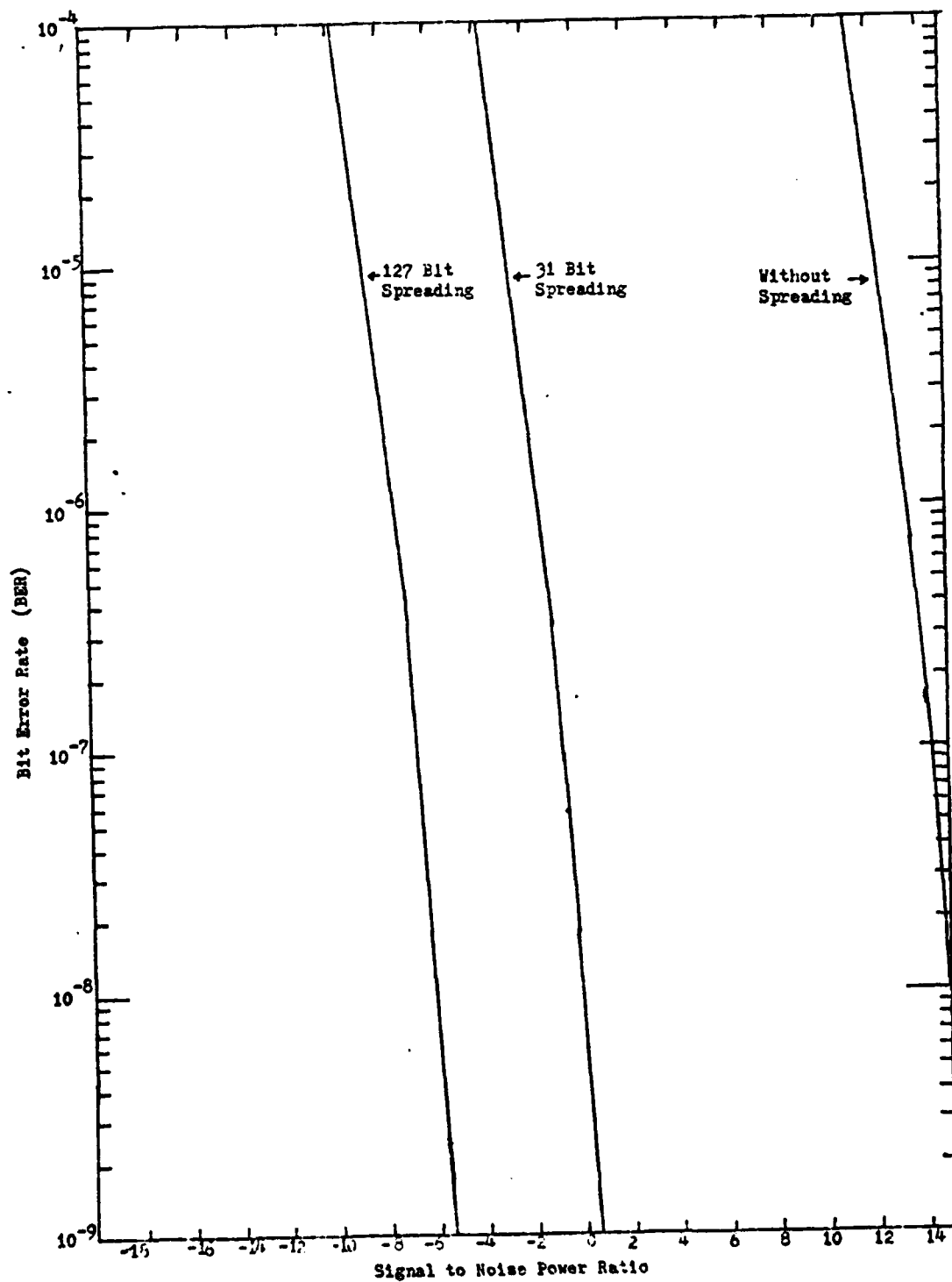


Figure 40. BER vs SNR For ASK Signals

transimpedance amplifier is reduced to -64 dBm and -70 dBm, respectively. On the 13 km link this results in an attenuation margin of 4.5 dB and 10.5 dB, respectively, when the LED and PIN diode are used. Therefore, using the original message and spread spectrum techniques allows the entire system to be designed using only the LED and PIN diode.

To obtain the theoretical processing gain advantage proper spread spectrum techniques must be applied. Because light transmitted in an optical fiber is unipolar, the spread spectrum technique must be unipolar. The simplest and most practical method for the shallow-water range application is direct sequence spreading utilizing maximal-length sequences, M-sequences. With direct sequence spreading a code of length  $L$  equal to the spreading factors is transmitted for every bit of information. The code is then detected using a matched filter. For short code lengths, less than  $10^3$ , the most practical matched filter is a shift-register-tapped-delay line. The codes selected must have good autocorrelation (maximum voltage out when the proper code arrives at the matched filter) and good cross-correlation (a maximum voltage well below the autocorrelation maximum when any other code arrives). M-sequences meet this criteria [1].

M-sequences are always of length  $2^n - 1$ . They are generated using feedback shift registers having  $n$  stages. A 31-bit M-sequence is generated using a five stage shift register and a 127-bit M-sequence requires a seven stage shift register. Feedback taps are made by Exclusively-NORing an even number of stages, one of which is always the  $n$ th stage, and feeding the result back into the first stage. For the 31-bit M-sequence there are 12 good codes while for the 127-bit M-sequence there are 32.

To investigate the merits of applying spread spectrum techniques to the shallow-water range fiber optics application a 31-bit M-sequence system was designed and built. The first circuit built generated four 31-bit

M-sequences, each of which was controlled by the detection of an  $\alpha$ ,  $\beta$ ,  $\gamma$  or  $\delta$ . The final circuit was a shift-register-tapped-delay line which was designed to detect that the  $\alpha$  or  $\gamma$  sequence had been sent.

The M-sequence generating circuit is shown in Fig. 41. Two basic sequences were generated utilizing an eight-bit serial-in parallel-out shift register (74164) and an Ex-NOR gate (74LS266). The sequences generated were designated  $\gamma$  and  $\delta$ . The sequences for  $\alpha$  and  $\beta$  were the complements of  $\gamma$  and  $\delta$  respectively and were generated by Ex-ORing the sequence with a "1". The inputs labeled  $\alpha$ ,  $\gamma$ ,  $\beta$  and  $\delta$  came directly from the 555 timer in the data recovery circuit. Referring to Fig. 41, during the 10 ms period when neither  $\alpha$  or  $\gamma$  are high, the leftmost 74164's master reset is low and each stage is cleared. As soon as the next  $\alpha$  or  $\gamma$  is detected, the shift register, which has the result of the Ex-NORing of stages five and three fed back into the first stage, begins generating the M-sequence. Simultaneously, the detected  $\alpha$  or  $\gamma$  sets or resets the 7473, JK Flip Flop, which determines if the generated code or its complement appears at the output of the Ex-OR gate (7486). The coded output then enters the 2/1 multiplexer (74157) of the original recovery circuit. Similarly a second shift register, controlled by the detection of  $\beta$  and  $\delta$ , with feed-back taps from stage five and two, is generating a different code and its complement. Thus, if the spreading circuit replaces the 7473 (JK Flip Flop) in the original data recovery circuit, the output of the 74157 multiplexer will be the original message spread 31 times.

The four M-sequences that were generated are shown in Figs. 42 through 45. The sequences for transmitting  $\alpha$ , Fig. 42, is designated  $[5,3]$ , where 5 and 3 are the feedback taps, and consists of the code  $[1111100011011101010000100101100]$ . The sequence for  $\gamma$ , Fig. 43, is designated  $[5,3]$  and consists of the complement of code  $\alpha$ . The sequence for  $\beta$ , Fig. 44, is designated

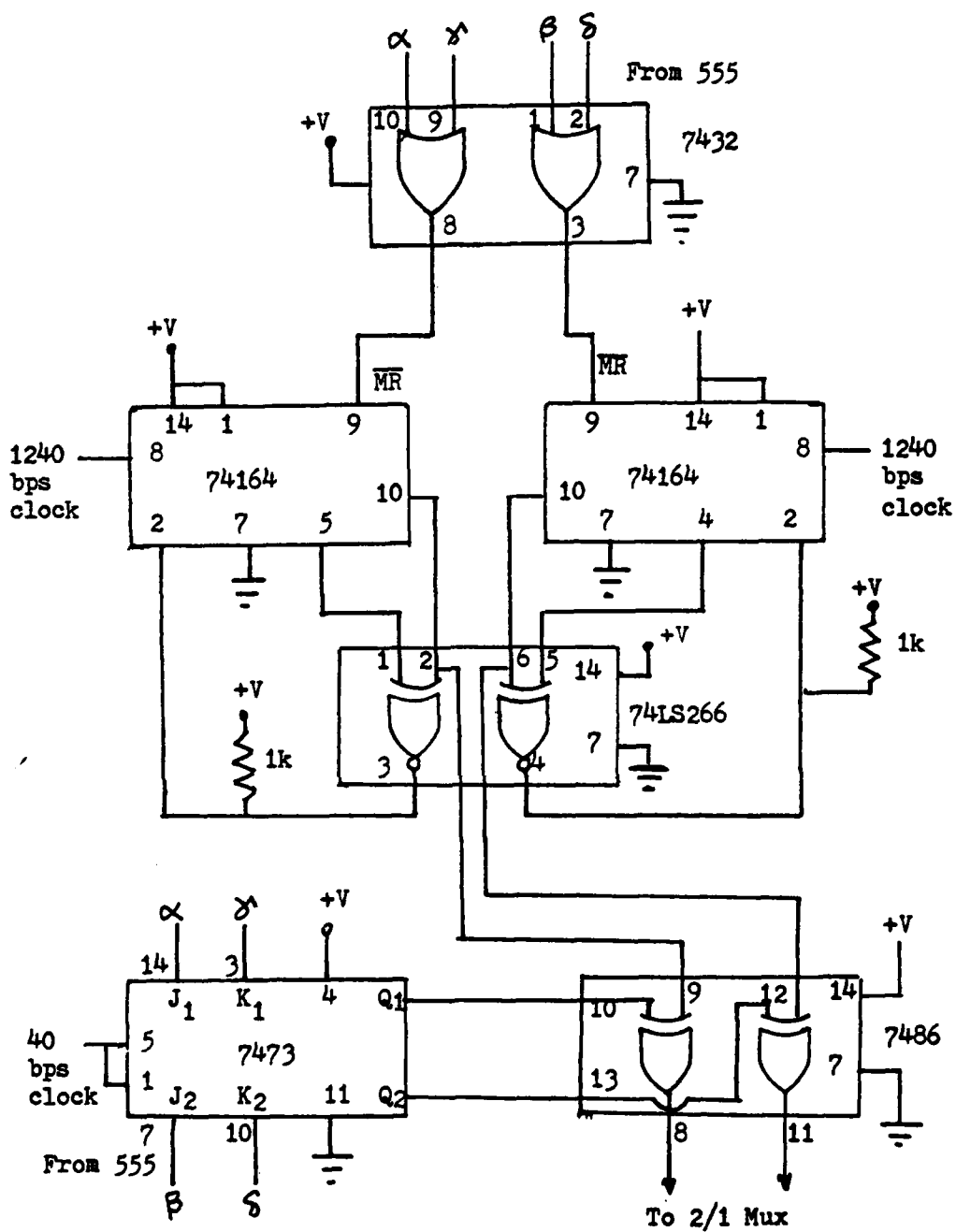


Figure 41. 31 Bit Spreading Circuit



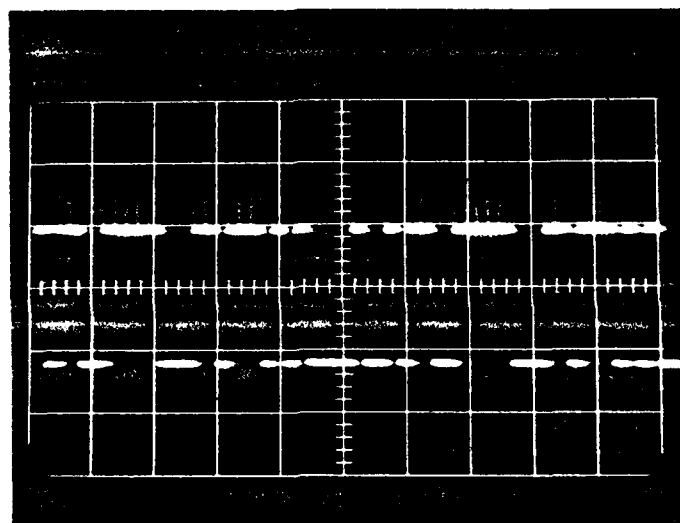


Figure 42. Spreading Sequence  $[5,3]$

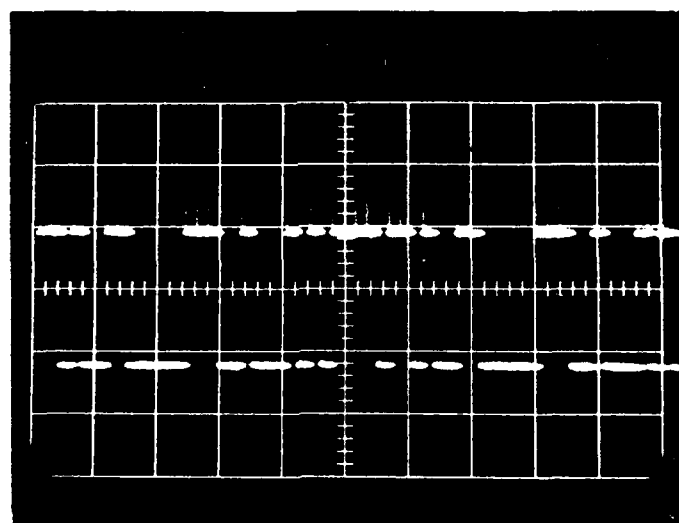


Figure 43. Spreading Sequence  $[\overline{5},3]$

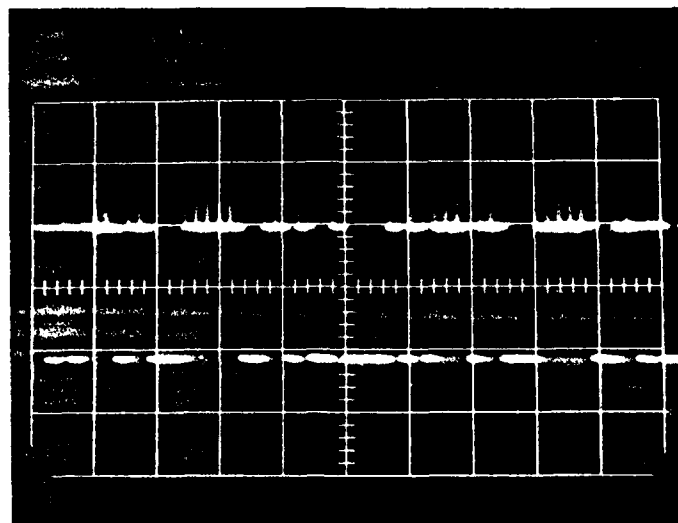


Figure 44. Spreading Sequence  $[5,2]$

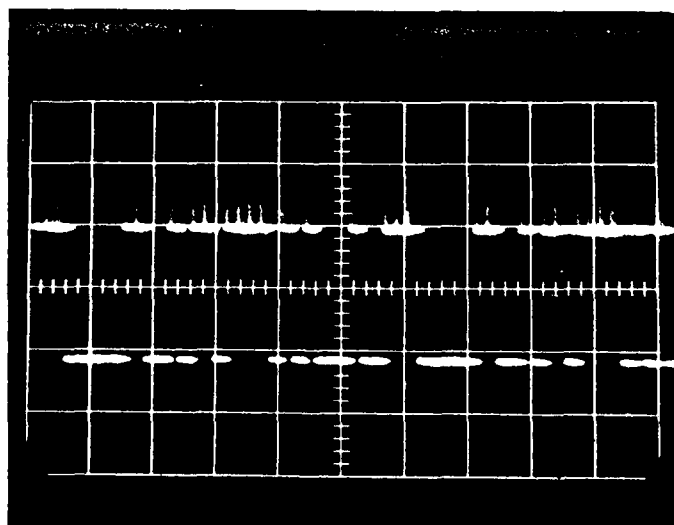


Figure 45. Spreading Sequence  $[\overline{5},2]$

$[5,2]$  and consists of the code  $[111110011010010000101011101100]$ . The sequence for  $\delta$ , Fig. 45, is designated  $[\overline{5},2]$  and is the complement of  $\beta$ .

The final circuit constructed was a de-spreader which detected the arrival of  $\alpha$  code and  $\gamma$  code. The circuit is shown in Fig. 46. The incoming signal is clocked into the shift register array at the bit rate of the spread signal. Each stage of the shift register is Ex-ORed with the desired code's value at that stage. For example, the first bit in the  $\alpha$  code is high. Therefore, Ex-OR 31's programmable input is tied high. At any instant the output of the Ex-OR will be high if the bit in the corresponding stage and the programmed Ex-OR input are the same. Otherwise the output of the Ex-OR will be low. The outputs of all the Ex-ORs were tied together using a resistive summing circuit.

To test the spreading and de-spreading circuit various sequences of the possible codes were initiated and the results observed. The results are shown in Figs. 47 through 57. In each case the top figure is a plot of the theoretical output and the bottom figure is the actual output observed on a strip recorder. Figures 47 through 50 depict the result when only one code is transmitted. Figures 51 through 54 depict the result when two codes are transmitted (e.g.  $[5,3]$   $[5,2]$   $[5,3]$   $[5,2]$  ...). Figures 55 and 56 depict the results when three codes are transmitted (e.g.  $[\overline{5},2]$   $[5,3]$   $[5,2]$   $[5,3]$   $[\overline{5},2]$  ...). Finally Fig. 57 depicts the results when all four codes are consecutively transmitted. In each case the expected and actual results are in close correlation.

The results indicate that only two de-spreaders are needed to recover all four codes. Whenever the programmed code arrived a high voltage out resulted. Likewise when the complement of the programmed code arrived a low voltage level occurred. By using voltage comparators set to trigger at the appropriate level, the arrival of the programmed code or its complement can be detected.

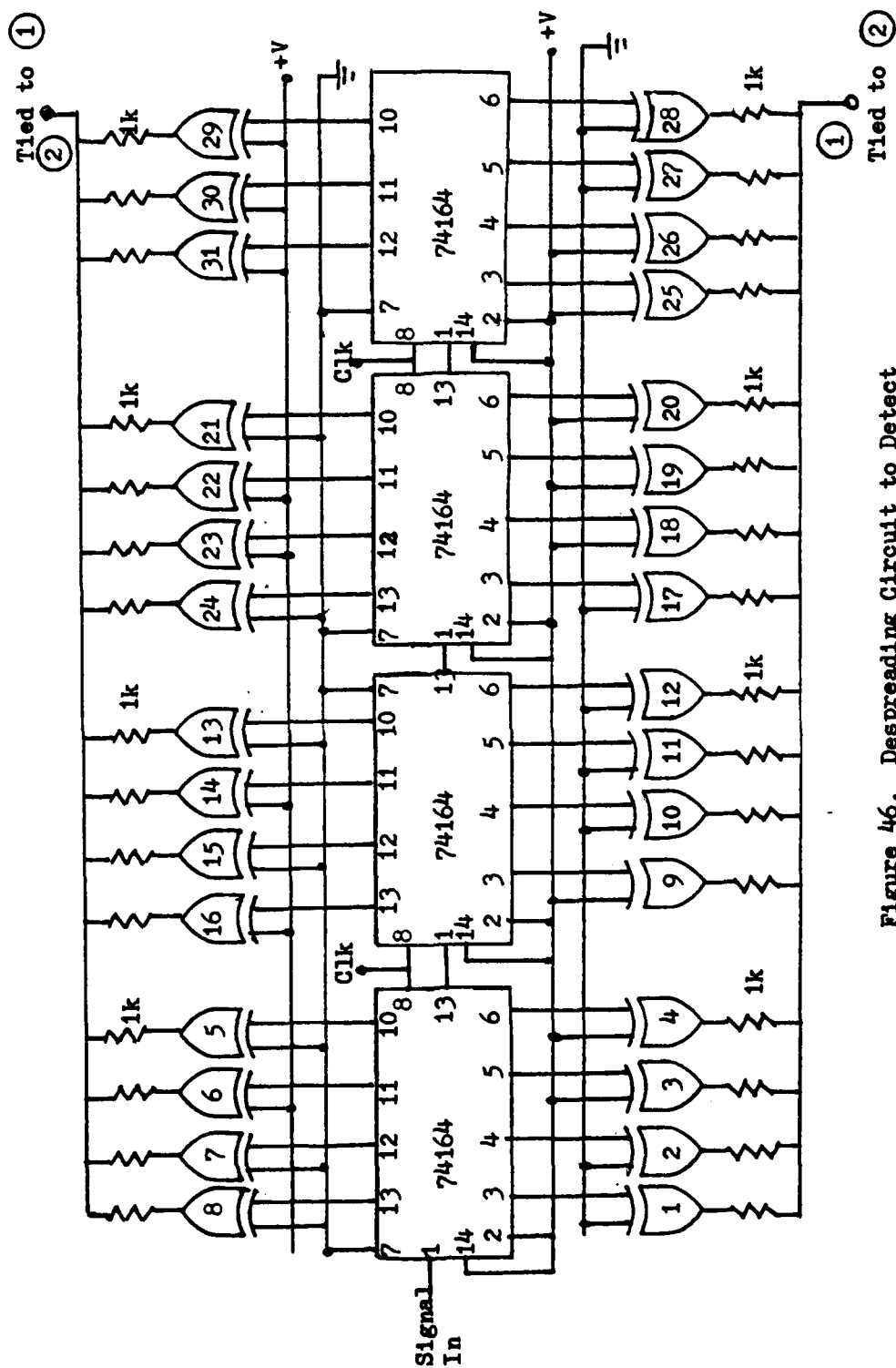


Figure 46. Despreading Circuit to Detect  
[5,3] or [5,3]

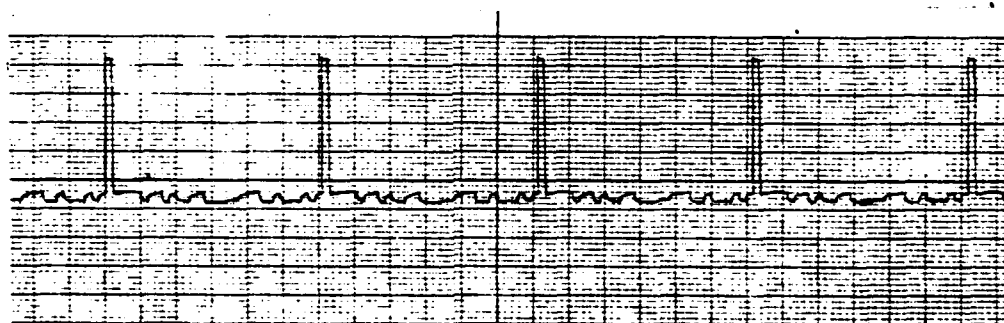
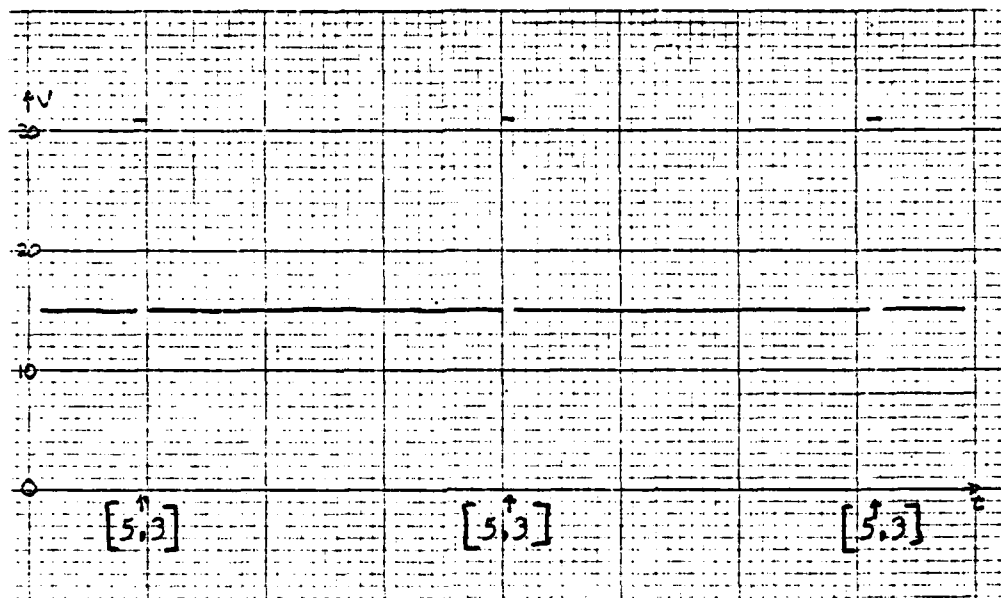


Figure 47. Theoretical and Measured Results  
 $[5,3]$  Transmitted

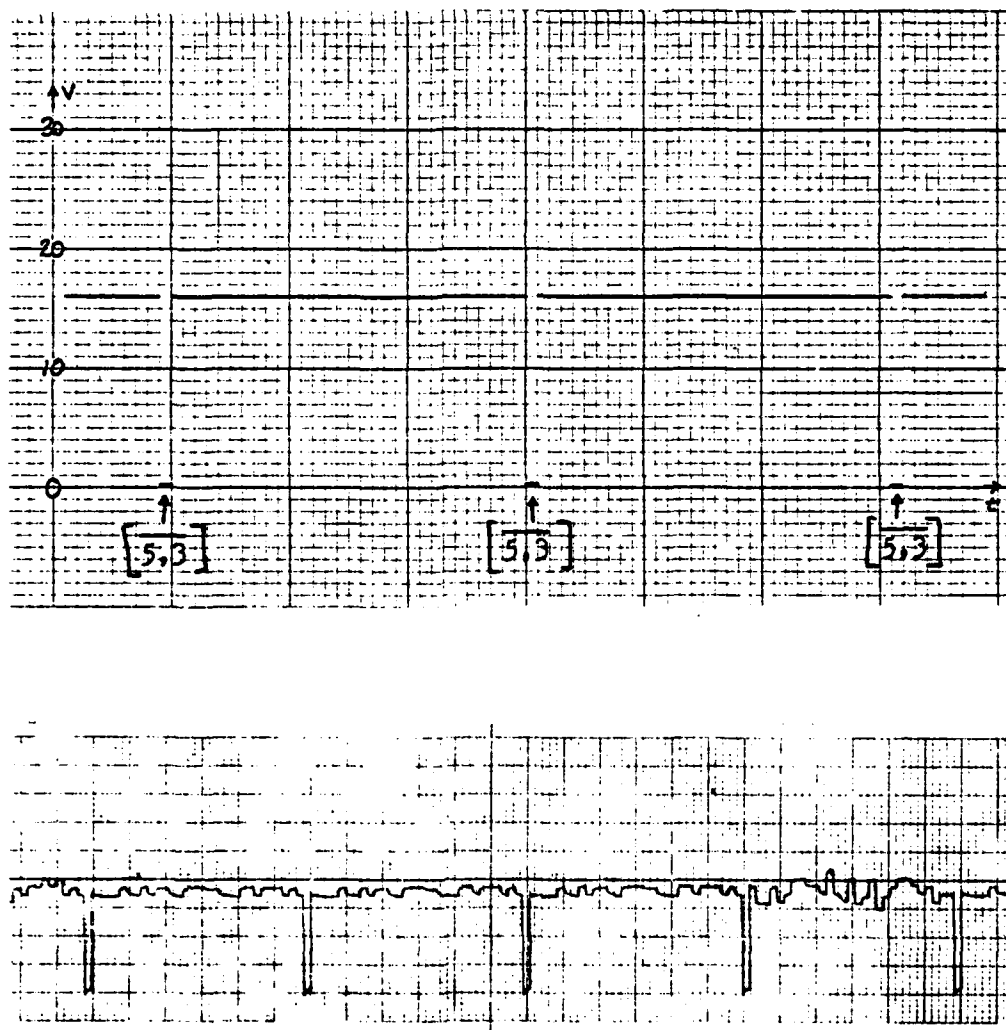


Figure 48. Theoretical and Measured Results  
 $[5,3]$  Transmitted

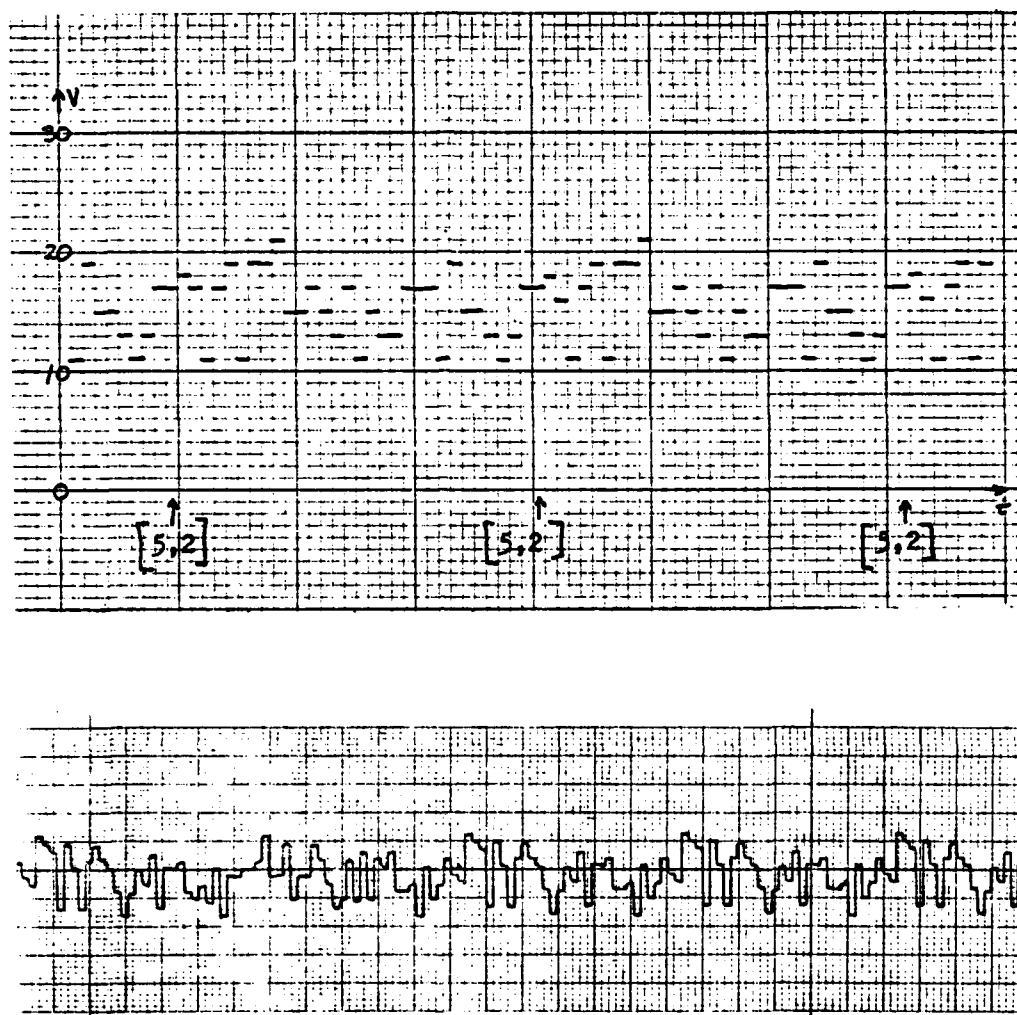


Figure 49. Theoretical and Measured Results  
 $[5,2]$  Transmitted

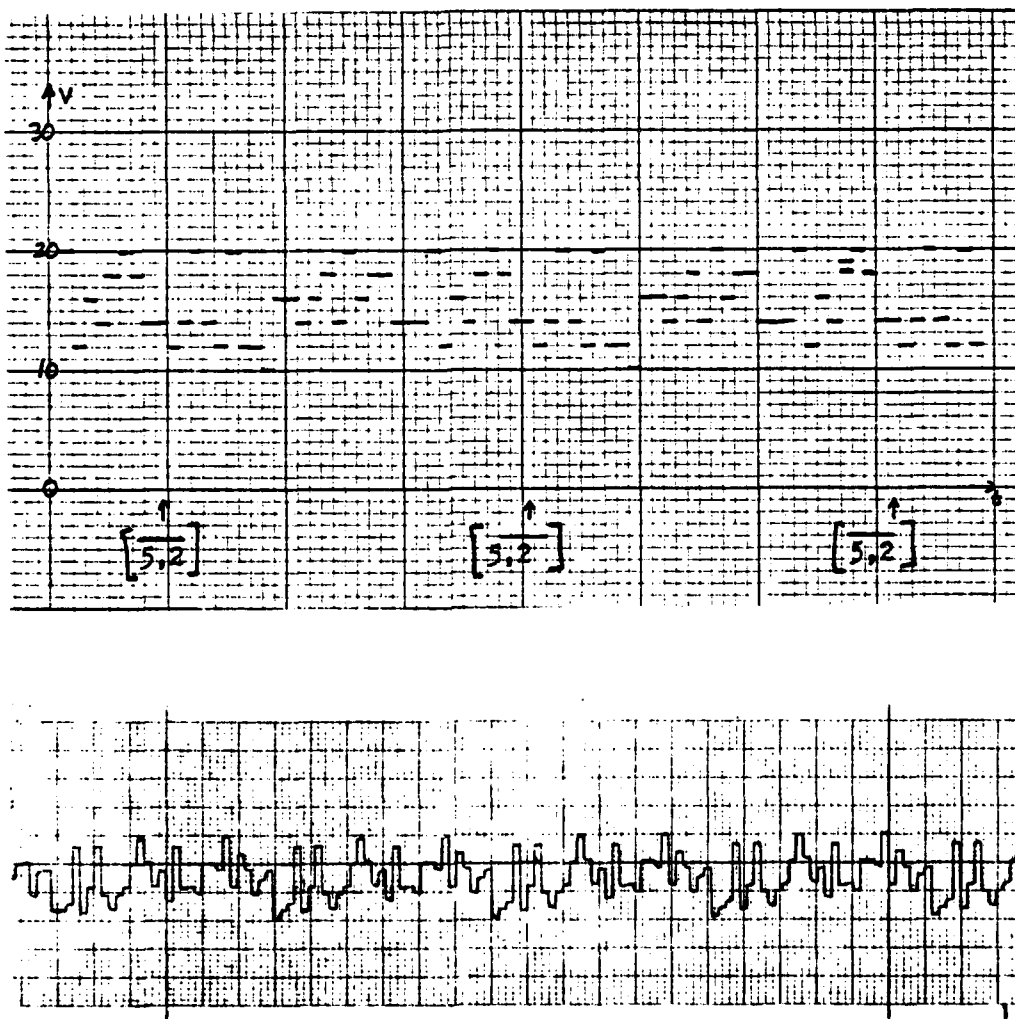


Figure 50. Theoretical and Measured Results  
 $[5,2]$  Transmitted



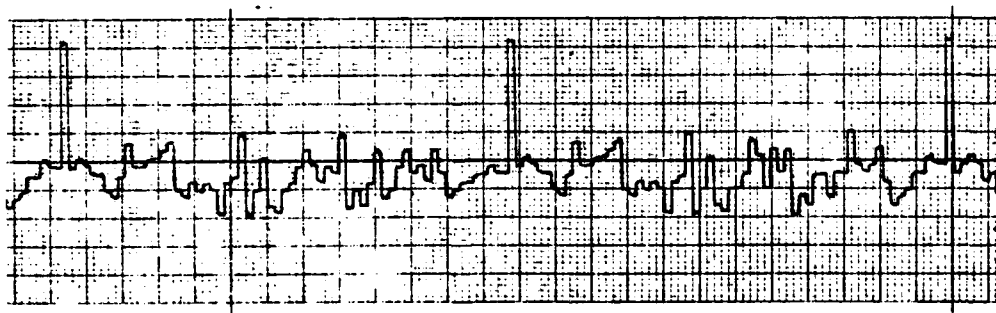
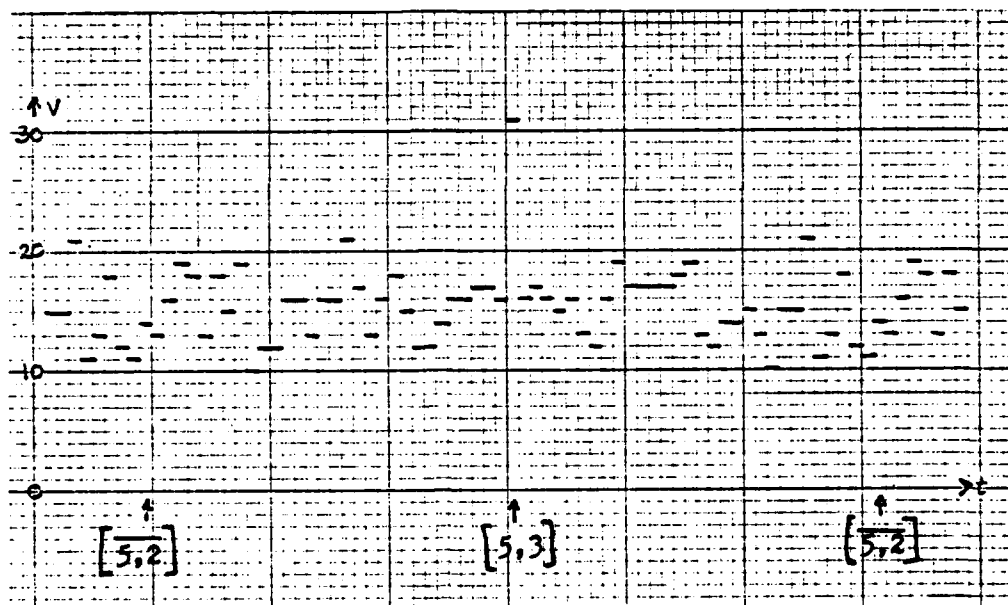


Figure 51. Theoretical and Measured Results  
 $[5,2], [5,3]$  Transmitted

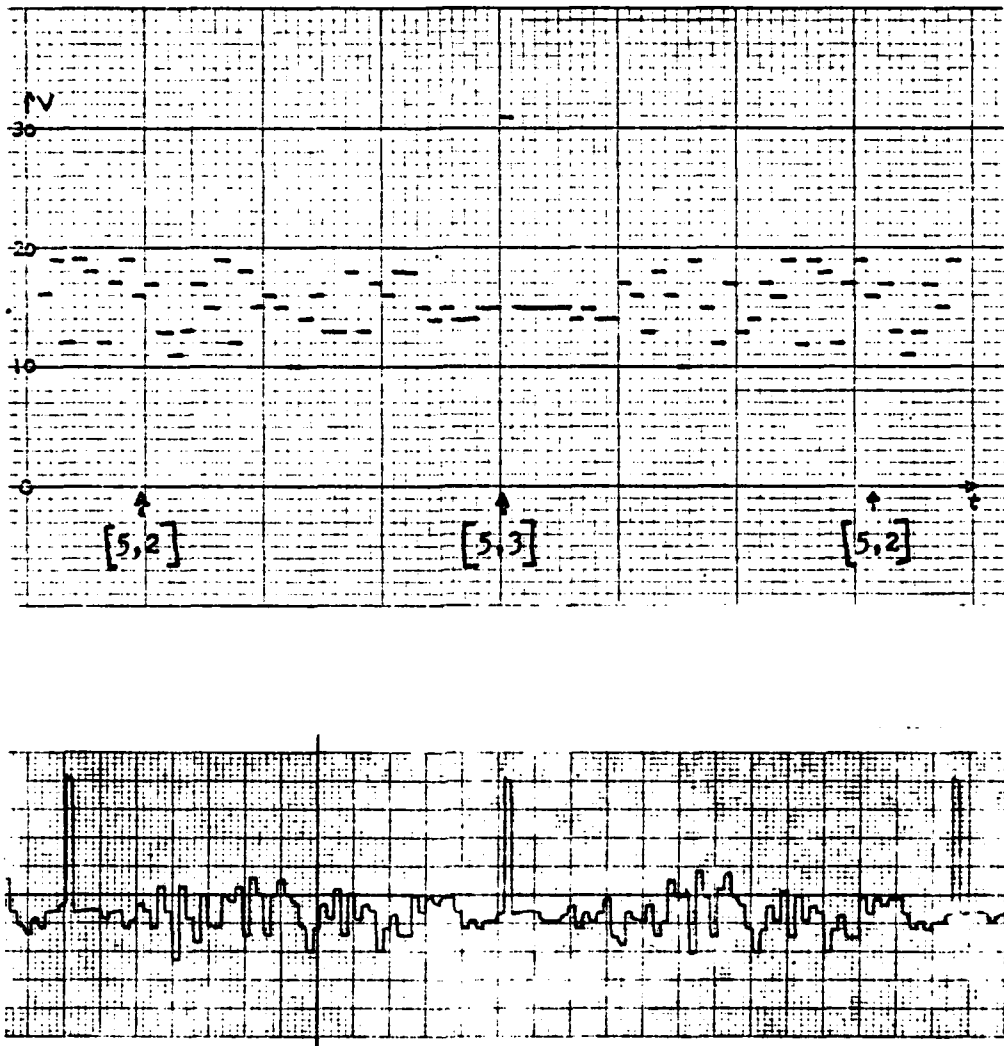


Figure 52. Theoretical and Measured Results  
 $[5,2], [5,3]$  Transmitted

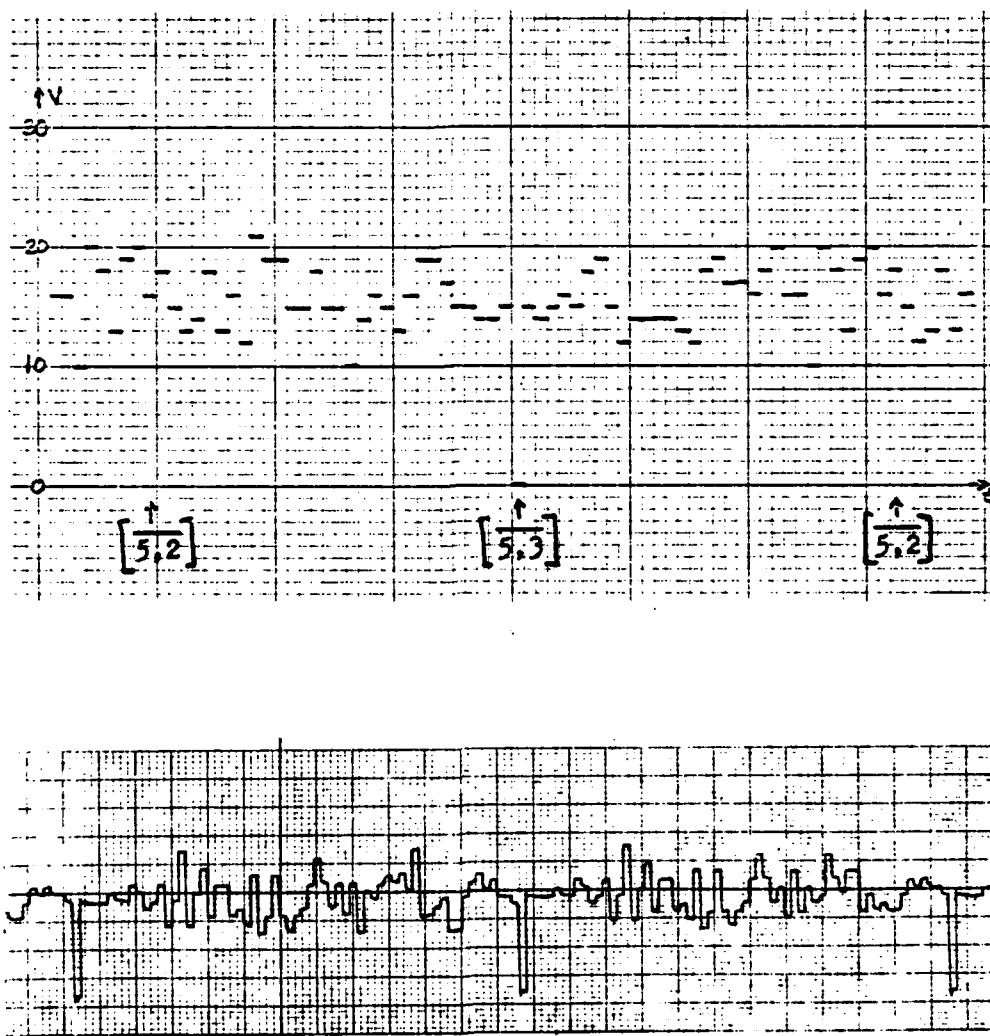


Figure 53. Theoretical and Measured Results  
 $\left[ \overset{\uparrow}{5}, 2 \right], \left[ \overset{\uparrow}{5}, 3 \right]$  Transmitted

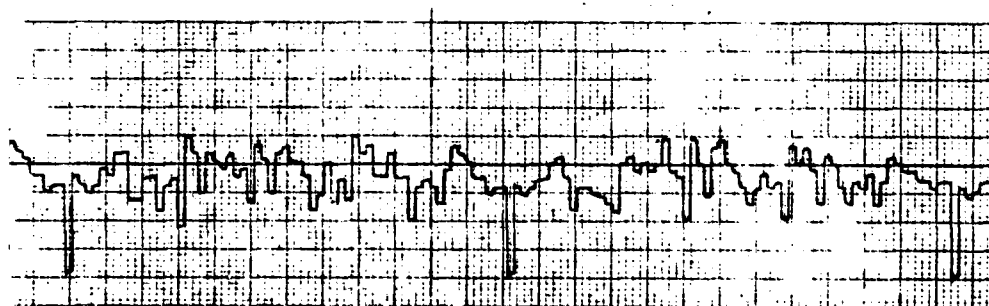
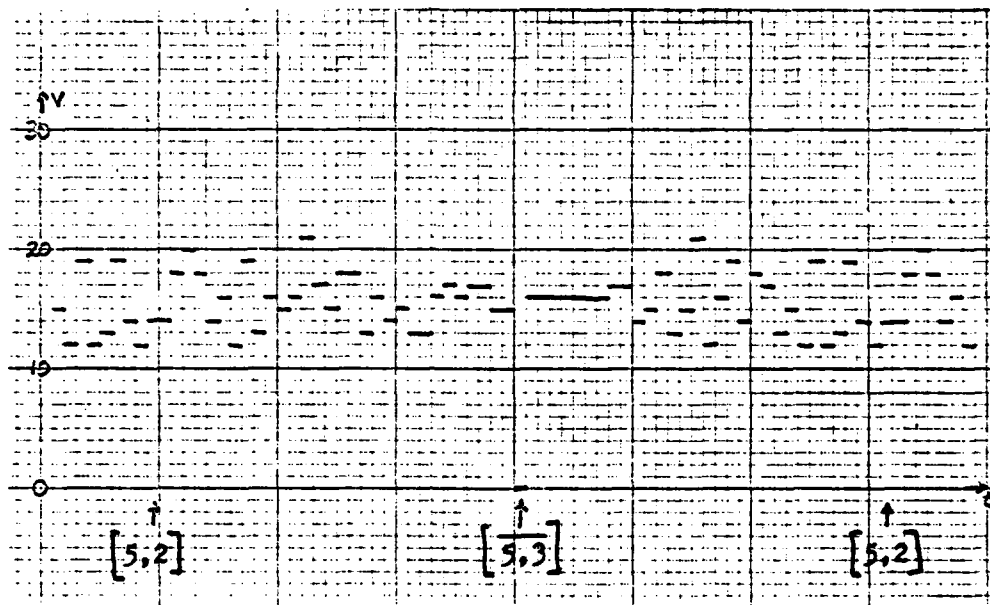


Figure 54. Theoretical and Measured Results  
 $[5,2], [5,3]$  Transmitted

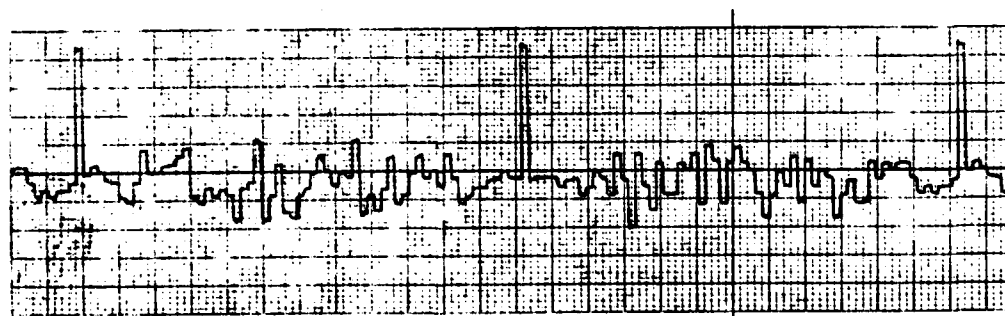
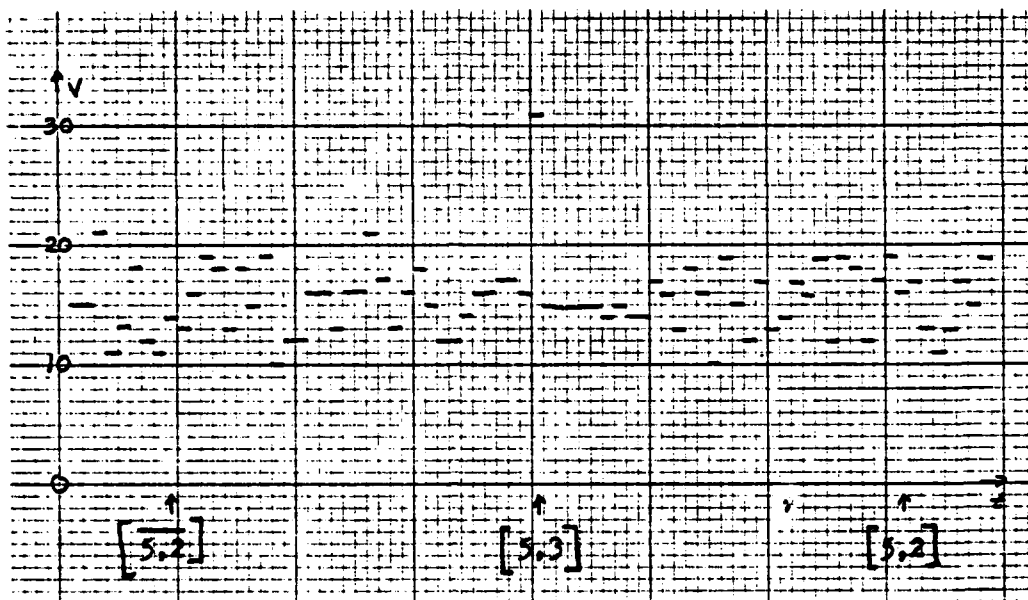


Figure 55. Theoretical and Measured Results  
 $[5,2], [5,3], [5,2], [5,3]$  Transmitted

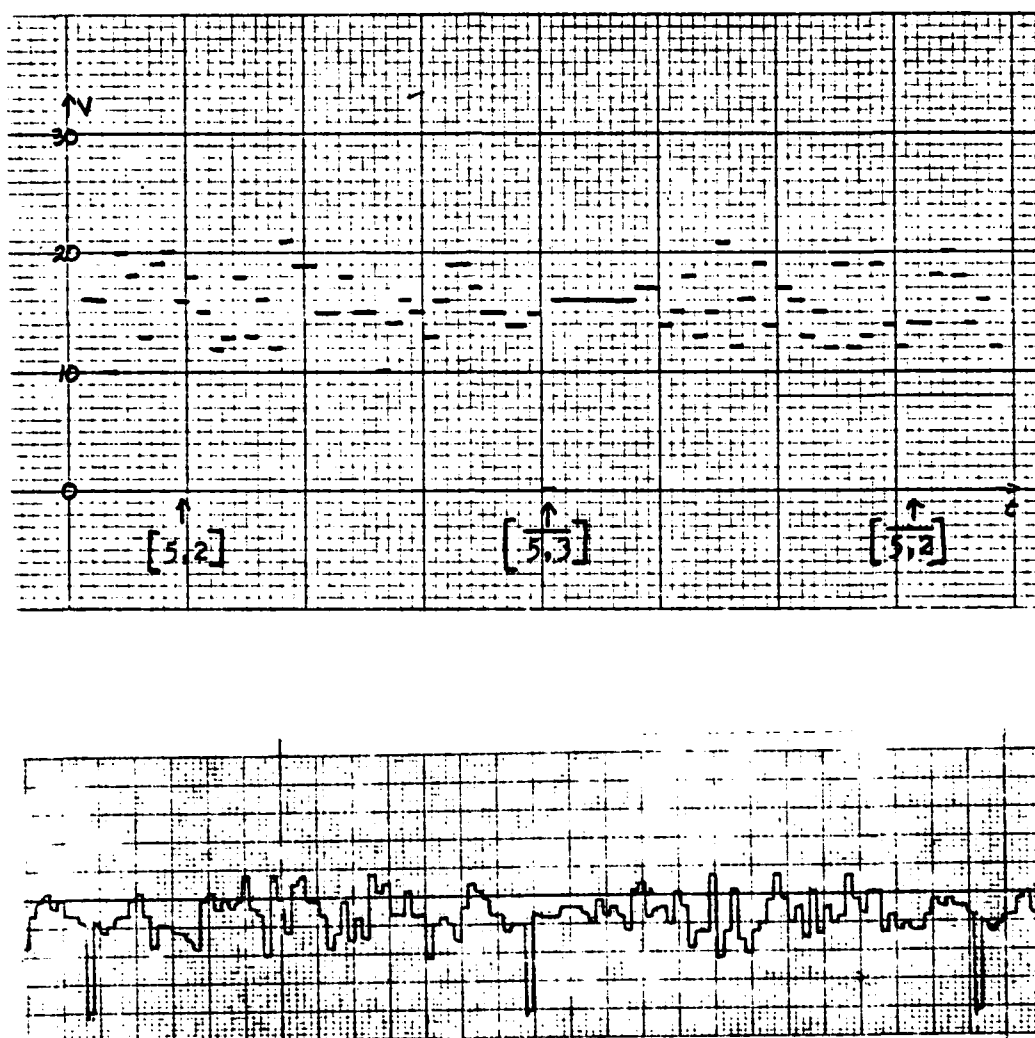


Figure 56. Theoretical and Measured Results  
 $[5,2], [5,3], [5,2], [5,3]$  Transmitted

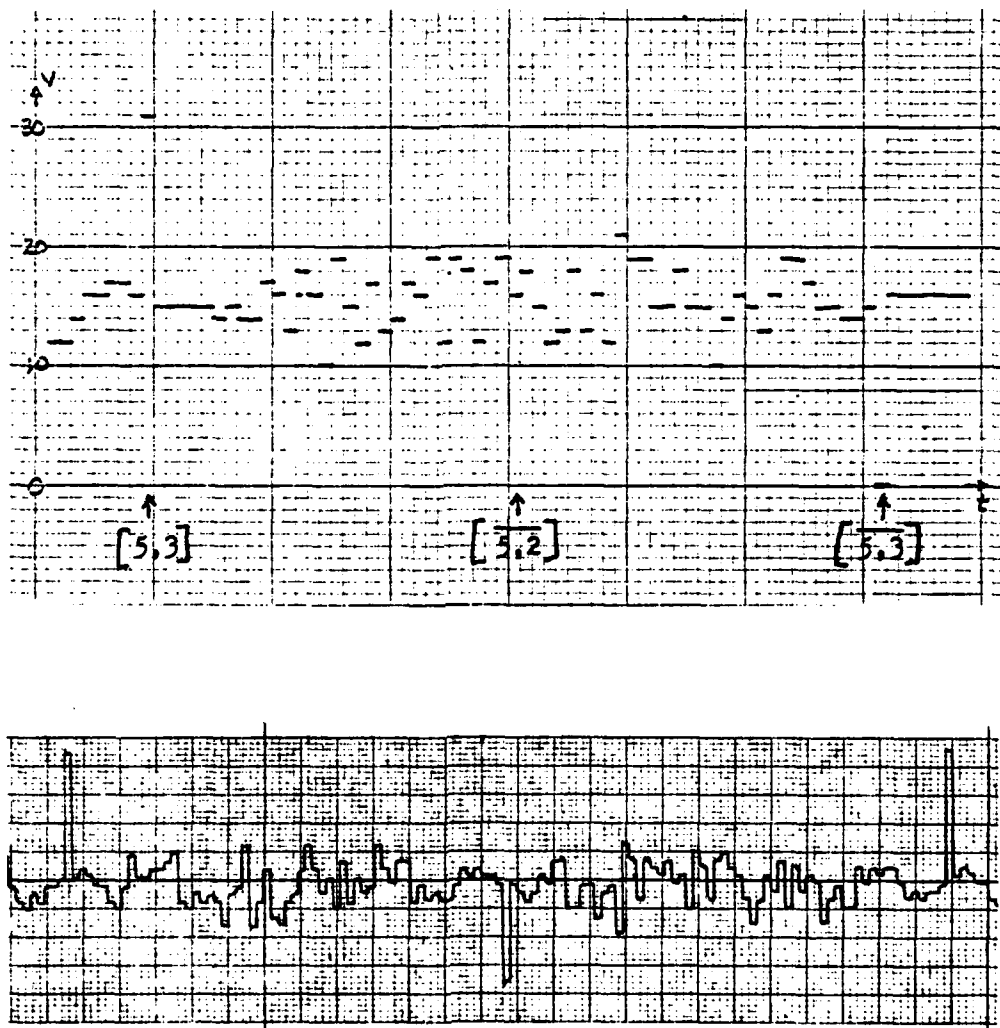


Figure 57. Theoretical and Measured Results  
 $[5,2], [5,3], [5,2], [5,3]$  Transmitted

Theoretically the output of the autocorrelation is 31 units high and any other sequence results in a maximum of 21 units. The output of the cross-correlation and its complement results in a level of 0 units while the minimum for any other arriving sequence is 10 units. If five errors occur in the desired code the maximum is reduced five units to a level of 26. Likewise for the complement code the output with five errors is increased to five units. If five errors occur in one of the other codes it is possible that the maximum could be increased five units to 26 or the minimum be reduced to five units. Therefore, the spread sequences can suffer five errors in 31 and the data can still be recovered. It is this feature which allows negative SNR's.

Because each hydrophone has three bands from which data can be recovered, at least six codes and their complements are required for the shallow-water range application. This criteria is capable of being met by both the 31-bit and 127-bit M-sequences. Although spreading by a factor of 127 provides 6 dB more attenuation margin than by a factor of 31, de-spreading the longer sequence requires four times as many integrated circuits. Therefore trade offs between processing gain and circuit cost would have to be considered in deciding which spread sequence length should be used.



## VI. CONCLUSIONS

As stated at the outset, the intention of this investigation was not to design a fiber optic link for the shallow-water tracking range. The objectives were to ascertain whether fiber optics were a viable mode of communications for the underwater cable link, to review the engineering parameters for fiber optics with sample calculations, and to investigate the various signal format alternatives.

From the investigation of optical cables it can be concluded that optical fiber cables can be constructed that survive in the ocean environment. With the many advantages of optical fibers over copper cables, the use of fiber optics merits strong consideration for application in the shallow-water tracking range and other future underwater projects at the Keyport facility.

A review of the procedures for engineering a fiber optic system revealed that a variety of commercially available optical sources and detectors can be used to successfully transmit the signal from the hydrophone to the shore-based signal processor. With proper selection of components, attenuation margins of greater than 10 dB can be obtained. It also appears that the simple transimpedance amplifier can be used as the front-end amplifier throughout the system.

A review of the available signal formats revealed that fiber optics favor digital signals. Analog signals require linearity which is difficult to obtain. It was seen that the large bandwidth required for PCM and TDM increases the thermal noise to a level where an APD must be used in the circuit. The third alternative considered was transmitting the original message. It was discovered, however, that for a BER of  $10^{-6}$  or better the original message resulted in a

multiplexed signal that could not be transmitted over the long 13 km link. It was then shown that by utilizing spread spectrum techniques the original message can be transmitted over the entire link with a BER of  $10^{-8}$  using only LEDs and PIN diodes. The only disadvantage of this technique is the loss of the Doppler information present in the SFSK signal. Thus if the range operation does not require the Doppler information it is apparent that the most practical fiber optic system utilizes a spread version of the original message as the signal.

#### LIST OF REFERENCES

1. R.C. Dixon, Spread Spectrum Systems, NY, NY: John Wiley & Sons, 1976, ch. 3, pp. 54-85.
2. G.R. Elion and H.A. Elion, Fiber Optics in Communications Systems, NY, NY: Marcel Dekker, Inc., 1978, pp. 94-158.
3. R.L. Gallawa, A User's Manual for Optical Waveguide Communications, Springfield, VA: NTIS, 1976, pp. 51-96, 195-204 and 213-225.
4. D. Kalish, P.L. Key, C.R. Kurkjian, B.K. Taryal, and T.T. Wang, "Fiber Characterization-Mechanical," in Optical Fiber Telecommunications, S.E. Miller and A.G. Chynoweth, Eds. New York: Academic Press, 1979, pp. 401-431.
5. R.E. Love, "Strength of Optical Waveguide Fibers," in Fibers & Integrated Optics, SPIE, vol. 77, 1976, pp. 69-77.
6. J.E. Midwinter, Optical Fibers for Transmission, NY, NY: John Wiley & Sons, ch. 12, pp. 260-307.
7. M.I. Schwartz, D. Gloge, and R.A. Kempf, "Optical Cable Design," in Optical Fiber Telecommunications, S.E. Miller and A.G. Chynoweth, Eds. New York: Academic Press, 1979, pp. 435-454.
8. "The Simplex Manual for Submarine Cables," Newington, NH: Simplex Wire & Cable Co., 1968, Section 3, pp. 1-31.
9. G.A. Wilkens, "Fiber Optic Cables for Undersea Communications," Fiber and Integrated Optics, vol. 1, no. 1, pp. 39-61, 1977.
10. G.A. Wilkens, "Recent Experience With Small, Undersea, Optical Cables," presented at EASCON '79, Washington, DC, October 8-11, 1979.

# INITIAL DISTRIBUTION LIST

	No. Copies
1. Defense Technical Information Center Cameron Station Alexandria, Virginia 22314	2
2. Library, Code 0142 Naval Postgraduate School Monterey, California 93940	2
3. Department Chairman, Code 63 Department of Electrical Engineering Naval Postgraduate School Monterey, California 93940	1
4. Professor John Powers, Code 62Po Department of Electrical Engineering Naval Postgraduate School Monterey, California 93940	6
5. Professor O.B. Wilson, Code 61W1 Department of Physics Naval Postgraduate School Monterey, California 93940	1
6. Mr. R.L. Marimon, Code 70 Naval Undersea Warfare Engineering Station Keyport, Washington 98345	1
7. Commander C. Gertner, Code 80 Naval Undersea Warfare Engineering Station Keyport, Washington 98345	1
8. Mr. R.L. Mash, Code 50 Naval Undersea Warfare Engineering Station Keyport, Washington 98345	1
9. Mr. Richard Peel, Code 7021 Naval Undersea Warfare Engineering Station Keyport, Washington 98345	3
10. Captain David N. Nicholson c/o MSG William Evans SAFSP-5 PO Box 92960 Worldway Postal Center Los Angeles, California 90009	3
11. Administrative Department, Code 0115 Naval Undersea Warfare Engineering Station Keyport, Washington 98345	5

# INITIAL DISTRIBUTION LIST (CONT)

	No. Copies
12. Mr. George Wilkens Naval Ocean Systems Center (Hawaii) PO Box 997 Kailua, Hawaii 96734	1
13. Dr. Steve Cowan, Code 5213 Naval Ocean Systems Center San Diego, California 92152	1
14. Cpt. John McHenry 203 Ashley Circle Martinez, Georgia 30907	1
15. Cpt. David Richards (S & I Branch) U.S. Army Electronic Proving Grounds Ft Huachuca, Arizona 85613	1